

EPA-R2-73-133
JANUARY 1973

Environmental Protection Technology Series

A User's Manual for Three-Dimensional Heated Surface Discharge Computations



**Office of Research and Monitoring
U.S. Environmental Protection Agency
Washington, D.C. 20460**

RESEARCH REPORTING SERIES

Research reports of the Office of Research and Monitoring, Environmental Protection Agency, have been grouped into five series. These five broad categories were established to facilitate further development and application of environmental technology. Elimination of traditional grouping was consciously planned to foster technology transfer and a maximum interface in related fields. The five series are:

1. Environmental Health Effects Research
2. Environmental Protection Technology
3. Ecological Research
4. Environmental Monitoring
5. Socioeconomic Environmental Studies

This report has been assigned to the ENVIRONMENTAL PROTECTION TECHNOLOGY series. This series describes research performed to develop and demonstrate instrumentation, equipment and methodology to repair or prevent environmental degradation from point and non-point sources of pollution. This work provides the new or improved technology required for the control and treatment of pollution sources to meet environmental quality standards.

A USER'S MANUAL FOR THREE-DIMENSIONAL
HEATED SURFACE DISCHARGE COMPUTATIONS

By

Keith D. Stolzenbach

E. Eric Adams

and

Donald R. F. Harleman

Project 16130 DJU

Project Officer

Frank H. Rainwater
National Environmental Research Center
Corvallis, Oregon 97330

Prepared for
OFFICE OF RESEARCH AND MONITORING
U.S. ENVIRONMENTAL PROTECTION AGENCY
WASHINGTON, D.C. 20460

EPA Review Notice

This report has been reviewed by the Environmental Protection Agency and approved for publication. Approval does not signify that the contents necessarily reflect the views and policies of the Environmental Protection Agency, nor does mention of trade names or commercial products constitute endorsement or recommendation for use.

ABSTRACT

In February 1971, a report by K. D. Stolzenbach and Donald R. F. Harleman entitled "An Analytical and Experimental Investigation of Surface Discharges of Heated Water" was published. (Technical Report No. 135, Ralph M. Parsons Laboratory for Water Resources and Hydrodynamics, Department of Civil Engineering, M.I.T.; also published as Water Pollution Control Research Series Report No. 16130 DJU 02/71 by the Water Quality Office, Environmental Protection Agency, Washington, D.C.) The report described above presented a literature review of previous analytical and experimental research on heated surface discharges, the development of a predictive theory for calculating three-dimensional temperature distributions in the near-field region and verification of the theory based on laboratory work at M.I.T. and elsewhere. The above report also contained a listing of the computer program as originally developed.

Subsequent work and experience in using the computer program for the calculation of temperature distributions have resulted in modifications and improvements in the program. In addition, a number of runs covering a wide range of input parameters have been carried out. These runs were done with two objectives: (1) to explore the limits of applicability of the theory and (2) to prepare design charts showing the important characteristics of the near field temperature distribution for heated surface discharges. These charts will enable the designer to make rapid estimates of surface isotherms and vertical thickness of surface jets.

This report presents a review of the theoretical background for the three-dimensional temperature prediction model, a detailed discussion of the revised computer program and a case study illustrating the procedure for optimizing the design of a surface discharge channel. The revised computer program flow chart, program listing and a sample of the input and output data are given in the appendices.

One difference between the revised computer program presented in this report and the original computer program of February 1971 deserves further comment. The original program contained the possibility of considering a sloping bottom in the receiving water. The sloping bottom, was assumed to extend downward

in a linear slope from the bottom of the discharge channel. In the revised computer program it is assumed that the bottom of the receiving water does not interfere with the development of the surface jet. Thus the revised program corresponds to $S_x = \infty$ in the original program. The reasons for eliminating the bottom slope effect in the revised program are two-fold: (1) the mathematical model, as originally constituted, did not adequately predict the point of separation of the heated jet from the bottom or lateral spreading when the jet is in contact with the bottom; (2) from the standpoint of environmental impact, it may be desirable to accept the depth of the receiving water as a constraint and to design the surface discharge channel to minimize interference of the heated jet with the bottom.

It is recognized that almost none of the operating power plants that employ surface discharge schemes have been designed to minimize bottom impact. This fact makes it difficult to compare field data from many existing plants with temperature predictions based on the mathematical model presented in this report.

Further analytical and experimental studies of bottom interference with heated surface jets are presently underway in the M.I.T. Parsons Laboratory and will be the subject of a future technical report.

Inquiries relating to the availability of the program source deck should be directed to Professor D.R.F. Harleman, Room 48-335, M.I.T., Cambridge, Massachusetts 02139.

TABLE OF CONTENTS

	<u>Page</u>
<u>ABSTRACT</u>	iii
<u>TABLE OF CONTENTS</u>	v
<u>LIST OF FIGURES</u>	vi
<u>I. INTRODUCTION</u>	1
1.1 Characteristics of Heated Discharges	1
1.2 Surface Discharges	3
<u>II. THE MATHEMATICAL MODEL</u>	3
2.1 Basic Assumptions	7
2.2 Discharge Structure	9
2.3 Integration of the Equations	16
2.4 Solution of the Equations	20
<u>III. THE PROGRAM</u>	39
3.1 Dimensionless Equations	39
3.2 The Computational Scheme	43
3.3 Input Formats	45
3.4 Output Format	46
<u>IV APPLICATION</u>	47
4.1 Schematization	47
4.2 Use of the Program Output	56
4.3 Case Study - Heated Surface Discharge into a Receiving Water Body of Finite Depth	57
<u>ACKNOWLEDGEMENT</u>	65
<u>REFERENCES</u>	67
<u>LIST OF SYMBOLS</u>	69
APPENDIX I. Flow Chart for Solution of $[a_{ij}] \frac{dy_j}{dx} = c_i$	73
APPENDIX II. Program Listing	75
APPENDIX III. Input and Output	97

LIST OF FIGURES

10

<u>Figure</u>		<u>Page</u>
1.1	Schematic of Heated Discharge	4
2.1	Coordinate Definitions	8
2.2	Discharge Structure	11
2.3	Calculated Surface Discharge Parameters: $IF_o = 4.4, A = 0.35, k/u_o = 4.2 \times 10^{-5}, V/u_o = 0$	22
2.4	Calculated Isotherms of $\Delta T/\Delta T_o$: $IF_o = 4.4, A = 0.35, k/u_o = 4.2 \times 10^{-5}, V/u_o = 0$	23
2.5	Centerline Temperature Rise $\Delta T_c/\Delta T_o$ and Dilution, D , in the Stable Region for $k/u_o = V/u_o = 0$	26
2.6	Maximum Vertical Depth of the Jet, $\frac{(h+r)_{\max}}{\sqrt{h_o b_o}}$ for $k/u_o = V/u_o = 0$	27
2.7a	Jet Parameters for $IF_o = 20.0, V/u_o = 0, k/u_o = 0$	29
2.7b	Jet Parameters for $IF_o = 10.0, V/u_o = 0, k/u_o = 0$	30
2.7c	Jet Parameters for $IF_o = 5.0, V/u_o = 0, k/u_o = 0$	31
2.7d	Jet Parameters for $IF_o = 2.0, V/u_o = 0, k/u_o = 0$	32
2.7e	Jet Parameters for $IF_o = 1.0, V/u_o = 0, k/u_o = 0$	33
2.7f	Jet Parameters for $IF_o = 20.0, V/u_o = 0.025, k/u_o = 0$	34
2.7g	Jet Parameters for $IF_o = 10.0, V/u_o = 0.05, k/u_o = 0$	35
2.7h	Jet Parameters for $IF_o = 5.0, V/u_o = 0.1, k/u_o = 0$	36
2.7i	Jet Parameters for $IF_o = 2.0, V/u_o = 0.1, k/u_o = 0$	37
4.1	Coefficient of Thermal Expansion for Fresh Water $\beta = \frac{1}{\rho} \frac{\partial \rho}{\partial T} (^{\circ}F^{-1})$ as a Function of Temperature $T(^{\circ}F)$	49
4.2	Discharge Channel Schematization	51

<u>Figure</u>		<u>Page</u>
4.3	Limitations on Maximum Jet Thickness by Bottom Topography	52
4.4	Two Layer Flow in the Discharge Channel	53
4.5	Temperature Distribution Plotting Aid	58
4.6	Schematic of Case Study Problem	59
4.7	Calculated Contours for the Case Study Example	64

I. Introduction

1.1 Characteristics of Heated Discharges

The discharge of heated condenser water into natural bodies of water can be broadly classified into two groups: surface discharges and submerged discharges. The latter class includes single port submerged discharges and multi-port diffusers. From the standpoint of minimizing the environmental impact of thermal effluents, the surface discharge has a number of advantages when compared with submerged discharges: (1) By careful design of a surface discharge it is possible to avoid temperature rises and high velocities along the bottom of the receiving water. (2) The time of travel of organisms entrained at the condenser water intake is short. (3) Heat dissipation from the surface of the receiving water is high because of the tendency of the discharge to form a stratified surface layer.

A typical open cycle system withdraws water from a natural water body through an intake structure and passes the flow through the turbine condensers where it undergoes a temperature rise before being returned to the receiving water through a discharge structure. In-plant technological considerations dictate condenser temperature rises of from 10-30°F with correspondingly large cooling water flows depending upon the amount of rejected heat.

The use of natural water bodies and coastal waters for disposal of waste heat must take into account the effect upon the environment of the flows and temperature rises induced in the receiving water. There is general agreement that water temperature increases which approach the sub-lethal range of impaired biological activity should be avoided. Practically all regulatory agencies provide this type of protection through controls on both maximum temperatures and allowable temperature rises and by designating the size of mixing zones for various types of receiving waters. In addition to environmental considerations the intake structure must be located and designed to prevent significant recirculation of heated water. Separation of the intake and discharge or the use of selective withdrawal structures are the most common techniques.

The temperature distribution induced in the receiving water by a heated discharge is determined by the characteristics of the discharge structure and by the local ambient heat transfer processes. Close to the point of discharge the momentum of the discharged water creates jet-like mixing of the heated and ambient water. Within this "near field" region the temperature and velocity

of the discharge decrease because of dilution by entrained water. The magnitude and extent of the dilution is determined primarily by the nature of the initial discharge flow, its submergence, velocity, dimensions and temperature rise above ambient. Mixing increases with increasing discharge momentum and decreases with increasing temperature rise. The greater the submergence of the discharge below the water surface, the lower the temperature rise at the surface will be after mixing. Mixing may also be affected by the presence of physical obstructions which tend to block the supply of dilution water. Surface discharges entrain a flow at least equal to the discharge flow in the near field, often up to twenty times as much.

Beyond the near field mixing region the discharge velocity and turbulence level are of the order of ambient values. In this "far field" region further entrainment does not occur and the temperature distribution is determined by natural turbulent convection and diffusion. Ultimately all of the rejected heat contained in the discharge passes to the atmosphere through the water surface, a process driven by the elevated surface temperatures. These far field heat transfers are highly variable, being determined by local water currents, wind, and meteorological conditions.

Consideration of either environmental impact or recirculation on discharge design must start with the near field temperature distribution. Far field processes are generally an order of magnitude less efficient in reducing temperatures and the far field temperature distribution tends to be more dependent upon the total amount of waste heat rather than the discharge design. In contrast, a wide range of dilutions is achievable in the near field through diverse types of discharge structures. It has been common practice to analyze near field temperatures by constructing scale models of the discharge structure. There is a pressing need for analytical models which relate the discharge characteristics to the flow and temperature distribution in the receiving water. Furthermore, since the analysis must almost always be performed in advance of actual plant construction, the analytical model must be totally predictive, containing no undetermined phenomenological coefficients.

This report describes the basis, structure, and use of a predictive model of the three-dimensional behavior of surface discharges of heated water. Emphasis is placed upon the assumptions underlying the theory, the scope of its validity,

the nature of its limitations, and the proper application to actual discharges. For similar treatments of submerged discharges, the reader is referred to references 1 and 2.

1.2 Surface Discharges

The theory presented herein considers a discharge of heated water from a rectangular open channel at the surface of an ambient body of water of infinite extent in which a current may be flowing (see Figure 1.1). The three-dimensional temperature distribution depends upon the mixing between the discharged and ambient water and upon the rate of heat transfer to the atmosphere at the water surface.

Experimental investigations of three-dimensional buoyant surface jets have been reported by Tamai (3), Wiegell (4), Jen (5), Stefan (6) and Hayashi (7). Buoyant surface discharges are distinguished from non-buoyant turbulent jets by lateral gravitational spreading and by reduction of vertical entrainment such as described by Ellison and Turner (8) for the two-dimensional case. The net result of these two processes is that the velocity and temperature distributions are much wider than deep with the increased surface area raising the possibility (as suggested by Hayashi) for significant surface heat loss. Previous analytical treatments (Hoopes (9), Motz (10)) of heated surface discharges have failed to take into account, in a single three-dimensional theory, the roles of buoyancy, initial channel shape, turbulent entrainment, and surface heat loss upon the temperature distribution.

In this treatment the discharge is assumed to be a free turbulent jet with a well defined turbulent region in which velocity and temperature are related to centerline values by similarity functions. An unsheared core region is accounted for. Turbulent entrainment is represented by entrainment coefficients as first introduced by Morton, Taylor, and Turner (11) and applied to other buoyant jet problems by Morton (12) and Fan (1) among others. A major contribution of this work is the treatment of lateral buoyant spreading by incorporating an assumed distribution for the lateral velocity into the set of integrated governing equations. Surface heat loss is assumed to be determined by a single heat loss coefficient as defined by Edinger (13). In the presence of a cross current in the receiving water the jet is deflected by entrainment of ambient lateral momentum.

The basic philosophy behind the formulation of the theory is that the

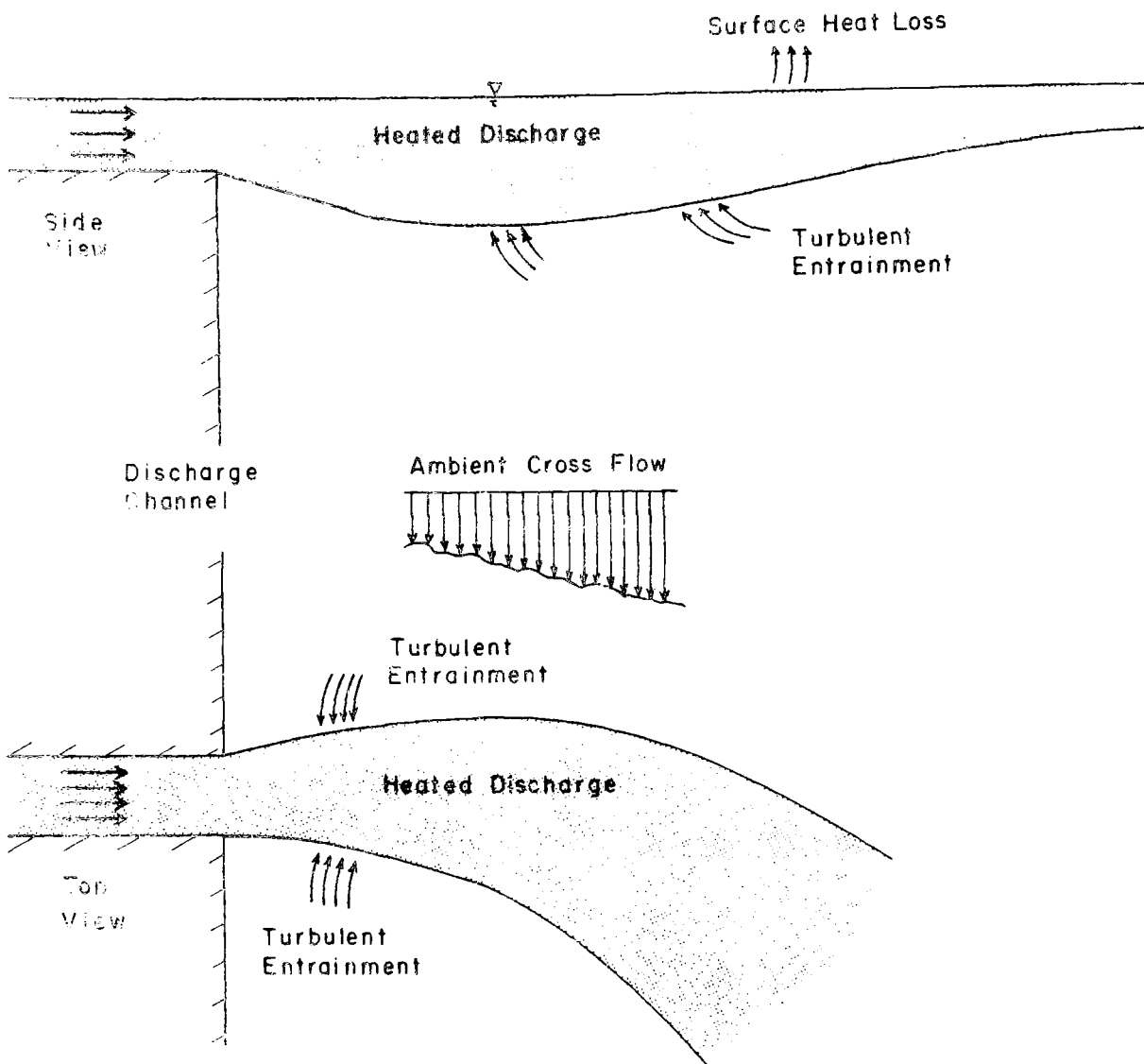


Fig. 1-1 Schematic of Heated Discharge

solution should match known non-buoyant jet behavior as the buoyancy terms go to zero. The effects of buoyancy are obtained by use of the basic equations and some judicious assumptions about the jet structure. In this way, the theory contains no undetermined coefficients and comparison of the theory with observations involves no curve fitting.

Because of the dependency of the treatment upon jet theory, the predictions of the model are valid only in the region where turbulence resulting from the discharge dominates ambient turbulent processes, i.e. in the near field.

II. The Mathematical Model

2.1 Basic Assumptions

The model considers a discharge Q_0 of heated water at temperature T_0 and density ρ_0 from a rectangular open channel of depth h_0 , width $2b_0$, and initial angle θ_0 at the surface of a receiving body of water at temperature T_a , density ρ_a and of large extent laterally and longitudinally. It is assumed that the bottom of the receiving water does not interfere with the vertical development of the surface jet. A non-uniform current V may be present in the receiving water. It is assumed that this current is parallel to the shoreline; however, its magnitude may vary in the offshore direction as shown in Figure 2.1. Far from the jet the water surface, η , is uniformly at $z = 0$. The flow in the receiving water is characterized by its velocity, density, pressure and temperature. These four variables are related by equations expressing conservation of mass, momentum and heat and an equation of state. The solution of the equations must be developed by setting certain terms in the basic equations equal to zero on the basis of the following assumptions:

- a) Steady flow: $\frac{\partial}{\partial t} = 0$
- b) Large Reynolds number: viscous terms negligible
- c) Boussinesq approximation: density gradients only important in pressure terms
- d) Hydrostatic pressure: $p = -\int_{\eta}^z \rho g dz$
- e) No jet induced motion at large depths: $\frac{\partial p}{\partial x} = \frac{\partial p}{\partial y} = 0$ as $z \rightarrow -\infty$
- f) Boundary layer flow: $\frac{\partial}{\partial x} \ll \frac{\partial}{\partial y}$ and $\frac{\partial}{\partial z}$
- g) Small density differences: $\frac{\rho_a - \rho_0}{\rho_a} \ll 1$
- h) Mild jet curvature: $V/u_0 < 1$

With the above assumptions the basic equations of mass, momentum and heat conservation may be simplified to the following form:

Mass Conservation

$$\frac{\partial u}{\partial x} + \frac{\partial v}{\partial y} + \frac{\partial w}{\partial z} = 0 \quad (2.1)$$

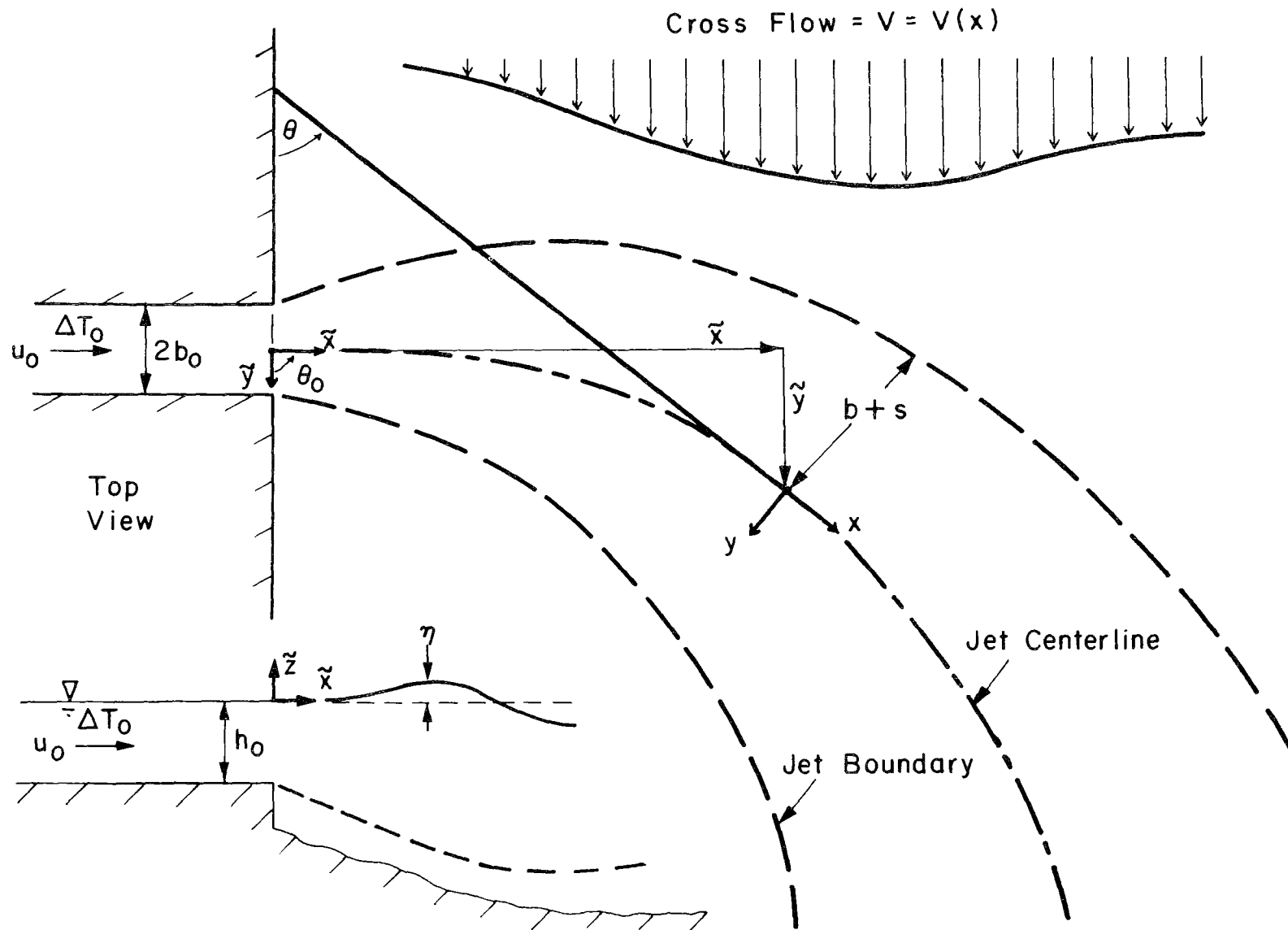


Fig. 2.1 Coordinate Definitions

x-Momentum Conservation

$$\frac{\partial u^2}{\partial x} + \frac{\partial uv}{\partial y} + \frac{\partial uw}{\partial z} = \beta g \int_z^{-\infty} \frac{\partial T}{\partial x} dz - \frac{\partial u'v'}{\partial y} - \frac{\partial u'w'}{\partial z} \quad (2.2)$$

y-Momentum Conservation

$$\frac{\partial uv}{\partial x} + \frac{\partial v^2}{\partial y} + \frac{\partial vw}{\partial z} = \beta g \int_z^{-\infty} \frac{\partial T}{\partial y} dz + u^2 \frac{\partial \theta}{\partial x} \quad (2.3)$$

Heat Conservation

$$\frac{\partial uT}{\partial x} + \frac{\partial vT}{\partial y} + \frac{\partial wT}{\partial z} = - \frac{\partial v'T'}{\partial y} - \frac{\partial w'T'}{\partial z} \quad (2.4)$$

where:

x,y,z = coordinate directions relative to the jet centerline
(see Figure 2.1)

u,v,w = mean velocity components

u',v',w' = turbulent fluctuating velocity components

T = mean temperature

T' = turbulent fluctuating temperature

θ = centerline deflection angle (see Figure 2.1)

g = gravitational acceleration

$\beta = \frac{1}{\rho} \frac{\partial \rho}{\partial T}$ where ρ = density

2.2 Discharge Structure

The governing equations (2.1-2.4) assumed for heated surface discharges may not be solved without further manipulation since the turbulent transfer terms are not determined. The technique used to develop the solution is to assume a structure for the velocity and temperature within the discharge, and boundary conditions at the outer edges, leaving as unknowns only certain values such as the centerline velocity and temperature. The governing equations may then be integrated over a cross-section perpendicular to the discharge centerline. This procedure eliminates the unknown turbulent terms and yields a set of first order differential equations which may be solved for the variables describing the discharge behavior.

The assumed structure of the discharge is shown in Figure 2.2. The longitudinal velocity and temperature distributions are taken to be as follows where η is the water surface elevation and u_c and $\Delta T_c = T_c - T_a$ are the centerline velocity and temperature rise above ambient at $z = \eta$, $y = 0$:

$$\begin{aligned}
 u &= u_c + V \cos \theta & 0 < |y| < s & & -r < z < \eta \\
 \Delta T &= \Delta T_c \\
 \\
 u &= u_c f(\zeta_z) + V \cos \theta & 0 < |y| < s & & -(r+h) < z < -r \\
 \Delta T &= \Delta T_c t(\zeta_z) \\
 \\
 u &= u_c f(\zeta_y) + V \cos \theta & s < |y| < s+b & & -r < z < \eta \\
 \Delta T &= \Delta T_c t(\zeta_y) \\
 \\
 u &= u_c f(\zeta_y) f(\zeta_z) + V \cos \theta & s < |y| < s+b & & -(r+h) < z < -r \\
 \Delta T &= \Delta T_c t(\zeta_y) t(\zeta_z)
 \end{aligned} \tag{2.5}$$

where $\zeta_y = \frac{|y|-s}{b}$ and $\zeta_z = \frac{-z-r}{h}$

The lengths r and s pertain to the initial core region and h and b to the turbulent region of the jet (see Figure 2.2).

The particular forms of the similarity functions are assumed to be as follows:

$$\begin{aligned}
 f(\zeta) &= (1 - \zeta^{3/2})^2 \\
 t(\zeta) &= 1 - \zeta^{3/2}
 \end{aligned} \tag{2.6}$$

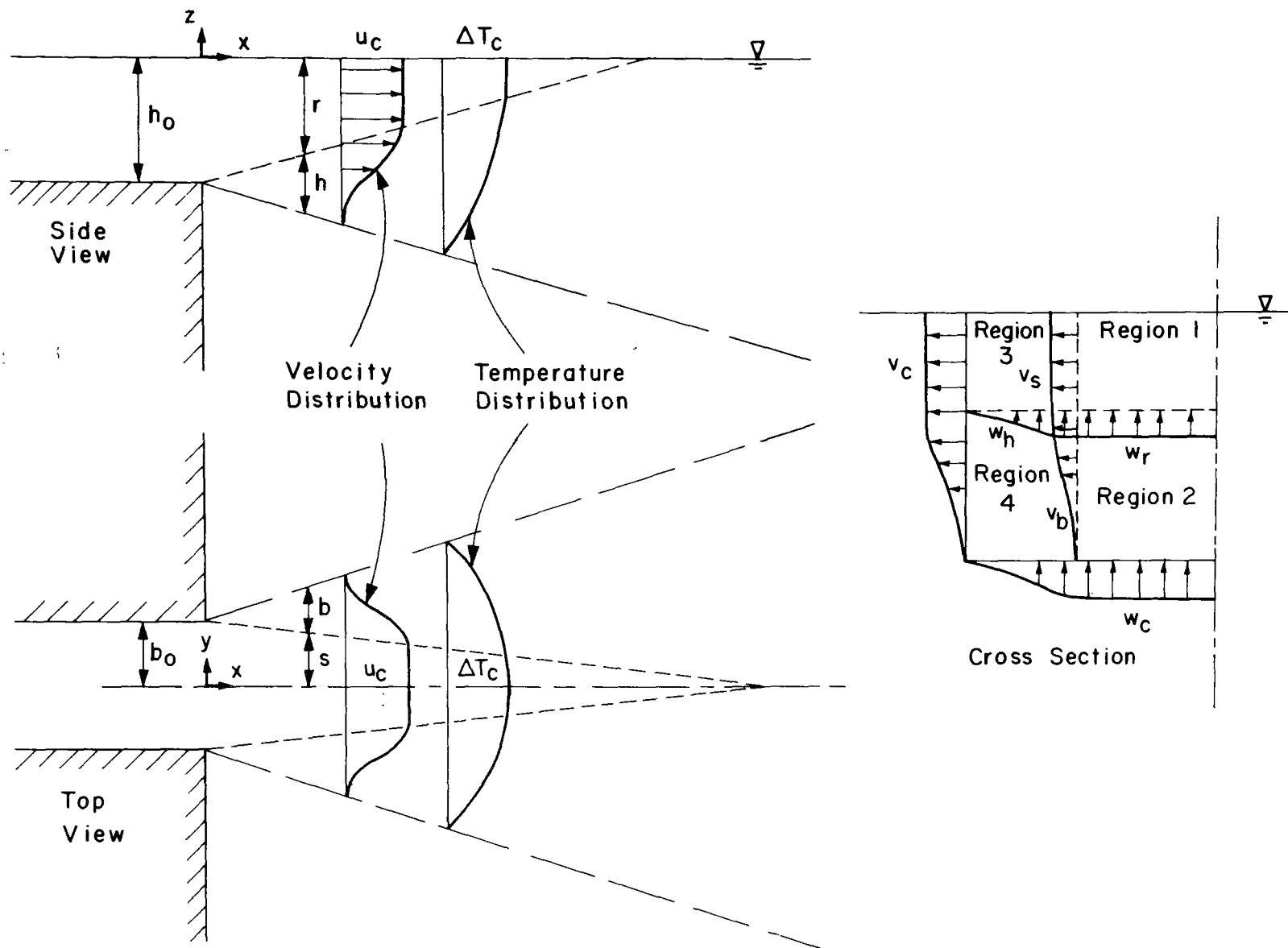


Fig. 2.2 Discharge Structure

The above functions were proposed by Abramovich (14). They have the desirable properties that a distinct jet boundary is defined at $\zeta = 1.0$ and that the velocity and temperature distributions are not identical but are related by $t = f^{1/2}$ as implied by Taylor's vorticity transfer theory.

The y momentum equation (2.3) expresses a balance between the lateral density gradients and lateral convective motions. It may be shown that for buoyant jets these lateral movements and thus the pressure gradient may be of the same order as convective transport in the x direction. The balance between lateral turbulent fluctuating pressures and Reynolds stresses, which is found in non-buoyant jets, is of second order and is neglected here. Since there are finite (but second order) lateral velocities in a non-buoyant jet, the lateral velocity v in equation (2.3) must be interpreted as the buoyant spreading velocity in excess of the non-buoyant value. To enable an integration of equation (2.3) over the jet cross section, the distribution of the lateral spreading velocity, v, must be specified. The lateral velocity is geometrically related to the longitudinal velocity by:

$$\frac{v}{u} = \tan \phi \quad (2.7)$$

where ϕ is the lateral jet streamline angle from the centerline in excess of the non-buoyant value. A distribution for u has already been given; it thus remains to choose a reasonable distribution for ϕ such that the following conditions are satisfied: (1) $\tan \phi = 0$ at $y = 0$ and (2) $\tan \phi = (\frac{db}{dx} - \epsilon)$ at $y = b+s$ where ϵ is the lateral spreading rate of a non-buoyant jet under the same conditions (cross flow, channel size, etc.). Since the gravitational spread is induced by the lateral temperature gradient, the y dependence of $\frac{\partial T}{\partial y}$ is used to distribute $\tan \phi$ between $y = 0$ and $|y| = b + s$. The result is:

$$\begin{aligned} v &= \pm \left(\frac{db}{dx} - \epsilon \right) u \zeta_y^{1/2} & s < |y| < s + b \text{ (v has the sign of y)} \\ v &= 0 & \text{elsewhere} \end{aligned} \quad (2.8)$$

The above distribution for v insures that for a non-buoyant jet in which

$\frac{db}{dx} = \epsilon$ the gravitational spreading velocity is identically zero everywhere.

Depending upon whether r or s are non-zero at a given centerline distance, the jet cross section will have 1, 2, or 4 regions (see Figure 2.2) on each side of the centerline ($y = 0$). To permit integration of the governing equations over each region separately, the velocities and the turbulent transfer of heat and momentum are specified at the boundaries of the regions. At the centerline of the jet, symmetry implies that there is no net transfer of mass, momentum or heat:

$$v = u'v' = v'T' = 0 \quad y = 0 \quad (2.9)$$

At the boundaries between the regions the velocities are assumed to be:

$$\begin{aligned} u'w' &= 0 \\ \left. \begin{aligned} w &= w_r & 0 < |y| < s \\ w &= w_h f(\zeta_y) & s < |y| < s + b \\ w &= 0 & s + b < |y| \end{aligned} \right\} z = -r \end{aligned} \quad (2.10)$$

$$\begin{aligned} u'v' &= 0 \\ \left. \begin{aligned} v &= \pm v_s & -r < z < \eta & (v \text{ has the sign of } y) \\ v &= \pm v_b f(\zeta_z) & -(r + h) < z < -r \\ v &= 0 & z < -(r + h) \end{aligned} \right\} |y| = s \end{aligned}$$

The internal velocities w_r , w_h , v_s , and v_b may be determined as part of the solution to the integrated governing equations but are of little interest in themselves.

The water surface is a boundary which permits no transfer of mass or momentum:

$$\left. \begin{aligned} u \frac{\partial \eta}{\partial x} + v \frac{\partial \eta}{\partial y} &= w \\ u'w' &= 0 \end{aligned} \right\} \quad z = \eta \quad (2.11)$$

The transfer of heat through the water surface is assumed to be proportional to the surface temperature rise above ambient:

$$w'T' = k(T - T_a) \quad z = \eta \quad (2.12)$$

The coefficient of heat loss, k , has units of velocity and is thus a kinematic quantity. It is related to the surface heat exchange coefficient, K , defined by Edinger (13) by:

$$k = \frac{K}{\rho c} \quad (2.13)$$

where ρ = density and c = specific heat of water. The determination of k (or K) for a particular case is discussed in a later section.

The outer boundaries of the jet is where entrainment of ambient water occurs but across which no heat is transferred. The boundary conditions are:

$$\begin{aligned} u'w' &= w'T' = 0 \\ w &= w_e - V \cos \theta \frac{dh}{dx} & 0 < |y| < s & \quad z = - (r+h) \\ w &= w_e f(\zeta_y) - V \cos \theta \frac{dh}{dx} & s < |y| < s + b & \\ & & & \quad (2.14) \end{aligned}$$

$$\begin{aligned} u'v' &= v'T' = 0 \\ v &= \frac{+v}{-v}_e + V \cos \theta \frac{db}{dx} & -r < z < \eta & \quad y = s+b \\ v &= \frac{+v}{-v}_e f(\zeta_z) + V \cos \theta \frac{db}{dx} & -(r+h) < z < -r & \end{aligned}$$

(v has the sign of y)

The velocities, w_e and v_e , are manifestations of the entrainment of ambient fluid into the turbulent region. In plane and axisymmetric non-buoyant jets, it is known that the entrainment velocity is proportional to the local center-line velocity. Note that Equation 2.8 gives $v = 0$ at $|y| = s + b$ where the boundary condition 2.14 specifies $|v| = v_e$. This is because the entrainment velocity v_e is an order of magnitude less than the spreading velocity v and its contribution to the integration of equation (2.3) is assumed to be balanced by the turbulent terms, which were neglected in the y equation. Ellison and Turner (8) have demonstrated that the vertical entrainment is a function of the gross Richardson number, $\frac{\beta g \Delta T_c h}{u_c^2}$, in two-dimensional jets. In this study the entrainment velocities are assumed to be given by

$$\begin{aligned} \frac{v_e}{u_c} &= \alpha_y \\ \frac{w_e}{u_c} &= \alpha_z \exp \left\{ -C \frac{\beta g \Delta T_c h}{u_c^2} \right\} \end{aligned} \quad (2.15)$$

Ellison and Turner's data indicate a value of $C = 5.0$ as appropriate. The entrainment coefficients, α_y and α_z , are to be determined such that the solution for the non-buoyant case ($T_o = T_a$) agrees with the experimental observations that the growth of a non-buoyant turbulent region is symmetrical:

$$\frac{db}{dx} = \frac{dh}{dx} = \epsilon \quad (2.16)$$

$$\frac{ds}{dx} = \frac{dr}{dx}$$

For non-buoyant jets discharging into a quiescent receiving water the spreading rate, ϵ_o , is constant. In these cases, Abramovich gives $\epsilon_o = .22$ for the similarity functions, f and t , used here.

The boundary condition at $x = 0$ is related to the discharge channel geometry, the flow rate Q_o , and the initial discharge temperature T_o .

$$\left. \begin{aligned} r &= h_o \\ s &= b_o \\ h &= b = 0 \\ u &= u_o = \frac{Q_o}{2h_o b_o} + V \cos \theta_o \\ \Delta T_c &= \Delta T_o \\ \theta &= \theta_o \\ \tilde{x} &= \tilde{y} = 0 \end{aligned} \right\} \quad x = 0 \quad (2.17)$$

2.3 Integration of the Equations

With the velocity and temperature distributions and boundary conditions stated in the previous section, the equations of motion may be integrated over the y-z cross section of the jet. The x momentum and mass conservation equations are integrated over each of the four possible jet regions on each side of the centerline plane. (Integration over both sides of the jet results in redundant equations because of the assumed symmetry.) This yields eight equations. The y-momentum and heat equations are integrated over the entire half-jet cross-section, yielding two more equations. With this choice of integrating limits, the terms in the integrated y-equation represent a balance between the lateral gravitational force and the lateral spreading of the discharge. Another equation is generated from the y-equation by integrating it over the entire cross section of the jet on both sides of the centerline. In this case the lateral spreading terms all drop out, being anti-symmetrical, and the remaining terms give the rate of deflection of the jet in the presence of a cross current. The equation set, completed by a simple geometrical relationship between the coordinates (x,y) referred to the jet centerline and the fixed centerline coordinates (\tilde{x}, \tilde{y}) is given in Table 2.1. Further details in the derivation of these equations are given in Stolzenbach and Harleman (15).

Region 1: continuity $rs \frac{d}{dx} [u_c + V\cos\theta] + rv_s - sw_r = 0$

Region 2: continuity $s \left[\frac{d}{dx} [h(u_c I_1 + V\cos\theta)] + (u_c + V\cos\theta) \frac{dr}{dx} + w_r - \alpha_{sz} u_c \right] + v_b h I_1 = 0$

Region 3: continuity $r \left[\frac{d}{dx} [b(u_c I_1 + V\cos\theta)] + (u_c + V\cos\theta) \frac{ds}{dx} - v_s + \alpha_y u_c \right] - w_r b I_1 = 0$

Region 4: continuity $\frac{d}{dx} \left[hb(u_c I_1^2 + V\cos\theta) \right] + (u_c I_1 + V\cos\theta) \left[b \frac{dr}{dx} + h \frac{ds}{dx} \right] + (w_h - \alpha_{sz} u_c) I_1 b - (v_b - \alpha_y u_c) I_1 h = 0$

Region 1: x momentum $(u_c + V\cos\theta) [2rs \frac{d}{dx} [u_c + V\cos\theta] + rv_s - sw_r] + \beta g s \left[\frac{d}{dx} (\Delta T_c \frac{r^2}{2}) + I_3 r \frac{d}{dx} (\Delta T_c h) \right] = 0$

Region 2: x momentum $s \left[\frac{d}{dx} [h (u_c^2 I_2 + 2V\cos\theta u_c I_1 + V^2 \cos^2 \theta)] + [u_c + V\cos\theta]^2 \frac{dr}{dx} + w_r [u_c + V\cos\theta] - \alpha_{sz} u_c V\cos\theta + \beta g \left[I_4 \frac{d\Delta T_c h^2}{dx} + I_3 \Delta T_c h \frac{dr}{dx} \right] \right] + v_b h (u_c I_2 + V\cos\theta I_1) = 0$

Table 2.1 Integrated Equations for Deflected Buoyant Jets

$$\begin{aligned}
 \text{Region 3: } x \text{ momentum } & r \left[\frac{d}{dx} [b(u_c^2 I_2 + 2V \cos \theta u_c I_1 + V^2 \cos^2 \theta)] + [u_c + V \cos \theta]^2 \frac{ds}{dx} - \right. \\
 & v_s [u_c + V \cos \theta] + \alpha_y u_c V \cos \theta \left. \right] - w_h b [u_c I_2 + V \cos \theta I_1] + \beta g \left[\frac{I_3}{2} \frac{d\Delta T_c b r^2}{dx} \right. \\
 & \left. + I_3^2 r \frac{d\Delta T_c b h}{dx} + \Delta T_c \left(\frac{r^2}{2} + I_3 h r \right) \frac{ds}{dx} \right] = 0
 \end{aligned}$$

$$\begin{aligned}
 \text{Region 4: } x \text{ momentum } & \frac{d}{dx} [h b (u_c^2 I_2^2 + 2V \cos \theta u_c I_1^2 + V^2 \cos^2 \theta)] + [u_c^2 I_2 + 2V \cos \theta u_c I_1 + V^2 \cos^2 \theta] \\
 & \left[b \frac{dr}{dx} + h \frac{ds}{dx} \right] + [w_h b - v_b h] [u_c I_2 + V \cos \theta I_1] - u_c I_1 [\alpha_{sz} b - \alpha_y h] V \cos \theta \\
 & + \beta g \left[I_3 I_4 \frac{d\Delta T_c h^2 b}{dx} + I_4 \Delta T_c h^2 \frac{ds}{dx} + I_3^2 \Delta T_c h b \frac{dr}{dx} \right] = 0
 \end{aligned}$$

$$\begin{aligned}
 \text{Jet } y \text{ momentum } & \frac{d}{dx} \left[\frac{db}{dx} - \epsilon \right] [u_c^2 b I_6 (r + h I_2) + 2V \cos \theta u_c b I_5 (r + h I_1) + V^2 \cos^2 \theta b (r + h)] \\
 & - \beta g \Delta T_c \left(\frac{r^2}{2} + I_3 r h + I_4 h^2 \right) = 0
 \end{aligned}$$

Table 2.1 (cont'd) Integrated Equations for Deflected Buoyant Jets

$$\text{Jet Heat} \quad \frac{d}{dx} \left[u_c \Delta T_c (s + bI_7) (r + hI_7) + V \cos \theta \Delta T_c (s + bI_3) (r + hI_3) \right]$$

$$+ k \Delta T_c (s + bI_3) = 0$$

$$\text{Jet Bending} \quad \left[u_c^2 (s + bI_2) (r + hI_2) + 2V \cos \theta u_c (s + bI_1) (r + hI_1) + \right. \\ \left. V^2 \cos^2 \theta (s + b) (r + h) \right] \frac{d\theta}{dx} - u_c V \sin \theta \left[-\alpha_{sz} (s + bI_1) + \alpha_y (r + hI_1) \right] = 0$$

$$\text{Jet x position} \quad \frac{d\tilde{x}}{dx} - \sin \theta = 0$$

$$\text{Jet y position} \quad \frac{d\tilde{y}}{dx} - \cos \theta = 0$$

$$I_1 = \int_0^1 f(\zeta) d\zeta = \int_0^1 (1 - \zeta^{3/2})^2 d\zeta = .4500$$

$$I_4 = \int_0^1 \int_{\zeta}^1 t(\zeta) d\zeta d\zeta = \int_0^1 \int_{\zeta}^1 (1 - \zeta^{3/2}) d\zeta d\zeta = .2143$$

$$I_2 = \int_0^1 f^2(\zeta) d\zeta = \int_0^1 (1 - \zeta^{3/2})^4 d\zeta = .3160$$

$$I_5 = \int_0^1 f(\zeta) \zeta^{1/2} d\zeta = \int_0^1 (1 - \zeta^{3/2})^2 \zeta^{1/2} d\zeta = .2222$$

$$I_3 = \int_0^1 t(\zeta) d\zeta = \int_0^1 (1 - \zeta^{3/2}) d\zeta = .6000$$

$$I_6 = \int_0^1 f^2(\zeta) \zeta^{1/2} d\zeta = \int_0^1 (1 - \zeta^{3/2})^4 \zeta^{1/2} d\zeta = .1333$$

$$I_7 = \int_0^1 f(\zeta) t(\zeta) d\zeta = \int_0^1 (1 - \zeta^{3/2})^3 d\zeta = .3680$$

Table 2.1 (cont'd) Integrated Equations for Deflected Buoyant Jets

The values of the non-buoyant ($\Delta T_o = 0$) entrainment coefficients which satisfy equations 2.16 in addition to Table 2.1 are:

$$\begin{aligned}
 \alpha_y &= -(I_1 - I_2) \varepsilon_o & \text{for} & \quad s > 0 \\
 \alpha_y &= -\frac{I_1 \varepsilon_o}{2} & \text{for} & \quad s = 0 \\
 \alpha_z &= (I_1 - I_2) \varepsilon_o & \text{for} & \quad r > 0 \\
 \alpha_z &= \frac{I_1 \varepsilon_o}{2} & \text{for} & \quad r = 0
 \end{aligned}
 \tag{2.18}$$

where I_1 and I_2 are integration constants as given in Table 2.1.

2.4 Solution of the Equations

The thirteen equations in Table 2.1 are a first order system of dimensional differential equations in x for the variables: u_c , ΔT_c , h , b , r , s , θ , \tilde{x} , \tilde{y} , v_s , v_b , w_r , and w_h . The actual solution proceeds first by writing the equations in a dimensionless form by normalizing each variable by the characteristic values: u_o , $\Delta T_o = T_o - T_a$, and $\sqrt{h_o b_o}$. The solution is then determined by the following dimensionless parameters:

$$F_o = \frac{u_o}{\sqrt{\beta g \Delta T_o h_o}} = \text{initial densimetric Froude number}$$

$$A = h_o / b_o = \text{aspect ratio}$$

$$k/u_o = \text{heat loss parameter}$$

$$V/u_o = \text{cross flow parameter}$$

The computer program which solves the equations is described in Section IV along with instructions for its use. The output consists of values of u/u_o , $\Delta T_c / \Delta T_o$, $h/\sqrt{h_o b_o}$, $b/\sqrt{h_o b_o}$, $r/\sqrt{h_o b_o}$, $s/\sqrt{h_o b_o}$, θ , $\tilde{x}/\sqrt{h_o b_o}$ & $\tilde{y}/\sqrt{h_o b_o}$ as a function of $x/\sqrt{h_o b_o}$. In addition to these variables which describe the jet structure (u_c , ΔT_c , . . . , etc.) other interesting dependent quantities which are functions of x may be defined. In the buoyant jet the vertical entrainment is a function of the local densimetric Froude number (an inverse Richardson number), F_L :

$$F_L = \frac{u_c}{\sqrt{\beta g \Delta T_c h}} \quad (2.19)$$

where u_c , ΔT_c , and h are local values at a given distance from the origin. The total flow in the jet may be determined by integrating the x velocity, u , over the jet cross section. The ratio of the flow at a given x to the initial flow is the jet dilution, D , or Q as labeled by the output,

$$D = \frac{u_c (r + I_1 h) (s + I_1 b) + V \cos \theta (r + h) (s + b)}{(u_o + V \cos \theta_o) h_o b_o} \quad (2.20)$$

Similarly the effect of surface heat loss may be evaluated by calculating the ratio of convected excess heat flow in the jet to the initial excess heat flow, HT .

$$HT = \frac{u_c \Delta T_c (r + I_1 h) (s + I_1 b) + V \cos \theta \Delta T_c (r + h) (s + b)}{\Delta T_o (u_o + V \cos \theta_o) h_o b_o} \quad (2.21)$$

Finally a dimensionless time of travel along the jet centerline from the end of the discharge channel to x is computed.

$$TM = \frac{u_o}{\sqrt{h_o b_o}} \int_o^x \frac{dx}{u_c} \quad (2.22)$$

The structure of a heated surface discharge is shown for a particular theoretical calculation in Figures 2.3 and 2.4. The main features are:

- 1) A core region in which the centerline velocity is constant and the centerline temperature rise decreases very slightly. The dilution, D , and the local densimetric Froude number, F_L , do not vary greatly in this region. The magnitude of F_L is much larger than F_o because the initial depth of the turbulent region, h , is zero. There is no significant surface heat loss in the core region.

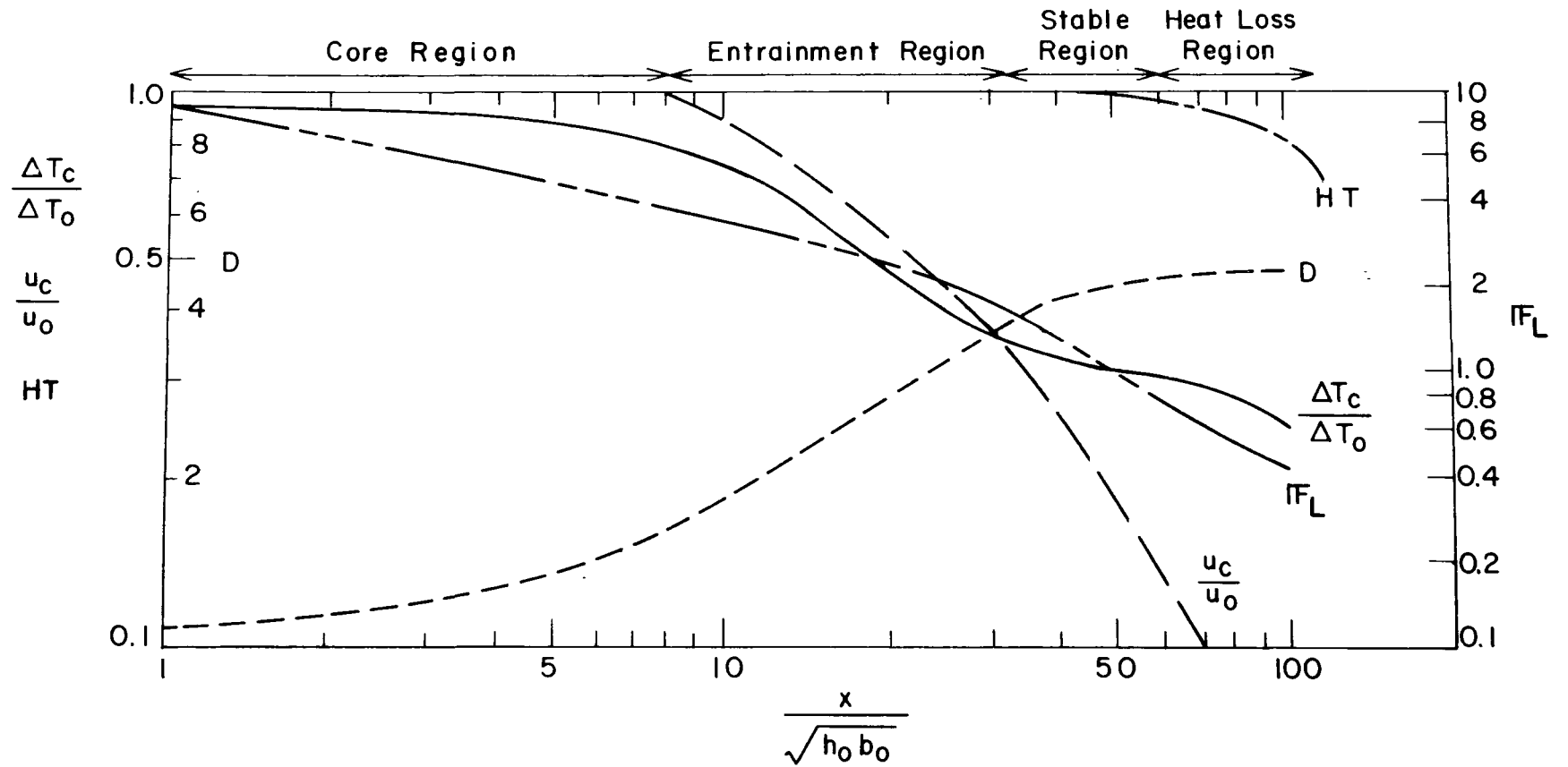


Fig. 2.3 Calculated Surface Discharge Parameters : $IF_0 = 4.4$, $A = 0.35$, $k/u_0 = 4.2 \times 10^{-5}$, $V/u_0 = 0$

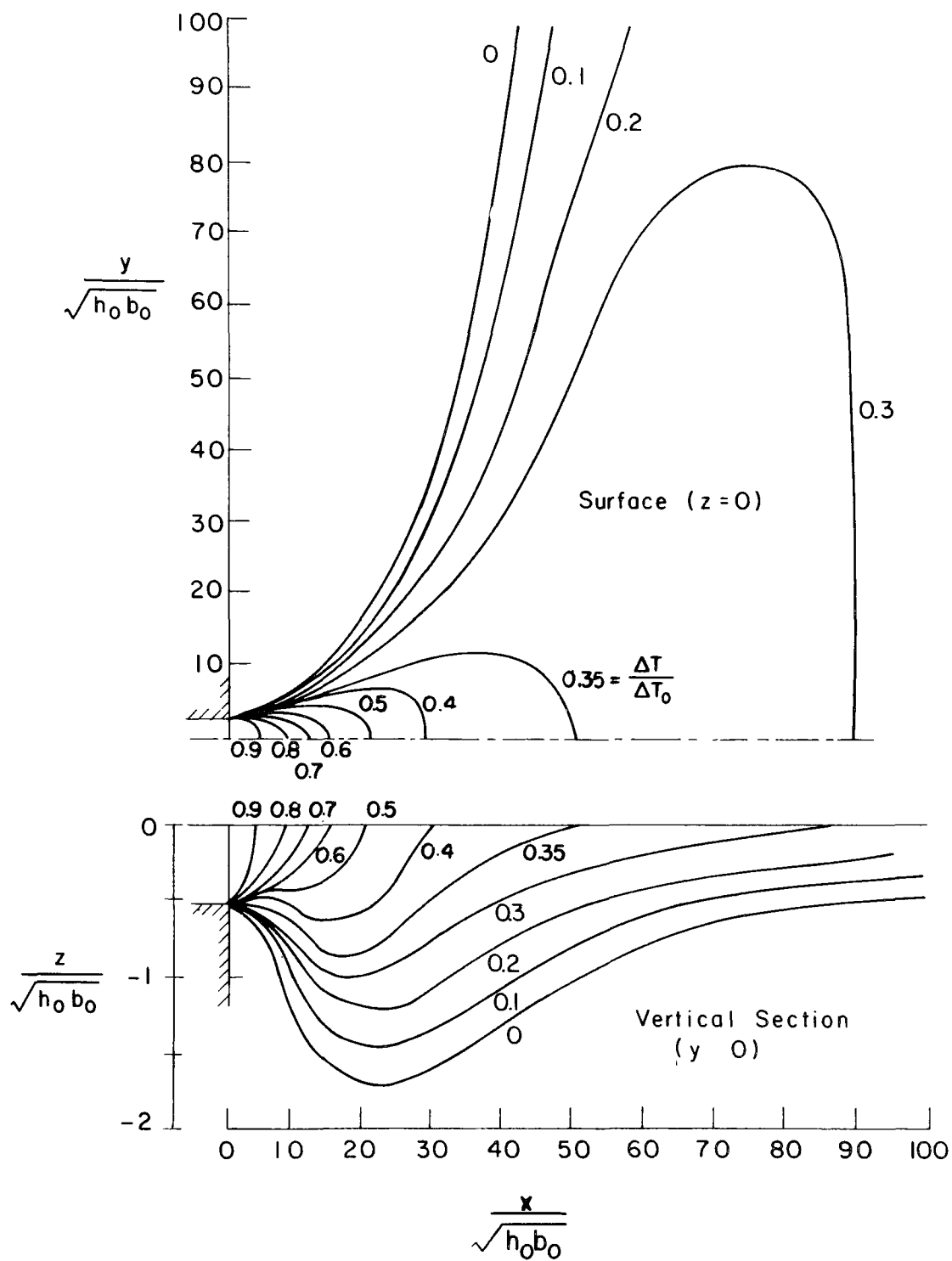


Fig. 2.4 Calculated Isotherms of $\Delta T / \Delta T_0$: $Pr_0 = 4.4$, $A = 0.35$, $k/u_0 = 4.2 \times 10^{-5}$, $V/u_0 = 0$

- 2) An entrainment region in which the centerline velocity and temperature drop sharply, approximately as $1/x$, as in a non-buoyant jet. The jet spreads vertically by turbulent processes. The lateral growth is dominated by gravitational spreading at a much greater rate than the vertical turbulent spread. Because of this large ratio of lateral to vertical spread, the jet reaches a maximum depth beyond which the bottom boundary rises to maintain mass conservation (see Figure 2.4). Local densimetric Froude numbers in this region decrease rapidly and the dilution rises sharply as a result of entrainment (see Figure 2.3). Surface heat loss remains negligible in this region, i.e., $HT = 1.0$.
- 3) A stable region in which vertical entrainment is inhibited by vertical stability as indicated by the local densimetric Froude number which is of order one or less. The jet depth continues to decrease because of lateral spreading. The small jet depths reduce the lateral entrainment, and the dilution and centerline temperature remain relatively constant in this region. The centerline velocity, however, drops sharply as a consequence of the large lateral spread. The surface temperature pattern is dominated by the wide, constant temperature stable region.
- 4) A heat loss region marking the end of the stable region. The lateral spread is sufficiently large to allow significant surface heat transfer and the temperature begins to fall again. Once surface heat loss becomes significant, the rate of temperature decrease is very rapid. However, at this point the centerline velocity is so low that the discharge may no longer be considered as a jet. In general it may be stated that surface heat loss, as determined by the value of k/u_o , is not an important factor in reducing the discharge temperature within the region of jet-like entrainment. Beyond the stable region, temperature distribution is controlled by passive diffusion processes acting upon the buoyant plume.

- 5) The primary effect of a current in the receiving water is to deflect the discharge without significantly affecting the dilution processes up to the point where the jet centerline velocity excess, u_c , is reduced to the magnitude of the cross current component in the centerline direction. For $u_c \leq V \cos \theta$ the ambient water may have a turbulence level comparable to the discharge turbulence and the basic assumptions of the theory will not be valid. This region is properly considered part of the far field.

The dilution and corresponding centerline temperature achieved in the stable region are of interest since the stable region constitutes a significant portion of the surface temperature distribution. Figure 2.5 is a plot of the dilution and surface temperature in the stable region as a function of IF_o with values of A indicated. It is clear that the ultimate stable dilution in a buoyant jet depends primarily upon IF_o and to a lesser extent upon A .

The maximum depth of the discharge, $h_{\max}/\sqrt{h_o b_o}$, is also of interest and may be determined from the theoretical calculations. Figure 2.6 indicates that the maximum vertical penetration of the jet is a function of IF_o with a very small dependence upon A .

For quick calculation involving the maximum jet penetration, centerline dilution, or centerline temperature rise, the results from Figure 2.5 and 2.6 can be condensed into three simplified formulas involving a new parameter, IF'_o , defined by

$$IF'_o = IF_o A^{1/4} = \frac{u_o}{\sqrt{g \left(\frac{\Delta \rho_o}{\rho_a} \right) (h_o b_o)^{1/2}}} \quad (2.23)$$

IF'_o is merely a "Froude number" whose characteristic length is the scaling length, $(h_o b_o)^{1/2}$, rather than a depth. The numerical results of Figures 2.5 and 2.6 are then approximated by

$$\left(\frac{\Delta T_o}{\Delta T_{c_s}} \right) = \sqrt{(IF'_o)^2 + 1} \approx IF'_o \quad (\text{for } IF'_o > 3) \quad (2.24)$$

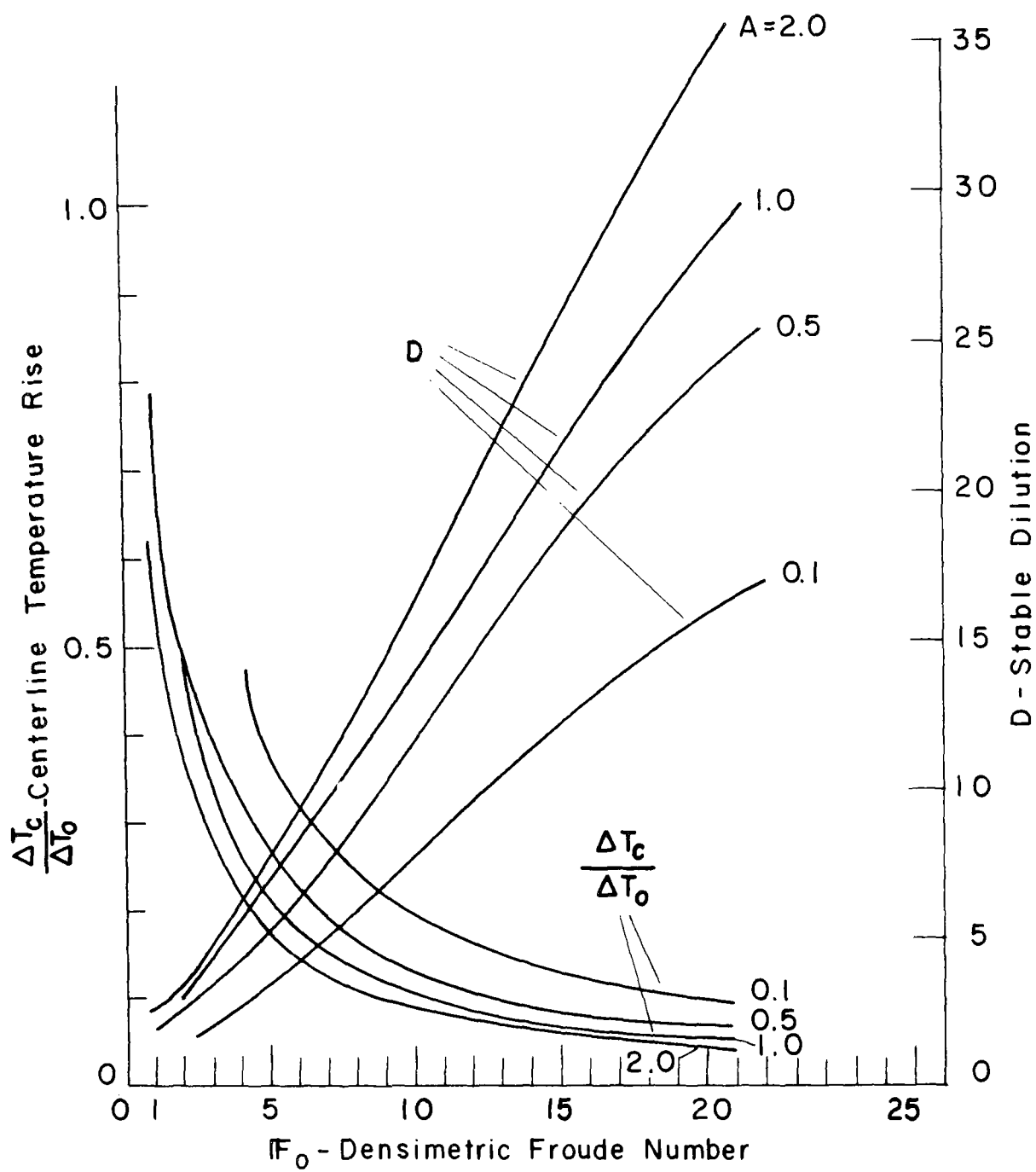


Fig. 2.5 Centerline Temperature Rise $\Delta T_c / \Delta T_0$ and Dilution, D , in the Stable Region for $k/u_0 = V/u_0 = 0$.

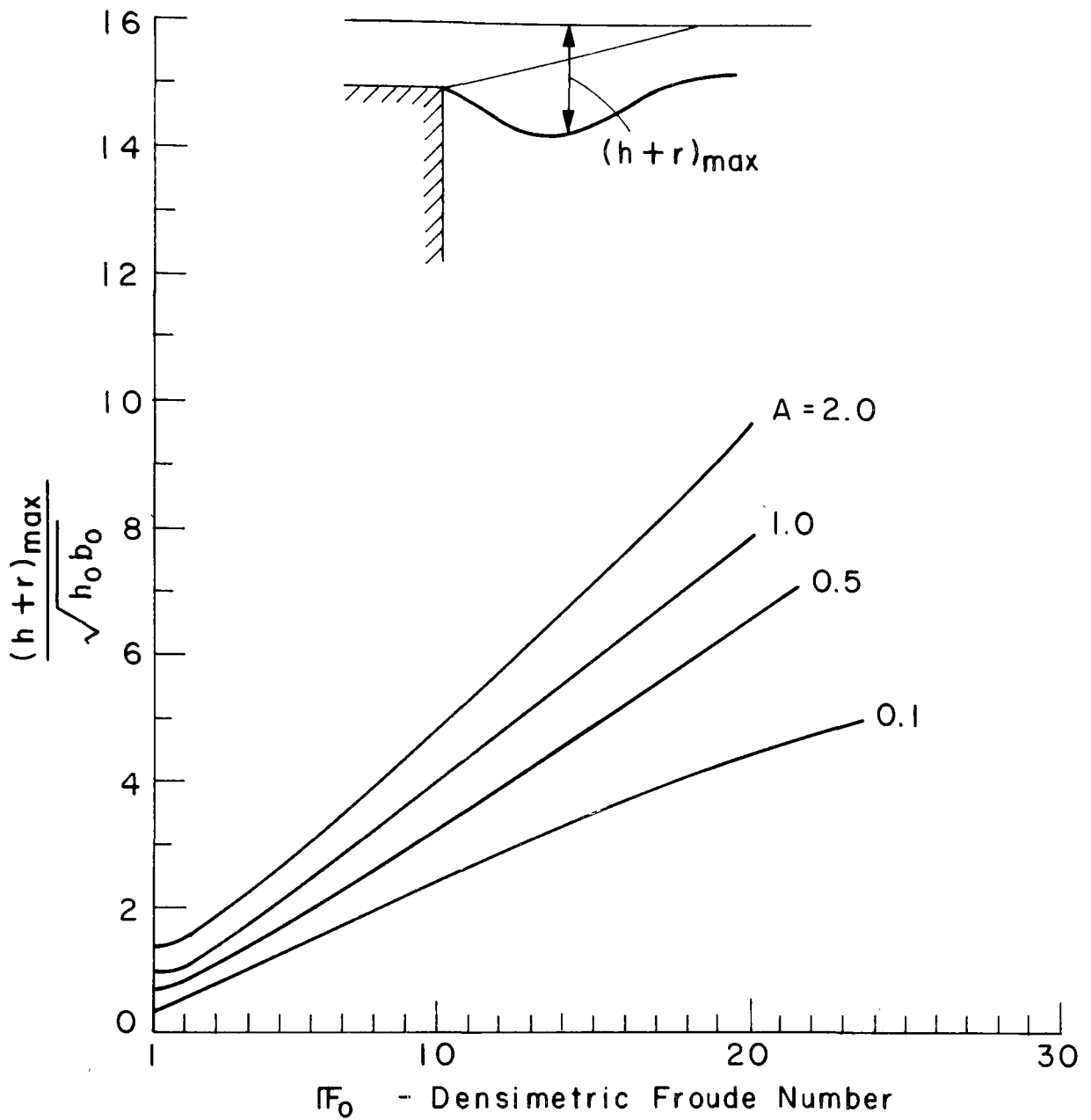


Fig. 2.6 Maximum Vertical Depth of the Jet, $\frac{(h+r)_{\max}}{\sqrt{h_0 b_0}}$
for $k/u_0 = V/u_0 = 0$

$$D_{\text{stable}} = 1.4 \sqrt{(F'_0)^2 + 1} \approx 1.4 F'_0 \text{ (for } F'_0 > 3) \quad (2.25)$$

$$\frac{(h + r)_{\text{max}}}{(h_0 b_0)^{1/2}} = 0.42 F'_0 \quad (2.26)$$

For $F'_0 > 3$, $h_{\text{max}} = (h + r)_{\text{max}}$ and (2.26) reduces to

$$\frac{h_{\text{max}}}{(h_0 b_0)^{1/2}} = 0.42 F'_0 \quad (2.27)$$

Equations 2.24 and 2.25 relate to properties of the jet in the stable region (stable centerline temperature rise and stable dilution respectively) and (2.26) relates to a maximum property of the jet. For the spatial history of the discharge or for information relating to lateral spreading or centerline deflection under a current, use of the generalized plots of the theoretical solution is suggested. Figures 2.7a to 2.7i give the basic calculated discharge properties for a range of values of F'_0 , A , and V/u_0 with k/u_0 set equal to zero. As discussed previously, a non-zero value of k/u_0 will have only secondary effect upon the temperature distribution and setting $k/u_0 = 0$ will always yield a slightly conservative result (i.e. higher temperatures). The next two chapters discuss the computer program and its application to actual discharge design.

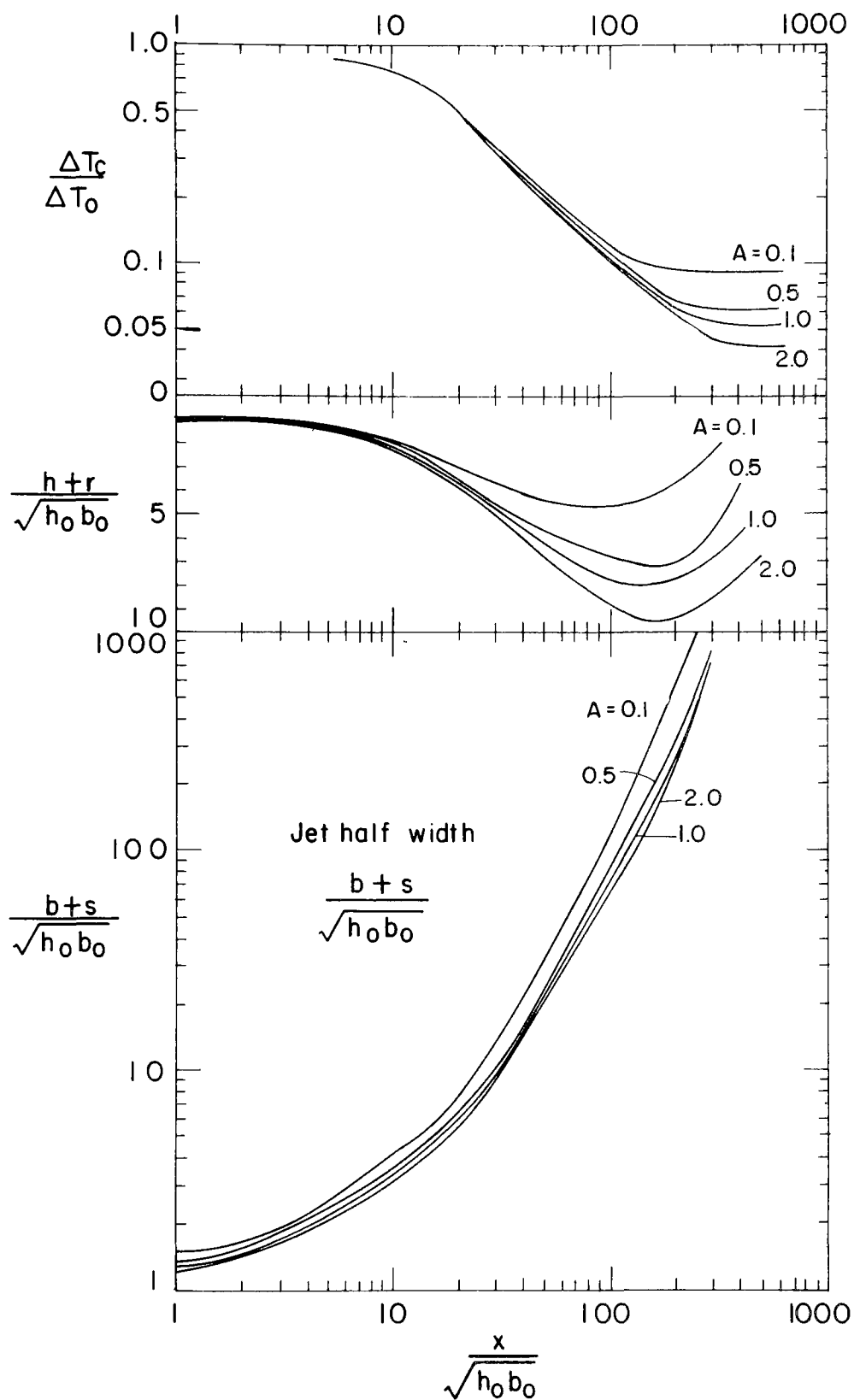


Fig. 2.7a Jet Parameters for $Pr_0 = 20.0$, $V/u_0 = 0$, $k/u_0 = 0$

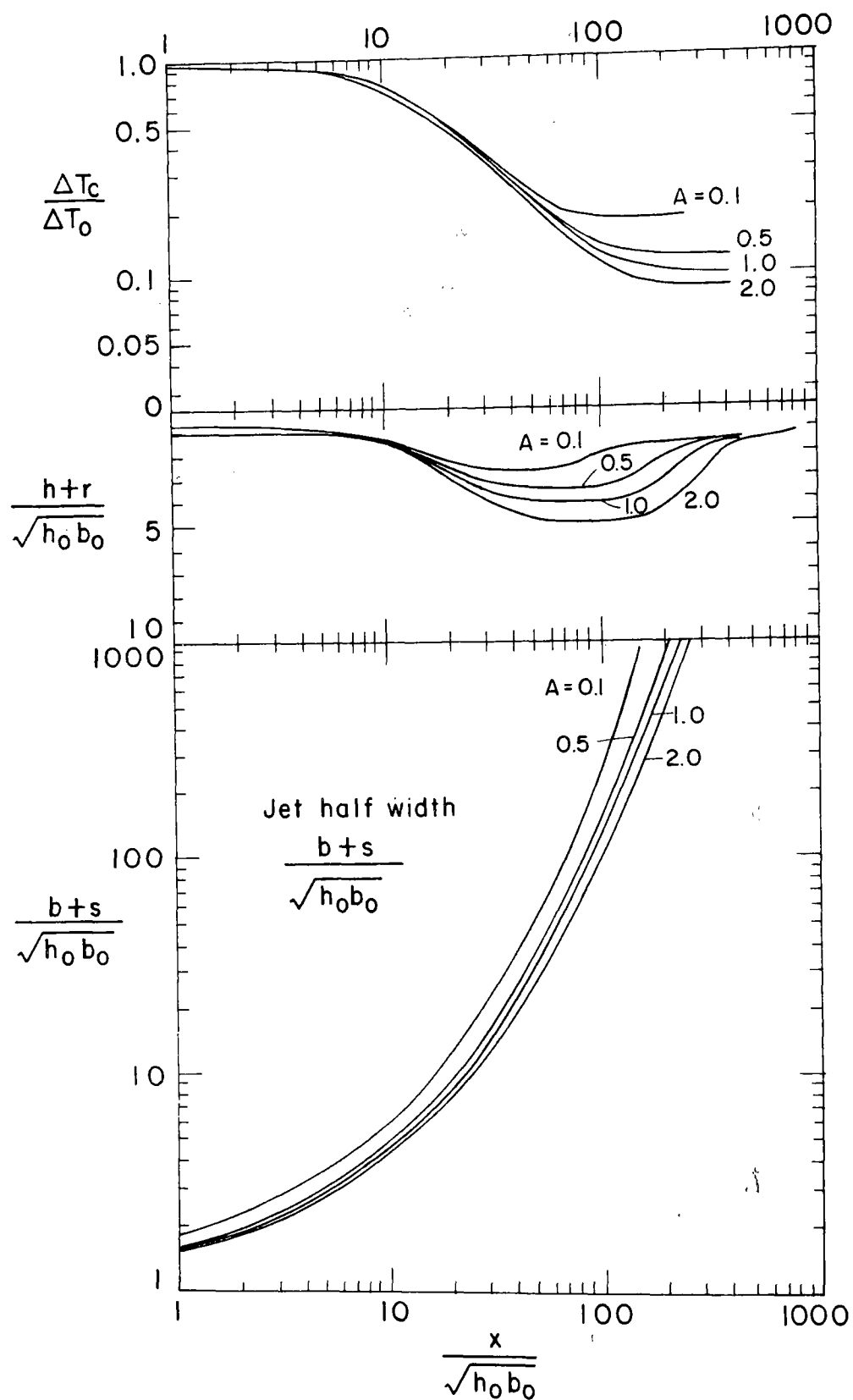


Fig. 2.7b Jet Parameters for $Pr_0 = 10.0$, $V/u_0 = 0$, $k/u_0 = 0$

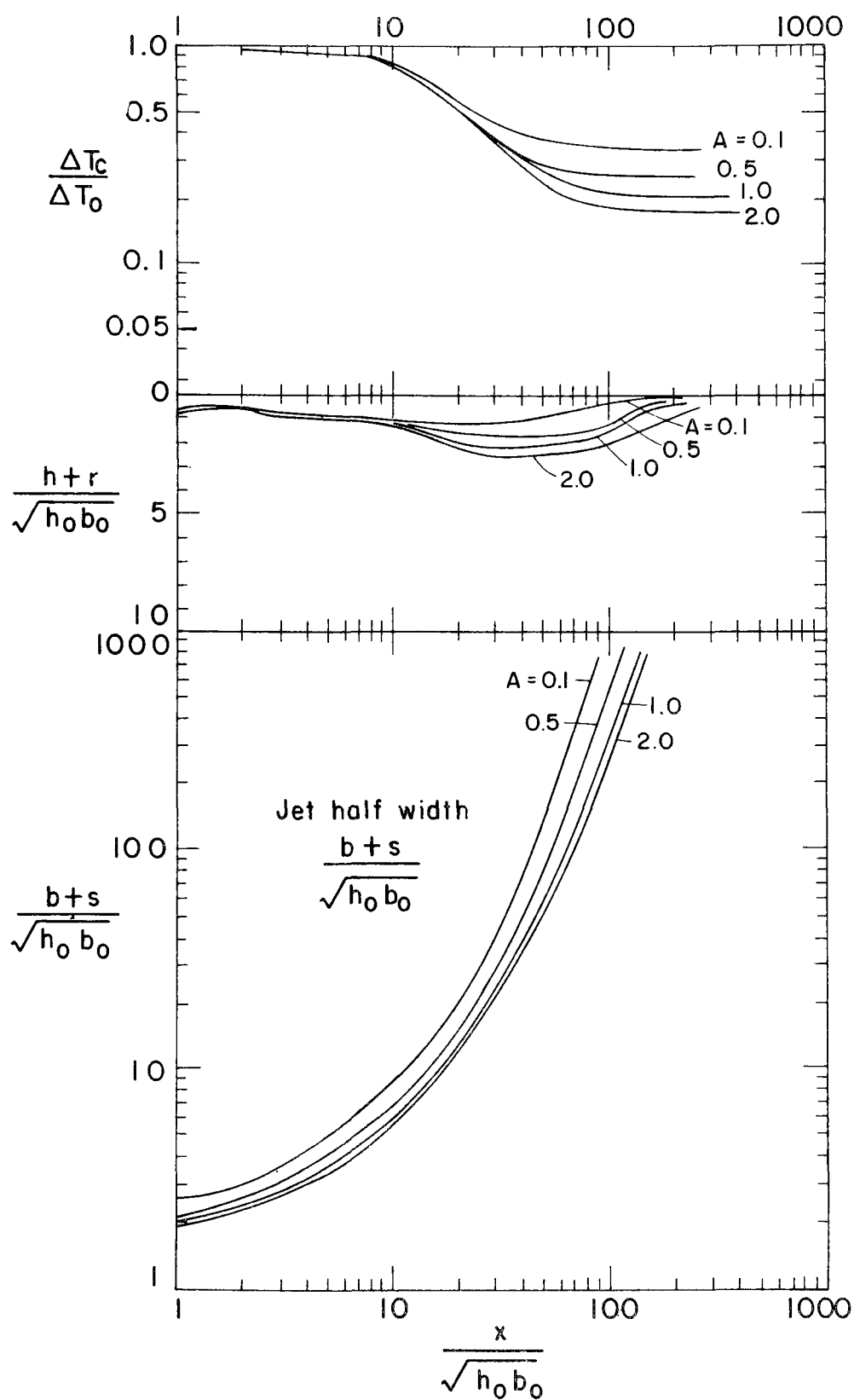


Fig. 2.7c Jet Parameters for $F_0 = 5.0$, $V/u_0 = 0$, $k/u_0 = 0$

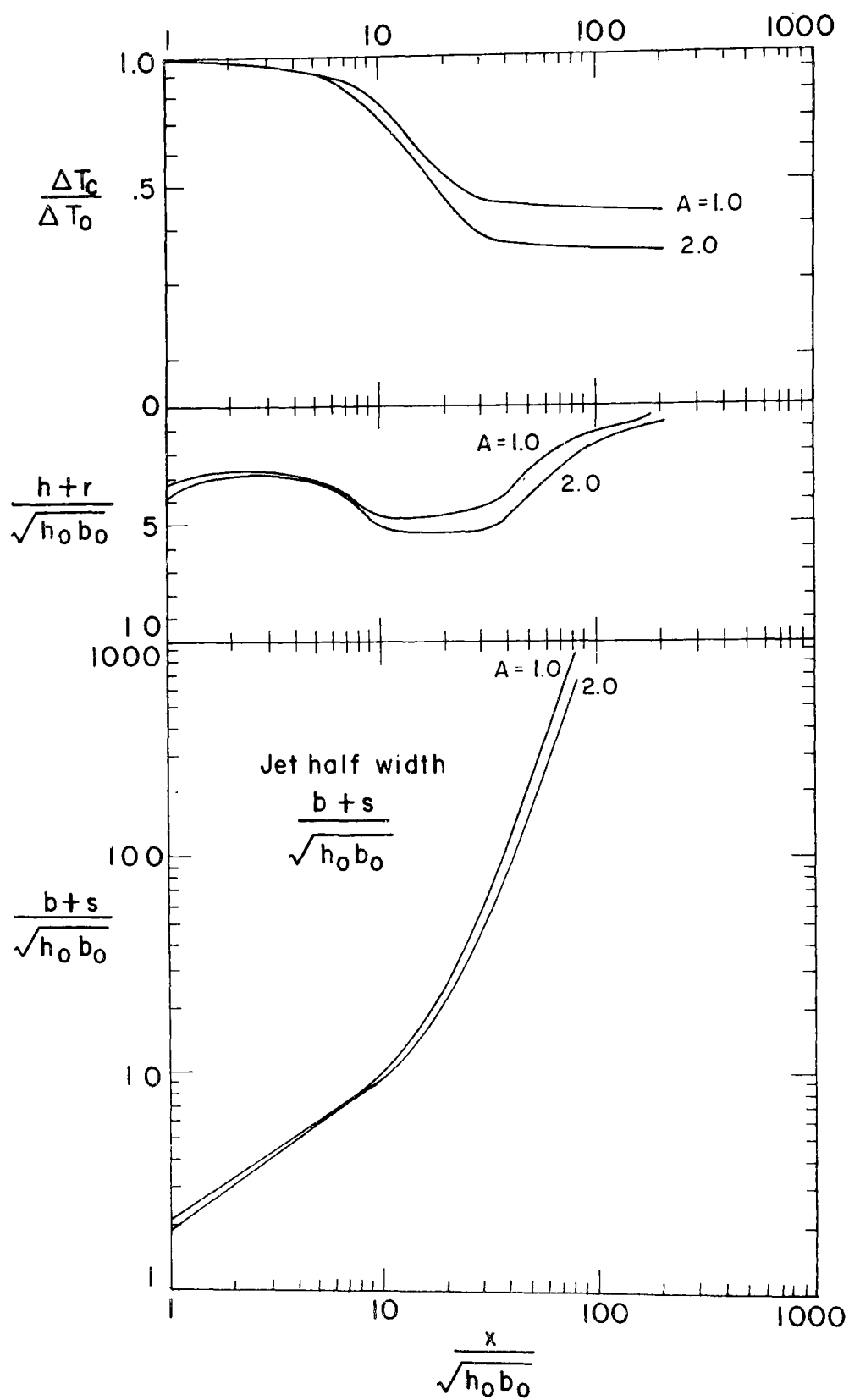


Fig. 2.7 d Jet Parameters for $W_0 = 2.0$, $V/u_0 = 0$, $k/u_0 = 0$

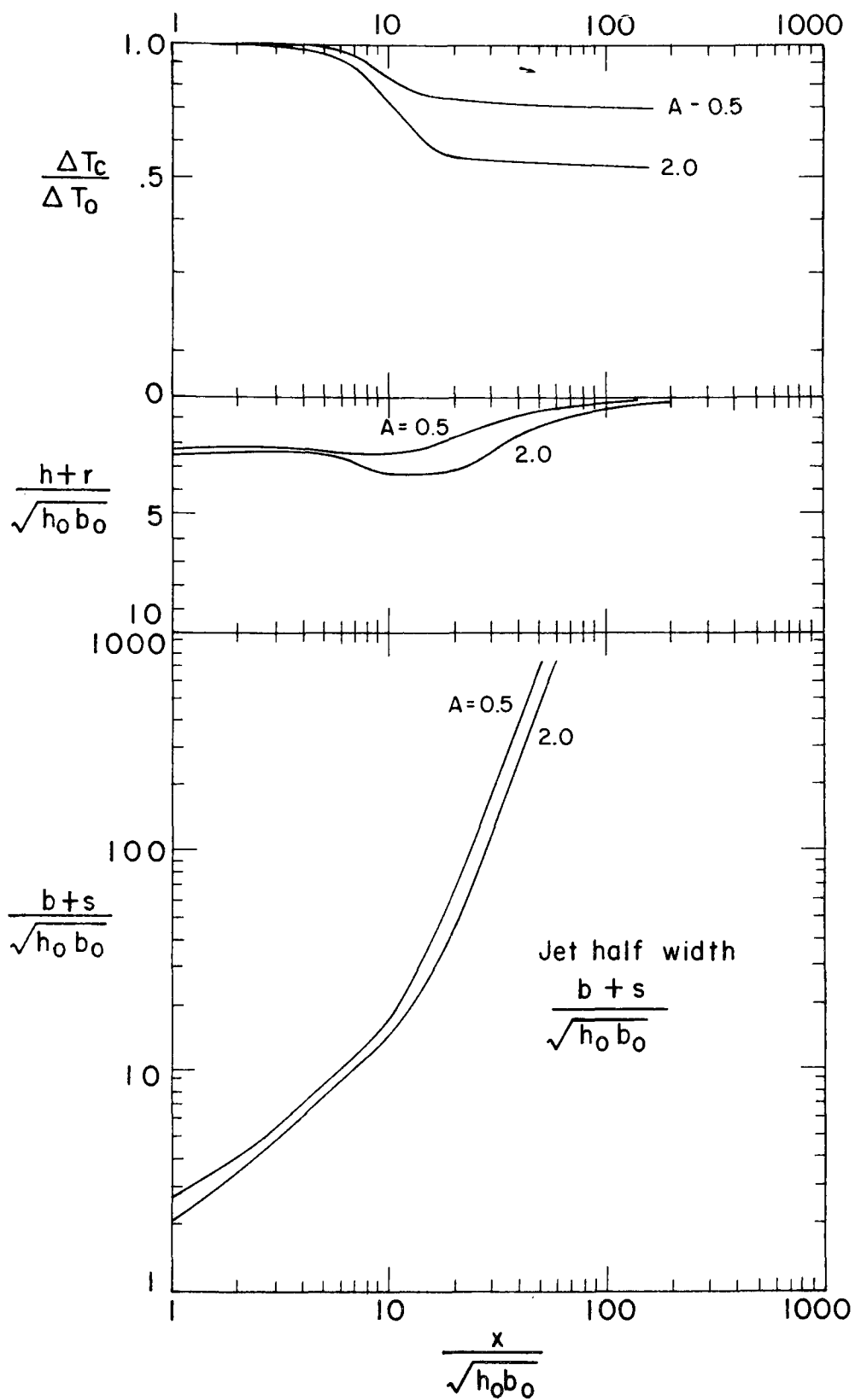


Fig. 2.7e Jet Parameters for $Fr_0 = 1.0$, $V/u_0 = 0$, $k/u_0 = 0$

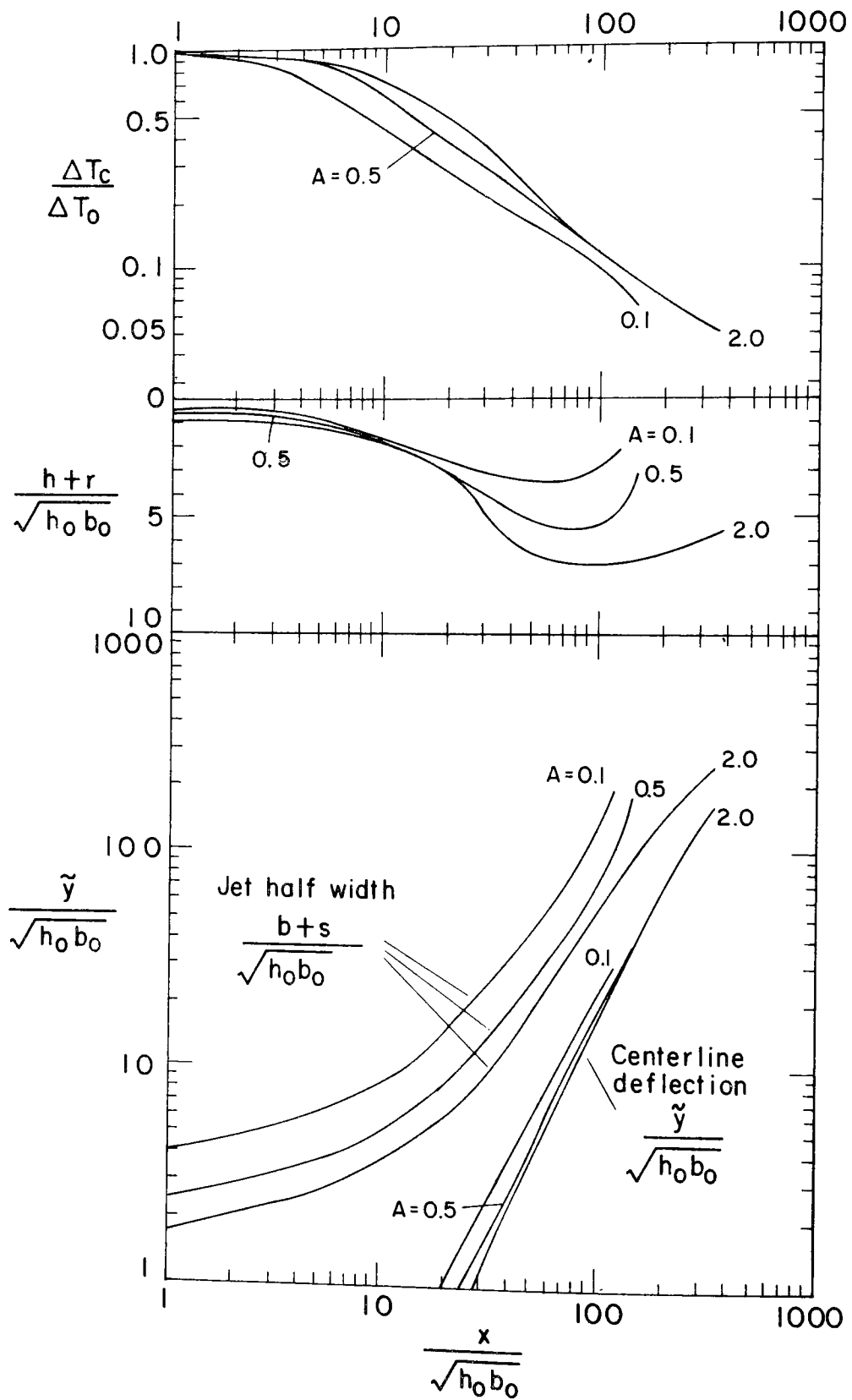


Fig. 2.7 f Jet Parameters for $Fr_0 = 20.0$, $V/u_0 = 0.025$, $k/u_0 = 0$

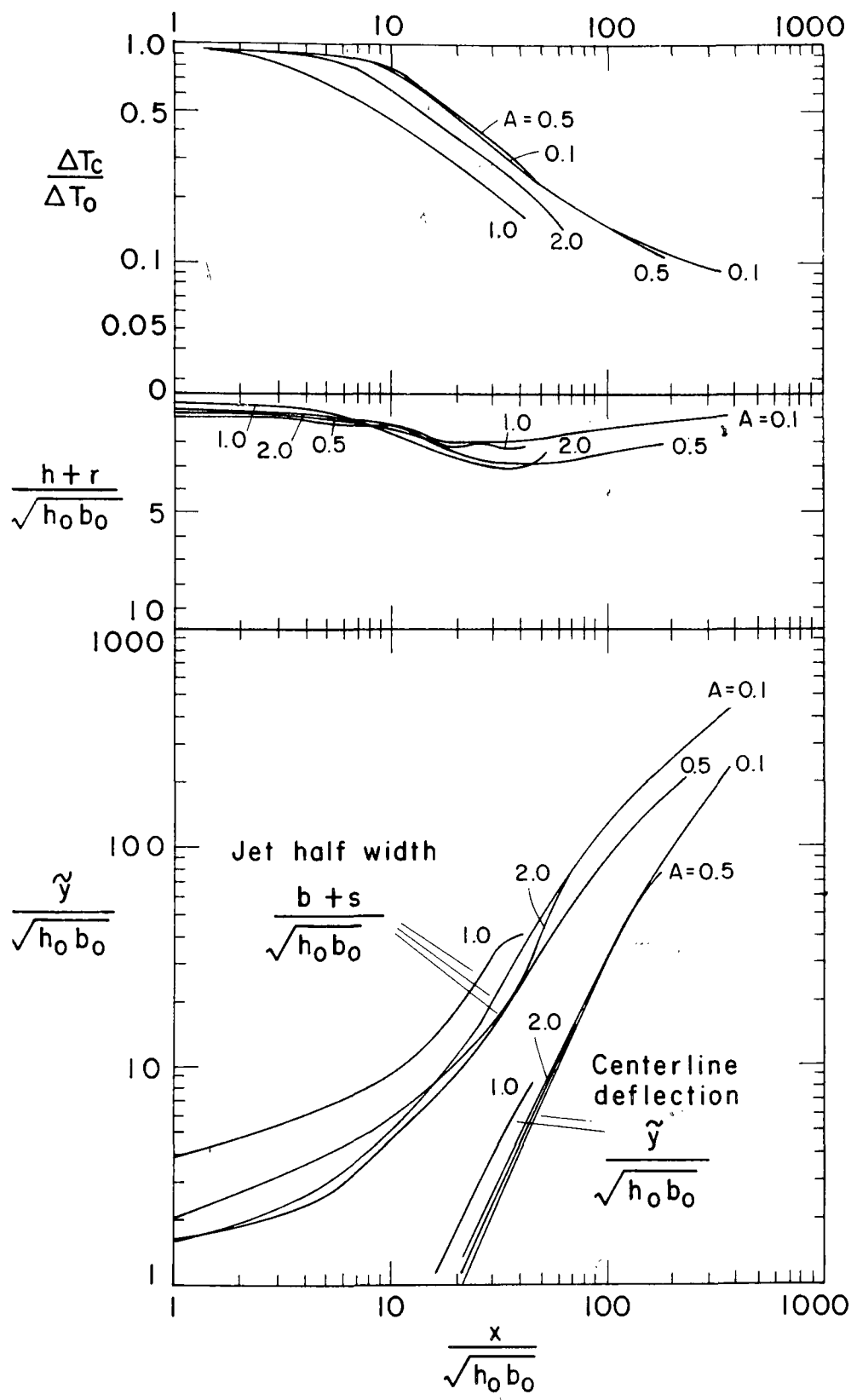


Fig. 2.7g Jet Parameters for $Fr_0 = 10.0$, $V/u_0 = 0.05$, $k/u_0 = 0$

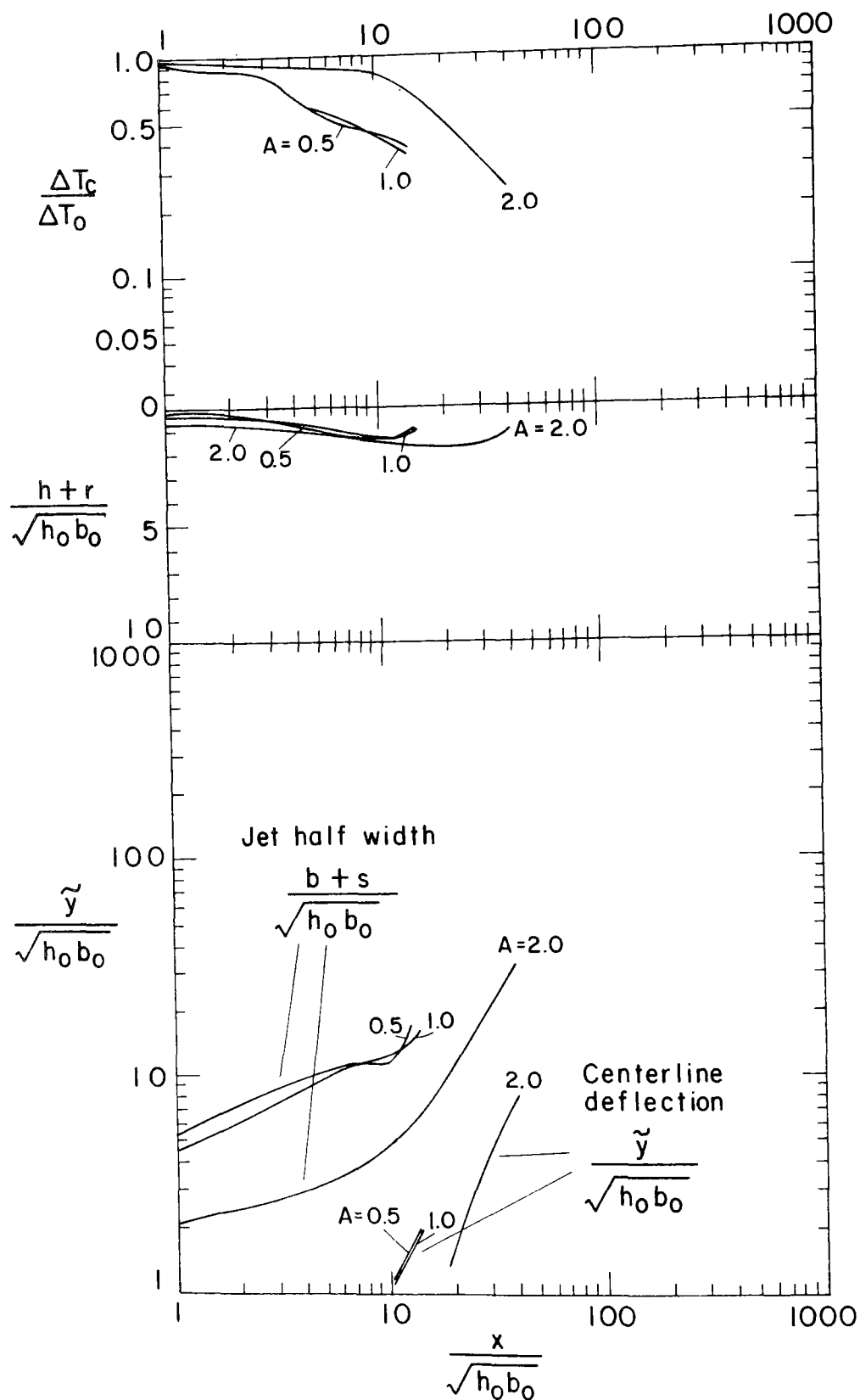


Fig. 2.7h Jet Parameters for $W_0 = 5.0$, $V/u_0 = 0.1$, $k/u_0 = 0$

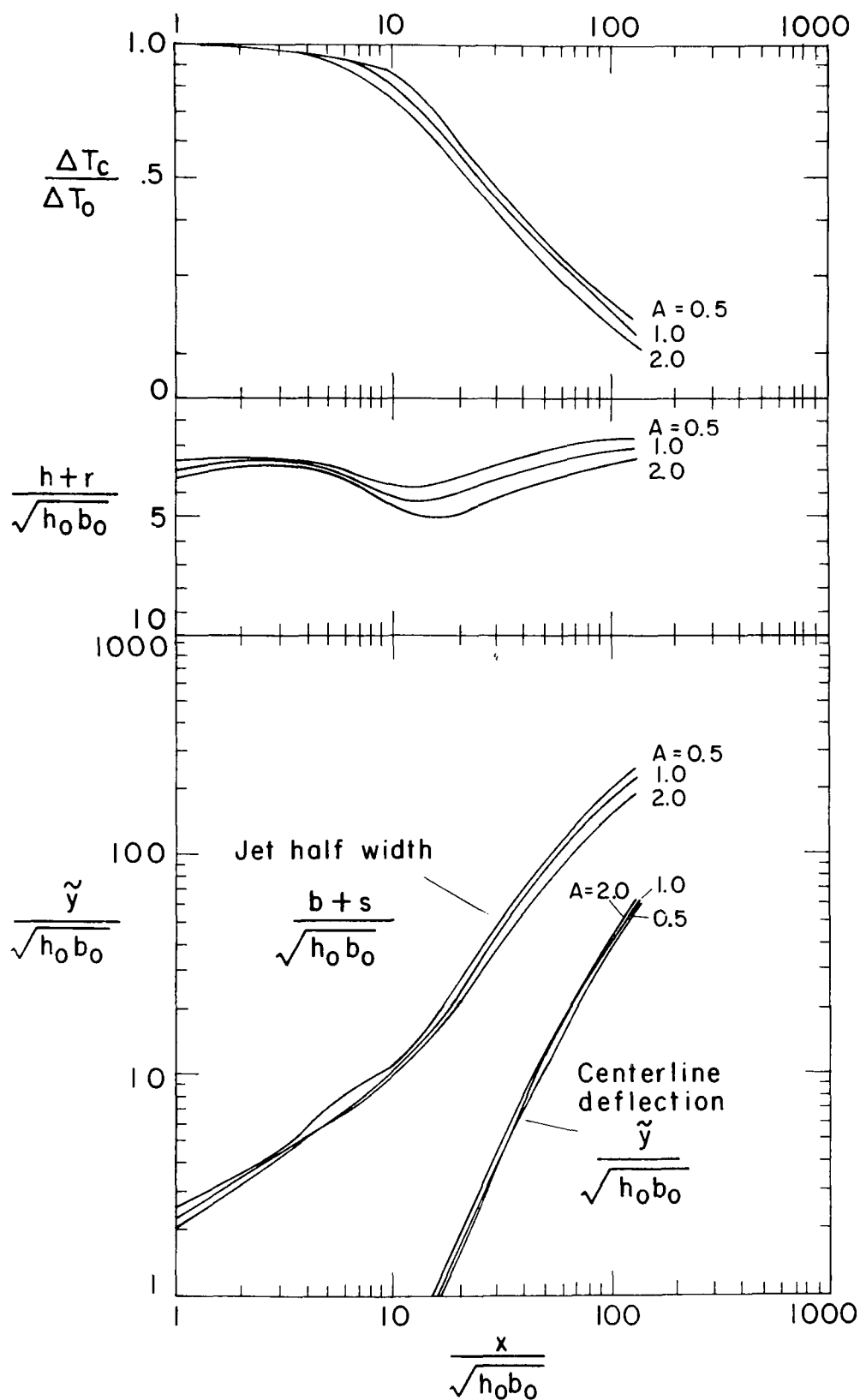


Fig. 2.7i Jet Parameters for $Fr_0 = 2.0$, $V/u_0 = 0.1$, $k/u_0 = 0$

III. The Program

This chapter is a detailed description of the program for computing the solution to the heated surface discharge equations. The solution method is described including the basic equations, and the computational scheme.

Lastly, the computer program input and output format are discussed.

3.1 Dimensionless Equations

The computations are performed with the following dimensionless variables:

$$\begin{aligned}\bar{x} &= x/\sqrt{h_o b_o} \\ \bar{\tilde{x}} &= \tilde{x}/\sqrt{h_o b_o} \\ \bar{\tilde{y}} &= \tilde{y}/\sqrt{h_o b_o} \\ \bar{u} &= u_c/u_o \\ \overline{\Delta T} &= \Delta T_c/\Delta T_o \\ \bar{h} &= h/\sqrt{h_o b_o} \\ \bar{b} &= b/\sqrt{h_o b_o} \\ \bar{r} &= r/\sqrt{h_o b_o} \\ \bar{s} &= s/\sqrt{h_o b_o} \\ \bar{V} &= V/u_o \\ \theta &\end{aligned}\tag{3.1}$$

The equation set in Table 2.1 is reduced by eliminating the internal velocities

v_s , u_b , w_r and w_h as follows:

- a) Sum all the mass conservation equations to form a
total mass conservative equation:

$$\frac{d}{dx} \left[\bar{u}(\bar{s}+\bar{b}I_1)(\bar{r}+\bar{h}I_1) + \bar{V}\cos\theta (\bar{s}+\bar{b})(\bar{r}+\bar{h}) \right] - \bar{u} \left[\alpha_{sz}(\bar{s}+\bar{b}I_1) - \alpha_y(\bar{r}+\bar{h}I_1) \right] = 0 \tag{3.2}$$

- b) Sum all the momentum conservation equations to form a
total momentum conservation equation:

$$\begin{aligned} \frac{d}{d\bar{x}} \left[\bar{u}^2 (\bar{s} + \bar{b}I_2) (\bar{r} + \bar{h}I_2) + 2\bar{u}\bar{V}\cos\theta (\bar{s} + \bar{b}I_1) (\bar{r} + \bar{h}I_1) + \bar{V}^2 \cos^2\theta (\bar{s} + \bar{b}) (\bar{r} + \bar{h}) \right. \\ \left. + \mathbb{F}_0^{-2} A^{-1/2} \bar{\Delta T} (\bar{s} + \bar{b}I_3) \left(\frac{1}{2} \bar{r}^2 + \bar{r}\bar{h}I_3 + \bar{h}^2I_4 \right) \right] - \bar{u}\bar{V}\cos\theta \left[\alpha_{sz} (\bar{s} + \bar{b}I_1) - \alpha_y (\bar{r} + \bar{h}I_1) \right] = 0 \end{aligned} \quad (3.3)$$

- c) The total heat equation:

$$\begin{aligned} \frac{d}{d\bar{x}} \left[\bar{u} \bar{\Delta T} (\bar{s} + \bar{b}I_7) (\bar{r} + \bar{h}I_7) + \bar{\Delta T} \bar{V}\cos\theta (\bar{s} + \bar{b}I_3) (\bar{r} + \bar{h}I_3) \right] \\ + \left[\frac{k}{u} \right]_0 \bar{\Delta T} (\bar{s} + \bar{b}I_3) = 0 \end{aligned} \quad (3.4)$$

- d) The y-momentum spreading equation:

$$\begin{aligned} \frac{d}{d\bar{x}} \left[\left[\frac{d\bar{b}}{d\bar{x}} - \epsilon \right] \left[\bar{u}^2 \bar{b}I_6 (\bar{r} + \bar{h}I_2) + 2\bar{u}\bar{V}\cos\theta \bar{b}I_5 (\bar{r} + \bar{h}I_1) + \bar{V}^2 \cos^2\theta \bar{b} (\bar{r} + \bar{h}) \right] \right] \\ - \mathbb{F}_0^{-2} A^{-1/2} \bar{\Delta T} \left(\frac{1}{2} \bar{r}^2 + \bar{r}\bar{h}I_3 + \bar{h}^2I_4 \right) = 0 \end{aligned} \quad (3.5)$$

- e) The y-momentum deflection equation:

$$\frac{d\theta}{d\bar{x}} + \frac{\bar{u}\bar{V}\sin\theta \left[\alpha_{sz} (\bar{s} + \bar{b}I_1) + \alpha_y (\bar{r} + \bar{h}I_1) \right]}{\bar{u}^2 (\bar{s} + \bar{b}I_2) (\bar{r} + \bar{h}I_2) + 2\bar{u}\bar{V}\cos\theta (\bar{s} + \bar{b}I_1) (\bar{r} + \bar{h}I_1) + \bar{V}^2 \cos^2\theta (\bar{s} + \bar{b}) (\bar{r} + \bar{h})} = 0 \quad (3.6)$$

f) Combine the region 1 mass and momentum conservation equations to eliminate v_s and w_r :

$$(\bar{u} + \bar{V} \cos \theta) \frac{d}{d\bar{x}} (\bar{u} + \bar{V} \cos \theta) + \mathbb{F}_o^{-2} A^{-1/2} \left[\frac{1}{2} \bar{r} \frac{d\bar{\Delta T}}{d\bar{x}} + \bar{\Delta T} \frac{d\bar{r}}{d\bar{x}} + I_3 \frac{d\bar{\Delta T}}{d\bar{x}} \bar{h} \right] = 0 \quad (3.7)$$

g) Combine the momentum and mass conservation equations from regions 1, 2, and 3 to eliminate v_s , v_b , w_t and w_h :

$$\begin{aligned} (\bar{r}\bar{b} + \bar{s}\bar{h}) & \left[(\bar{u}I_2 + \bar{V} \cos \theta I_1) \frac{d\bar{u}}{d\bar{x}} + (\bar{u}(2I_1 - \frac{I_2}{I_1}) + \bar{V} \cos \theta) \frac{d\bar{V} \cos \theta}{d\bar{x}} \right] \\ & + \bar{u} \bar{V} \cos \theta (I_1 - \frac{I_2}{I_1}) (\bar{s} \frac{d\bar{h}}{d\bar{x}} + \bar{r} \frac{d\bar{b}}{d\bar{x}}) + \bar{u} (1 - \frac{I_2}{I_1}) \frac{d}{d\bar{x}} [\bar{r}\bar{s} (\bar{u} + \bar{V} \cos \theta)] \\ & + \mathbb{F}_o^{-2} A^{-1/2} \left[\bar{s} (I_4 \frac{d\bar{\Delta T}}{d\bar{x}} \bar{h}^2 + I_3 \bar{\Delta T} \bar{h} \frac{d\bar{r}}{d\bar{x}}) + \frac{1}{2} I_3 \frac{d\bar{\Delta T}}{d\bar{x}} \bar{b} \bar{r}^2 + I_3 \bar{r}^2 \frac{d\bar{\Delta T}}{d\bar{x}} \bar{b} \bar{h} + \right. \\ & \left. \bar{\Delta T} (\frac{1}{2} \bar{r}^2 + \bar{r}\bar{h} I_3) \frac{d\bar{s}}{d\bar{x}} \right] + \bar{u} (\alpha_{sz} \bar{s} - \alpha_y \bar{r}) \frac{I_2}{I_1} = 0 \quad (3.8) \end{aligned}$$

h) The geometrical relationships:

$$\frac{d\bar{x}}{d\bar{x}} - \sin \theta = 0 \quad (3.9)$$

$$\frac{d\bar{y}}{d\bar{x}} - \cos \theta = 0$$

Using the similarity functions defined in the theory, the integration constants have the values:

$$\begin{aligned}
 I_1 &= .4500 \\
 I_2 &= .3160 \\
 I_3 &= .6000 \\
 I_4 &= .2143 \\
 I_5 &= .2222 \\
 I_6 &= .1333 \\
 I_7 &= .3680
 \end{aligned} \tag{3.10}$$

The entrainment coefficients are as follows assuming $\epsilon_o = .22$:

$$\begin{aligned}
 \alpha_z &= .0295 & \bar{r} > 0 \\
 \alpha_z &= .0495 & \bar{r} = 0
 \end{aligned} \quad \alpha_{sz} = \alpha_z \exp \left[-5 \frac{\overline{\Delta T} \bar{h}}{\bar{u}^2} \bar{F}_o^{-2} A^{-1/2} \right]$$

$$\begin{aligned}
 \alpha_y &= -.0295 & \bar{s} > 0 \\
 \alpha_y &= -.0495 & \bar{s} = 0
 \end{aligned} \tag{3.11}$$

It should be noted that the computer program may be used for other choices of similarity functions and spreading rate than those assumed here by simply changing the program statements which specify the values of I_1 - I_7 and ϵ_o . The entrainment coefficients are automatically computed from these variables using equations (2.18)

The above nine equations may be solved for the \bar{x} derivatives of \bar{x} , \bar{y} , \bar{u} , $\overline{\Delta T}$, \bar{h} , \bar{b} , \bar{r} , \bar{s} , and θ . (Note that \bar{V} is given as an input and thus is known. The "initial" conditions at $\bar{x} = 0$ are:

$$\begin{aligned}
 \bar{x} = \bar{y} &= 0 & \bar{h} = \bar{b} &= 0 \\
 \bar{u} &= 1 - \bar{V} \cos \theta_o \quad (\bar{V} \text{ taken at origin}) & \bar{r} &= A^{1/2} \\
 \overline{\Delta T} &= 1 & \bar{s} &= A^{-1/2} \\
 & & \theta &= \theta_o
 \end{aligned} \tag{3.12}$$

3.2 The Computational Scheme

The computer program is conceptually simple. After all inputs are read the variables are initialized to their values at the discharge origin. The solution proceeds by advancing along the discharge centerline (increasing \bar{x}) using the calculated derivatives of each variable to calculate its behavior. The differential equation technique is a fourth order Runge-Kutta scheme which has been taken, in modified form, from the IBM Scientific Subroutine Package. The program consists of a main program and five subroutines:

MAIN: This program reads the input data, sets up the initial conditions for each calculation, and calls the subroutine SRKGS which performs the calculations.

SRKGS: This subroutine is a modified version of the IBM Scientific Subroutine Package DRKGS for solving a system of differential equations. The form of the equation system is:

$$[a_{ij}] \frac{dy_j}{dx} = c_i \quad (3.13)$$

where a_{ij} is a coefficient matrix, y_j is a vector of the variables (\bar{u} , ΔT , etc.) and c_i is a vector of the constants in the i equations. Subroutine SRKGS advances the solution by successively calling subroutine FCT which solves the system of equations for $\frac{dy_j}{dx}$. The results of the calculations are periodically printed by calling subroutine OUTP.

FCT: This subroutine uses the current values of the variables, computes the coefficient matrix, a_{ij} , the vector c_i , and solves the resulting system of linear equations for $\frac{dy_j}{dx}$ by calling routine SGELG. The following details concerning this routine may be of interest:

a) To reduce the equation set to first order the equation $\frac{d}{d\bar{x}} \left[\frac{db}{d\bar{x}} \right] = \frac{d^2 b}{d\bar{x}^2}$ is added where $\frac{d^2 b}{d\bar{x}^2}$ is computed from the y-spreading Equation (3.5) and $\frac{db}{d\bar{x}}$ becomes a variable.

b) Because of their relatively simple form, the y-deflection Equation (3.6) and the geometrical relationships (3.9) are not included in the matrix

solved by SGELG but are solved separately within FCT.

- c) When an ambient current is present, ($V \neq 0$) the value of ϵ is computed by setting $\overline{\Delta T} = 0$ and solving a reduced set of equations from which the heat equation (3.4) is omitted and the y-spreading equation (3.5) is replaced by $\frac{db}{dx} = \frac{dh}{dx}$. The full buoyant equation set is then solved using the calculated value of ϵ . When there is no ambient current, ($V=0$) the spreading rate is $\epsilon_0 = .22$, and the full equation set is solved directly.

SGELG: This subroutine is a modified form of the IBM Scientific Subroutine Package routine DGELG. It solves the system of linear equations by Gauss-Jordan reduction.

OUTP: The values of the calculated variables (y_j) are printed in formatted form. Certain other quantities of interest are also printed (see Section 3.4).

CROSS: This subroutine is called by the other routines whenever the velocity of the cross flow is required. The routine uses the input values V_1 to V_8 to compute the cross flow as a function of \bar{x} . This subroutine may be modified by any user to any particular functional form with the only requirement being that the routine place the value of the cross flow at the current value of \bar{x} in V and the value of $\frac{dV}{d\bar{x}}$ in DV . The cross flow function used in the present version is described in the next section.

The computations for a particular case will be terminated for one of the following reasons:

- 1) the limit on \bar{x} specified by the input has been reached (see next section). This is the normal termination.
- 2) $\bar{u} \leq \bar{V} \cos \theta$: This termination occurs when the centerline velocity excess is reduced to the same magnitude as the ambient current in which case the basic assumptions of the theory are not valid.
- 3) $\bar{u} \leq .02$: The limiting value .02 for \bar{u} is an arbitrarily chosen small number below which the assumptions of jet-like behavior are not valid.

- 4) The total dimensionless momentum, $M = \bar{u}^2(\bar{r} + \bar{h}I_2)(\bar{s} + \bar{b}I_2) + 2\bar{u}\bar{V}\cos\theta(\bar{r} + \bar{h}I_1)(\bar{s} + \bar{b}I_1) + \bar{V}^2\cos^2\theta(\bar{r} + \bar{h})(\bar{s} + \bar{b}) + \bar{F}_0^2A^{-1/2} \frac{\Delta T}{\bar{u}_o}(\bar{s} + \bar{b}I_3) \left(\frac{1}{2}\bar{r}^2 + \bar{r}\bar{h}I_3 + \bar{h}^2I_4 \right)$, which should be constant for $\frac{\bar{V}}{\bar{u}_o} = 0$ and nearly constant for $\frac{\bar{V}}{\bar{u}_o}$ near zero has deviated from its initial value by more than 25%. This termination indicates that the computation is accumulating a large numerical error.

3.3 Input Formats

	<u>Input Data</u>	<u>Format</u>
	Number of cases to be calculated	I3
One Set for each Calculation	$\bar{F}_0, A, k/\bar{u}_o, \theta_o, \bar{x}_L, \text{ERR}, \text{STEP}$	2F10.5, F10.7, 4F10.5
	$V_1, V_2, V_3, V_4, V_5, V_6, V_7, V_8$	8F10.5

where $\bar{F}_0 = \text{initial densimetric Froude number} = \frac{\bar{u}_o}{\sqrt{\frac{\Delta\rho_o}{\rho_a}gh_o}} = \frac{\bar{u}_o}{\sqrt{\beta\Delta T_o gh_o}}$

$A = \text{aspect ratio} = h_o/b_o$

$k/\bar{u}_o = \text{surface heat loss parameter}$

$\theta_o = \text{initial angle (in degrees) between the discharge centerline and the boundary of the ambient region}$

$\bar{x}_L = \text{the value of } x/\sqrt{h_o b_o} \text{ at which the program should terminate for this case}$

ERR = maximum allowable average error in the variables at each time step

STEP = interval of \bar{x} at which variable values should be printed

$V_1-V_8 = \text{constants describing the cross flow. In the present program version only } V_1 - V_5 \text{ are used as follows}$

$$\bar{V} = V_1 + V_2 \exp \left[-V_3 \left[V_4 \bar{x} - V_5 \right]^2 \right]$$

$$\frac{d\bar{V}}{d\bar{x}} = 2(V_4 \bar{x} - V_5)V_2V_3V_4 \exp \left[-V_3(V_4 \bar{x} - V_5)^2 \right]$$

A sample input listing is given in Appendix III.

3.4 Output Format

The output is paged for each calculation with the basic input variables printed on the heading of each page. The values of the variables are printed in column form under the following headings

$$\begin{aligned}
 X &= \bar{x} \\
 H &= \bar{h} \\
 B &= \bar{b} \\
 R &= \bar{r} \\
 S &= \bar{s} \\
 IF_L &= IF_o A^{1/4} / \left(\frac{\Delta T}{\bar{u}^2} \bar{h} \right)^{1/2} \\
 Q &= \bar{u}(\bar{r} + \bar{h}I_1)(\bar{s} + \bar{b}I_1) + \bar{V}\cos\theta (\bar{r} + \bar{h})(\bar{s} + \bar{b}) \\
 M &= \bar{u}^2(\bar{r} + \bar{h}I_2)(\bar{s} + \bar{b}I_2) + 2\bar{u}\bar{V}\cos\theta(\bar{r} + \bar{h}I_1)(\bar{s} + \bar{b}I_1) \\
 &\quad + \bar{V}^2\cos^2(\bar{r} + \bar{h})(\bar{s} + \bar{b}) + IF_o^{-2}A^{-1/2} \Delta T(\bar{s} + \bar{b}I_3) \left(\frac{1}{2}\bar{r}^2 + \bar{r}\bar{h}I_3 + \bar{h}^2I_4 \right) \\
 U &= \bar{u} \\
 T &= \Delta T \\
 HT &= \Delta T [\bar{u}(\bar{r} + \bar{h}I_7)(\bar{s} + \bar{b}I_7) + \bar{V}\cos\theta(\bar{r} + \bar{h})(\bar{s} + \bar{b})] \\
 V &= \bar{V} \\
 XP &= \tilde{x} \\
 YP &= \tilde{y} \\
 THD &= \theta \\
 TM &= \int_0^{\tilde{x}} \frac{d\tilde{x}}{\bar{u}}
 \end{aligned}$$

An example of program output is shown in Appendix III.

IV. Applications

The theoretical model presented in the preceding sections permits determination of the behavior of a heated surface discharge as a function of relatively few controlling parameters: IF_o , h_o/b_o , k/u_o , V/u_o . The geometry of actual field configurations are rarely as simple as those assumed in the theory and judgement must be applied in the schematization of the discharge to a form for which the dimensionless parameters may be given. Similarly, the output of the program must be interpreted in the light of the basic assumptions of the model. The following sections discuss in detail the generation of input data for the computations and the construction of the temperature distribution from the program output. Finally, a case study is presented as an example of the use of the theory and computer program.

4.1 Schematization

This section is a discussion of the data requirements and schematization techniques for preparing input to the program. The following are the physical data needed as input to the theoretical calculations.

The ambient temperature, T_a , is assumed in the theory to be constant in space and time. Actual ambient receiving water temperatures are often stratified vertically or horizontally and may be unsteady due to wind, tidal action or diurnal variations in solar heating. The natural stratification of the ambient water may be increased by accumulation of heat at the water surface if the discharge is in a semi-enclosed region. The value of the ambient temperature, for a given initial temperature rise, ΔT_o , determines the initial density difference between the discharged and ambient water. Also the effectiveness of the entrainment of ambient water in reducing the discharge temperatures is a function of the ambient stratification.

If the temperature differences resulting from ambient stratification in the vicinity of the discharge are the same magnitude as the initial discharge temperature rise, the theoretical model of this study should not be applied without further development to account for the ambient stratification. The theory is valid if an ambient temperature, T_a , may be chosen which is representative of the receiving water temperatures, that is, if the temporal or spatial variations in ambient temperature do not differ from T_a by more than a few degrees Fahrenheit.

The initial discharge temperature rise, ΔT_o , is determined from the discharge temperature, T_o , and the chosen ambient temperature, T_a . The value of ΔT_o will be equal to the temperature rise through the condensers only if the intake temperature is equal to T_a . Actual discharge temperatures should be relatively steady unless the power plant has several different condenser designs in which case the discharge temperature will vary with the plant load. Use of the theory requires that a constant value of ΔT_o be specified, the choice being based on the likely steady value of the discharge temperature.

The initial relative density difference, $\Delta \rho_o / \rho_a$ may be related to T_a and ΔT_o by $\Delta \rho_o / \rho_a = \beta \Delta T_o$ where β is a function of T as given in Figure 4.1 for fresh water. The curve of β vs. T is not linear but only a small error will be introduced if T is set equal to $T_a + \Delta T_o / 2$. A more accurate value of $\Delta \rho_o / \rho_a$ may be obtained by using tabulated values of water density vs. temperature, or in the case of salt water, water density vs. salinity and temperature.

The initial condenser water discharge velocity, u_o , is a function of the power plant condenser water pumping rate and the discharge channel area.

The discharge channel geometry is important since the theory uses the square root of one half of the discharge channel flow area as a scaling length. Calculation of the discharge densimetric Froude number, Fr_o , requires specification of the initial depth, h_o ; and the aspect ratio, A , requires both h_o and the initial width, b_o . The following procedure is suggested for any channel shape:

- a) Let h_o be the actual maximum discharge channel depth so that calculation of Fr_o is not affected by the schematization.
- b) Let b_o be such that the correct discharge channel area is preserved:

$$b_o = \frac{\text{channel area}}{2h_o} \quad (4.1)$$

Then the aspect ratio is given by:

$$A = \frac{h_o}{b_o} = \frac{2h_o^2}{\text{channel area}} \quad (4.2)$$

As an example, the aspect ratio of a circle is $8/\pi = 2.55$.

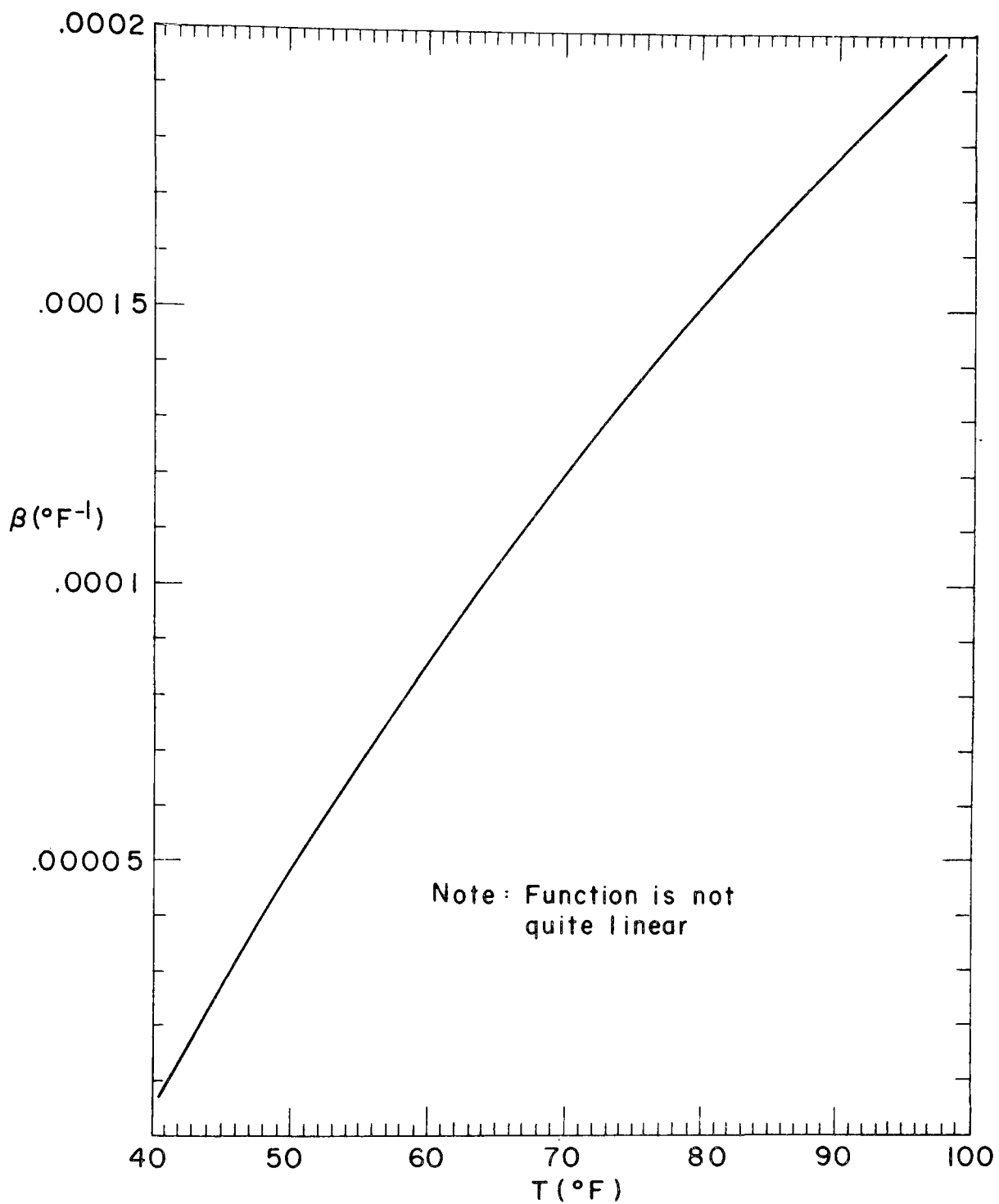


Fig. 4-1 Coefficient of Thermal Expansion for Fresh Water

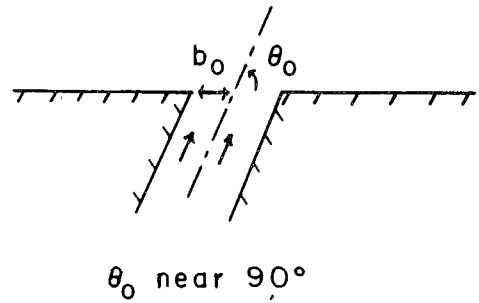
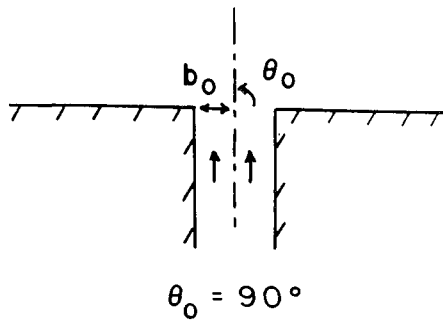
$$\beta = \frac{1}{\rho} \frac{\partial \rho}{\partial T} \text{ } (^{\circ}\text{F}^{-1}) \text{ as a Function of Temperature } T (^{\circ}\text{F})$$

The discharge channel geometry may vary with time if the elevation of the receiving water changes due to tidal motion or other causes. In this case separate calculations for each elevation of the receiving water must be made, assuming that the steady state theory predicts the instantaneous temperature distribution.

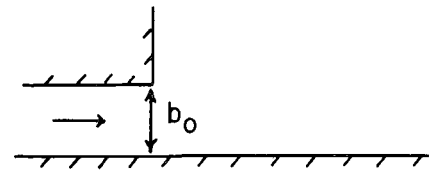
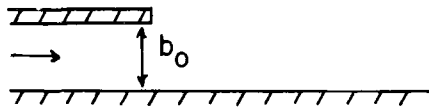
Very complicated arrangements of the discharge channel relative to the boundaries of the ambient receiving waters are beyond the capabilities of the theory of this study. If the discharge channel is nearly at right angles to the solid boundaries, the theory may be used as developed, or if the discharge is directed parallel to a straight boundary, the discharge may be schematized by assuming that the solid boundary is the centerline of a jet whose discharge channel is twice the width of the actual discharge (see Figure 4.2). The width b_o is then twice the width calculated by the procedure discussed previously. However, if it is not clear whether the jet will entrain water from one or both sides or if irregularly shaped solid boundaries will deflect the jet or distort it from the form assumed in the theory, a meaningful schematization is not possible.

The densimetric Froude number Fr_o and the aspect ratio A of the surface discharge channel should be chosen to be consistent with the bottom topography of the receiving water body. If optimum dilution is to be obtained, the vertical development of the surface jet should not be limited by the bottom of the receiving water. This is generally considered to be a desirable objective by the aquatic or marine biologist inasmuch as it avoids exposure of benthic organisms to high velocities and temperature rises. Designs which contain minimum interaction between the surface jet and the bottom topography are shown on the left side of Figure 4.3. Examples of surface jets in which there are substantial interactions in relation to the bottom topography are shown on the right side of Figure 4.3. In the latter case, vertical entrainment and dilution are reduced by the interference of the jet and the bottom.

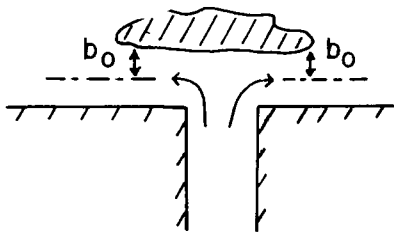
If the discharge channel densimetric Froude number, Fr_o , is less than unity, a wedge of ambient water will intrude into the discharge channel and the heated flow will be forced to obtain a densimetric Froude number of unity at the discharge point (see Figure 4.4). The depth of the heated flow in the presence of a wedge, h_o^* , is given by:



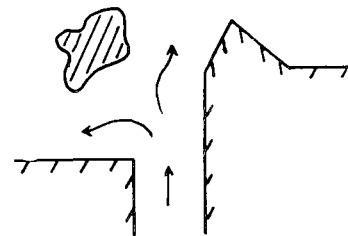
Discharges with Entrainment from Both Sides



Discharges with Entrainment from One Side



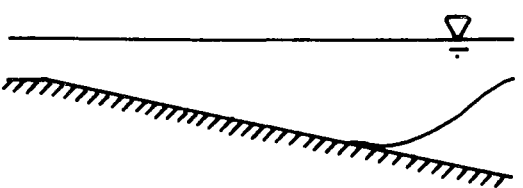
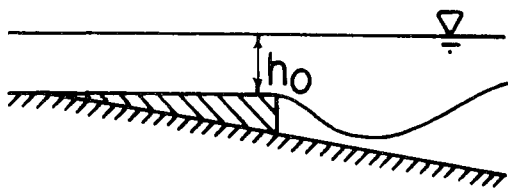
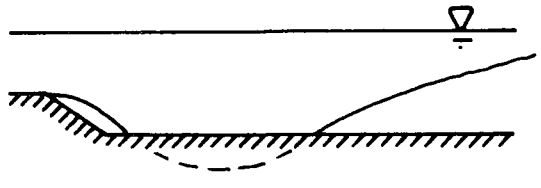
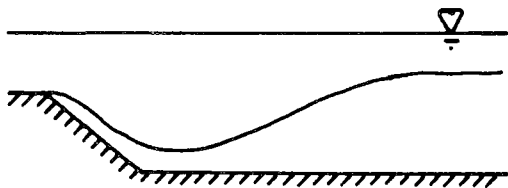
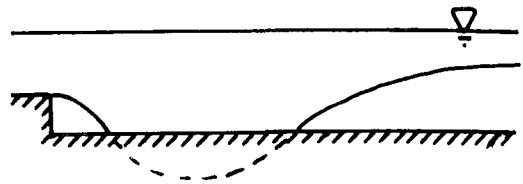
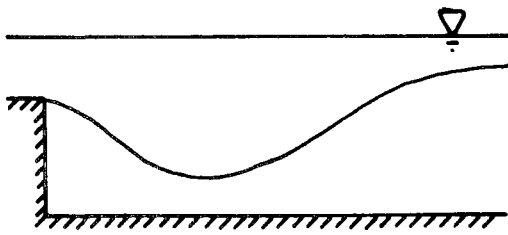
Schematization Possible



Schematization not Possible
Because of Irregular Geometry

Discharges with Obstructions

Fig. 4.2 Discharge Channel Schematization



Minimum Interaction

Substantial Interaction

Fig. 4.3 Limitations on Maximum Jet Thickness by Bottom Topography

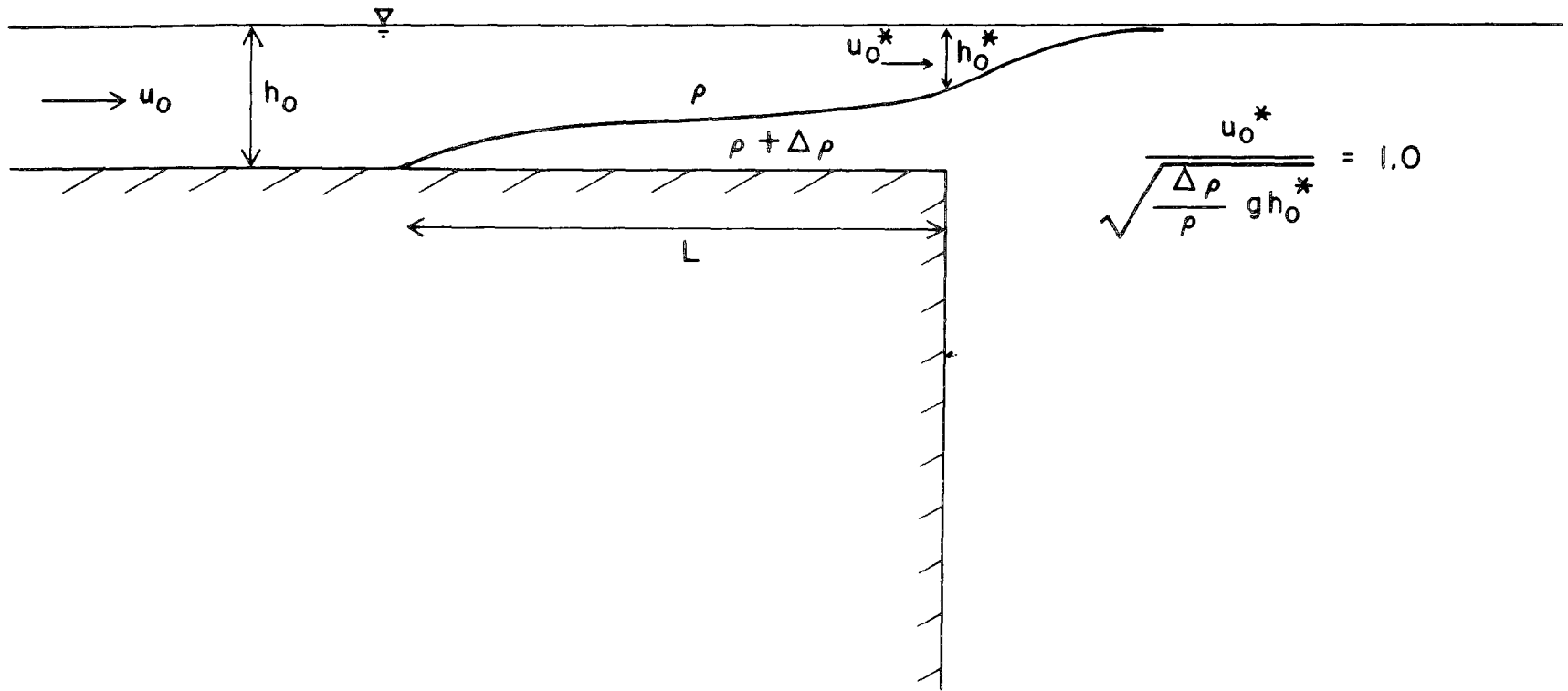


Fig. 4.4 Two Layer Flow in the Discharge Channel

$$\frac{h_o^*}{h_o} = F_o^{2/3} \quad (4.3)$$

where h_o and F_o are based on the channel dimensions. A flow area may be calculated based on the depth h_o^* and the aspect ratio calculated as described previously in this section.

The surface heat loss coefficient, k , may be estimated from local meteorological variables, principally wind speed, and the ambient water temperature. Care should be taken to use values for k which are appropriate for local conditions. Edinger (13) and Ryan (16) discuss methods for determining values of $K = \rho ck$.

The cross flow velocity, V , in the receiving water may be measured directly or estimated from flow measurements in the case of a channel flow. The theory accepts as input values of V/u_o as a function of $\tilde{x}/\sqrt{h_o b_o}$ (see Chapter 3).

Once the schematization of the discharge configuration is achieved, the theoretical calculation is performed by the computer program described in Chapter 3. The inputs to the program for each calculation are F_o , $A = h_o/b_o$, k/u_o and V/u_o (as a function of $\tilde{x}/\sqrt{h_o b_o}$).

It should be noted that the theoretical model may not necessarily be applied to any arbitrary set of input parameters. In general the value of k/u_o has little effect; however, depending upon the value of the other parameters, F_o , A , and V/u_o , and upon the specified error size, ERR, the program may fail to generate a solution. This problem may take one of the following forms:

- 1) Little or no advancement of solution, i.e. the step size remains very small.
- 2) Abrupt discontinuities noticeable either in the values of the variables or in the total mass, momentum, or heat.
- 3) Unstable behavior in one or more variables, culminating usually in an overflow error.

The chance of the program encountering one of the above problems increases with decreasing F_o and A and increasing V/u_o . The value of ERR produces no consistent result except that too large a value of ERR most often yields

unstable behavior or discontinuities, and too small a value may prevent advancement.

The causes of this anomolous behavior in certain cases are not totally understood at the present time, but are thought to be related to the following:

- 1) accumulation of round-off error where the solution should be stable, i.e. a totally numerical problem,
- 2) genuinely unstable solutions, probably caused by the determinant of the differential equation coefficient matrix being zero or near zero.

The first of these could probably be solved by paying greater attention to round off error generation than is now done. To the extent that the second cause has no physical significance it may also be desirable to eliminate this problem by numerical manipulation. However, the governing equations for the heated discharge are similar to open channel flow equations which possess critical flow points at which the equations strictly have no solution and the coefficient matrix is zero. It is not clear to what extent the degeneracy of the three-dimensional heated discharge equations corresponds to critical flow behavior; the answer will only come by observing actual discharges in the laboratory and field. Thus for the time being the limitation on the computational range of this theory must be accepted.

Of course the values of IF_0 , A , and V/u_0 are pre-determined by the case being considered, leaving ERR as the only free parameter. Figures 2.7a to 2.7i indicate the range of each variable and the various combinations of values for which calculations may be successfully performed. Table 4.1 gives a rough guideline as to the best value of ERR to be used for different cases. In general if the solution is not advancing, a larger ERR might be tried and if the solution appears unstable a smaller value should be tried. Experience has shown that the behavior of the solution may also depend upon the type of computer used. The results quoted herein are based on calculations done on an IBM 360 either -65 or -75. Users employing different systems than this are encouraged first of all to try several values of ERR in an attempt to make an unsuccessful calculation work and secondly to take up the challenge of illuminating more clearly than is done here the properties of the governing equations, the physical relevance of these properties, and their efficient numerical treatment.

Table 4.1

Guideline to Choice of Maximum Error Value, ERR

Fr_o	A	A	A	A
	0.1 - 0.5	0.5 - 1.0	1.0 - 1.5	2.0 - ∞
1 - 2	.005 with no crossflow .05 with cross-flow	.005	.005	.005
2 - 5	.005 with no crossflow .05 with cross-flow	.005	.01	.01
5 - 10	.01	.01	.01	.01
10 - ∞	.01	.01	.01	.01

4.2 Use of the Program Output

An example of the program output is shown in Appendix III. All of the outputs are in dimensionless form and must be transformed by the following steps

- 1) Multiply \tilde{x} , \tilde{y} , \bar{x} , \bar{r} , \bar{s} , \bar{b} , and \bar{h} by $\sqrt{h_o b_o}$
- 2) Multiply \bar{u} by u_o
- 3) Multiply $\overline{\Delta T}$ by ΔT .
- 4) Multiply TM by $\sqrt{h_o b_o}/u_o$

The calculated isotherms may be constructed as follows:

- 1) Locate the centerline using \tilde{x} and \tilde{y} .
- 2) Assign values of $T_c = T_a + \Delta T_c$ along the centerline.
- 3) Plot the boundaries of the core and turbulent regions using s , b , r and h .
- 4) Assign temperatures within the discharge using the assumed temperature distribution (Equation 2.5).

Figure 4.5 may be used as an aid in the construction of isotherm contours; lines of constant $\zeta_y = \frac{y-s}{b}$ or $\zeta_z = \frac{z-r}{h}$ are plotted and then the temperature contours are drawn by referring to the figure. The values of temperature rise above ambient are expressed as fractions of ΔT_o , the initial temperature rise.

If the surface area within a given temperature rise ΔT_* is of interest, the following formula may be used:

$$A_* = 2h_o b_o \int_0^{\bar{x}_*} \left[\bar{s} + \bar{b} (1 - \overline{\Delta T}_* / \overline{\Delta T})^{2/3} \right] d\bar{x} \quad (4.4)$$

where

$$\left. \begin{aligned} \bar{s} &= s / \sqrt{h_o b_o} \\ \bar{b} &= b / \sqrt{h_o b_o} \\ \overline{\Delta T} &= \Delta T_c / \sqrt{h_o b_o} \end{aligned} \right\} \quad \text{As given in the program output as a function of } \bar{x}.$$

$$\overline{\Delta T}_* = \Delta T_* / \Delta T_o$$

$$\bar{x}_* = \text{the value of } x / \sqrt{h_o b_o} \text{ where } \overline{\Delta T} = \overline{\Delta T}_*$$

A simple computer program may be written which performs the above integration numerically.

Finally, the travel time along the centerline to a given temperature, $T_a + \Delta T_*$, is given by $TM(\bar{x}_*) \frac{\sqrt{h_o b_o}}{u_o}$.

It is important to note that although the theory calculates the temperature distribution out to very small values of temperature rise above ambient, these extreme regions of the discharge will be subject to distortion by random ambient processes especially wind stresses.

The calculated temperature distribution must be interpreted with this in mind and no critical significance should be given to the exact calculated position of isotherms of small temperature rise.

4.3 Case Study - Heated Surface Discharge into a Receiving Water Body of Finite Depth

Consider a proposed discharge into a large body of water at ambient temperature T_a with a uniform depth H as shown on Figure 4.6. A constraint is

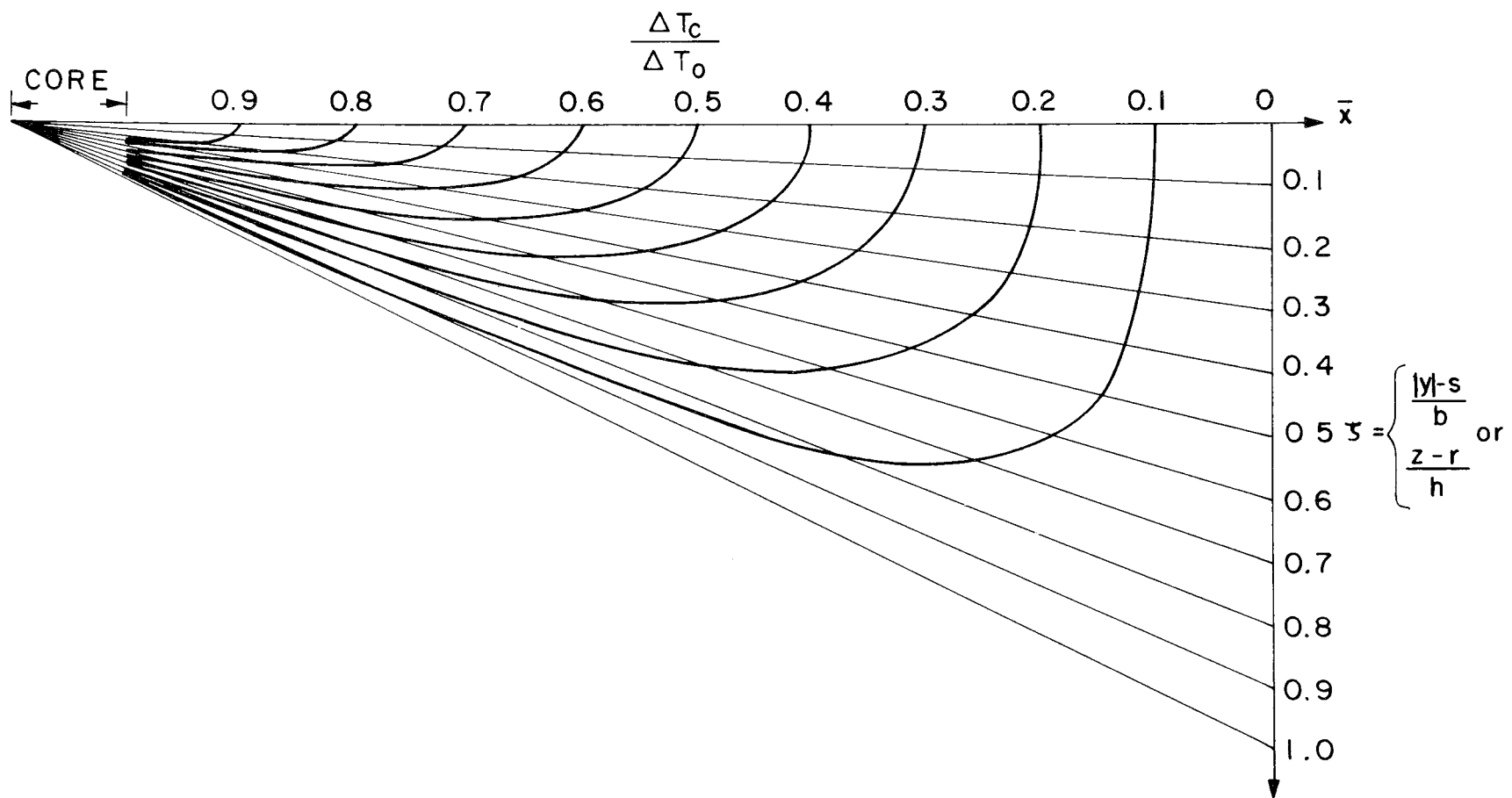


Fig. 4.5 Temperature Distribution Plotting Aid

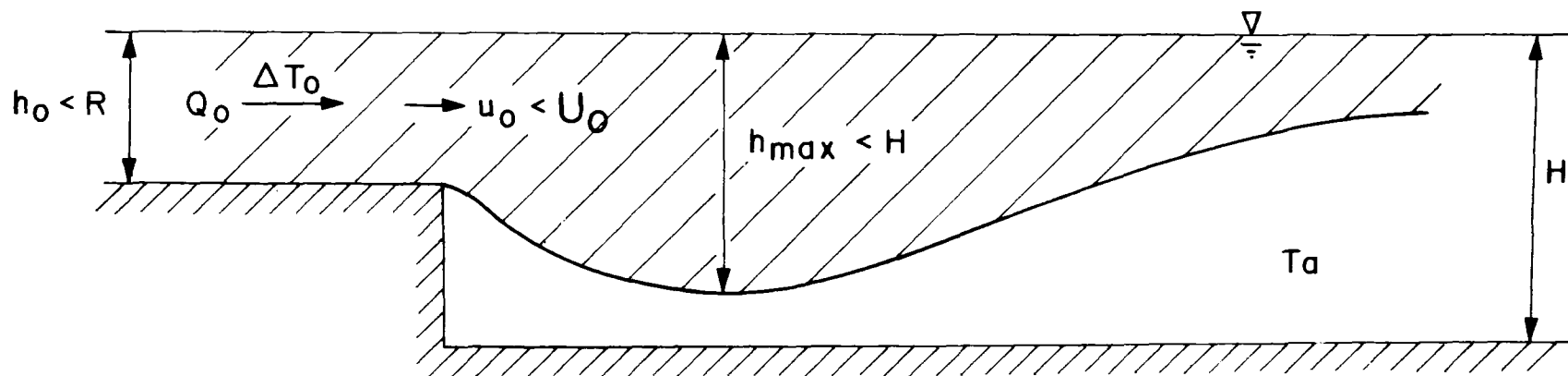


Fig. 4.6 Schematic of Case Study Problem

placed upon the discharge velocity such that $u_o \leq U_o$. Because the theory applies only to discharges which are not influenced significantly by solid boundaries in the receiving water, it is desirable that $h_{\max} \leq H$ where h_{\max} is the maximum vertical penetration of the discharge (see Figure 4.6). The choice of h_{\max} as the "critical" boundary of the jet is an arbitrary one but is probably conservative considering the assumed structure of the jet which sets $u = 0$ at that point. Entrainment should not be significantly affected by contact with the bottom at the point of maximum depth only.

A third constraint may be imposed by local topography. For instance h_o must be less than or equal to the water depth, and $2b_o$ may be constrained by some critical width. Thus in general $h_o < R$ and $b_o < S$.

The discharge is characterized by an initial temperature rise, ΔT_o , and a condenser water flow, Q_o . The problem treated in this case study is to design a discharge channel for maximum ultimate (stable) dilution (see Figure 2.5) while meeting all the imposed constraints. This case study will illustrate the generation of temperature contours and isotherm areas from the computer output in addition to treating the more specific, but often relevant, problem of optimizing a channel design with one or more constraints imposed.

The definition of IF'_o and the following approximate formulas may be recalled from Chapter 2 for IF'_o greater than 3.

$$IF'_o = IF_o A^{1/4} = \frac{u_o}{(g\beta\Delta T_o)^{1/2} (h_o b_o)^{1/4}} \quad (4.5a)$$

$$= \frac{Q_o}{2(g\beta\Delta T_o)^{1/2} (h_o b_o)^{5/4}} \quad (4.5b)$$

$$= \frac{2^{1/4} u_o^{5/4}}{(g\beta\Delta T_o)^{1/2} Q_o^{1/4}} \quad (4.5c)$$

$$\left(\frac{\Delta T_o}{\Delta T_{c_s}} \right) \approx IF'_o \quad (4.6a)$$

$$D_s \approx 1.4 F'_o \quad (4.6b)$$

$$\frac{h_{\max}}{(h_o b_o)^{1/2}} \approx 0.42 F'_o \quad (4.7)$$

Equation (4.5) defines F'_o , (4.6a and b) relates centerline dilution and overall dilution to F'_o and (4.7) relates the maximum jet penetration to F'_o . Note that for a given $\Delta\rho_o/\rho$ and Q_o both the maximum stable dilution and the maximum penetration are dependent only on discharge velocity u_o and not on the aspect ratio. This provides freedom in selecting channel geometry.

The constraint that $h_m \leq H$ may be restated using (4-7) as

$$F'_o \leq \frac{6.8 H^{5/3} (g\beta\Delta T_o)^{1/3}}{Q_o^{2/3}} \quad (4.8)$$

and from (4.5c) the constraint that $u_o \leq U_o$ may be restated as

$$F'_o \leq \frac{1.19 U_o^{5/4}}{(g\beta\Delta T_o)^{1/2} Q_o^{1/4}} \quad (4.9)$$

Because ultimate dilution increases monotonically with F'_o (see Eqn. 4.6), the channel should be designed with F'_o equal to the smaller of the two expressions in (4.8) and (4.9). From (4.5b) it may be shown that

$$h_o b_o = \frac{Q_o^{4/5}}{2^{4/5} F_o'^{4/5} (g\beta\Delta T_o)^{2/5}} \quad \text{and} \quad (4.10)$$

$$u_o = \frac{Q_o}{2h_o b_o} \quad (4.11)$$

where F'_o is picked from (4.8 and 4.9). If there is a constraint on either the width or depth of the discharge structure, this constraint may be included with (4.10) to determine h_o and b_o . If there is a constraint on both width and depth

such that $h_o < R$ and $b_o < S$ and the product $RS < h_o b_o$ as determined by (4.10), then a discharge channel cannot be designed with the desired constraints.

Example: Design a discharge channel no more than 12 feet deep to achieve maximum stable dilution of a heated discharge of 2,000 cfs and 15°F temperature rise into a water body 31 ft. deep at an ambient temperature of 70°F. Maximum discharge velocity is $U_o = 6$ ft/sec. The area within the 4°F surface isotherm should be calculated.

1. The value of β is taken from Figure 4-1 using $T = 77.5^\circ\text{F}$, $\beta = .000144^\circ\text{F}^{-1}$ and $(g\beta\Delta T_o) = .069 \text{ ft/sec}^2$.
2. Using (4.8) the constraint on depth is

$$F'_o \leq \frac{6.8(31)^{5/3}(.069)^{1/3}}{2000^{2/3}} = 5.3$$

Using (4.9) the constraint on velocity is

$$F'_o \leq \frac{(1.19)(6)^{5/4}}{(.069)^{1/2}(2000)^{1/4}} = 6.4$$

Hence F'_o should equal 5.3 and the jet should just touch the bottom.

3. From (4.10) and (4.11)

$$h_o b_o = \frac{2000^{4/5}}{2^{4/5}(5.3)^{4/5}(.069)^{2/5}} = 192 \text{ ft}^2,$$

$$(h_o b_o)^{1/2} = \text{scaling length} = 13.9 \text{ ft.}$$

and $u_o = \frac{2000}{2(192)} = 5.2 \text{ ft/sec}$

4. No constraint has been placed on b_o so any number of combinations of $h_o b_o$ will be satisfactory. As an example, $h_o = 11$ ft. and $b_o = 17.5$ feet satisfies the requirement on channel depth and results in a $F_o \approx 6.0$; aspect ratio, $A \approx 0.6$; and $F'_o = 5.3$.

5. Theoretical calculation (computer output) for these values are shown in Appendix III.
6. Figure 4.5 is used to plot the isotherms in two planes (horizontal at the surface and vertical at the jet centerline) in Figure 4.7.
7. Equation 4.4 is used to calculate the area within the 4° isotherm with $\frac{\Delta T_*}{\Delta T} = 4/15 = .27$ and $\bar{x}_* = 45$. The computations are organized as follows:

\bar{x}	\bar{s}	\bar{b}	$\frac{\Delta T}{\Delta T_*}$	$\frac{\Delta T_*}{\Delta T}$	$(1 - \frac{\Delta T_*}{\Delta T})^{2/3}$	$\bar{s} + \bar{b}(1 - \frac{\Delta T_*}{\Delta T})^{2/3}$	$\sum [\bar{s} + \bar{b}(1 - \frac{\Delta T_*}{\Delta T})^{2/3}] \Delta \bar{x}$
1.131	1.52	.585	.971	.278	.805	1.99	2.25
2.62	1.37	1.16	.940	.287	.798	2.30	5.67
5.24	1.44	2.39	.884	.305	.784	3.31	14.3
⋮	⋮	⋮	⋮	⋮	⋮	⋮	⋮
10.5	1.48	5.27	.692	.390	.719	5.27	39.3
⋮	⋮	⋮	⋮	⋮	⋮	⋮	⋮
41.9	0	41.5	.282	.957	.122	5.05	267.

The first and last column may be multiplied by the scaling length, $\sqrt{h_o b_o} = 13.9$ ft. and plotted against each other to produce the 74° isotherm shown in Fig. 4.7. The integration in Equation 4.4 results in an $A_* = 2(192)(267) = 103,000$ sq. ft. or 2.4 acres.

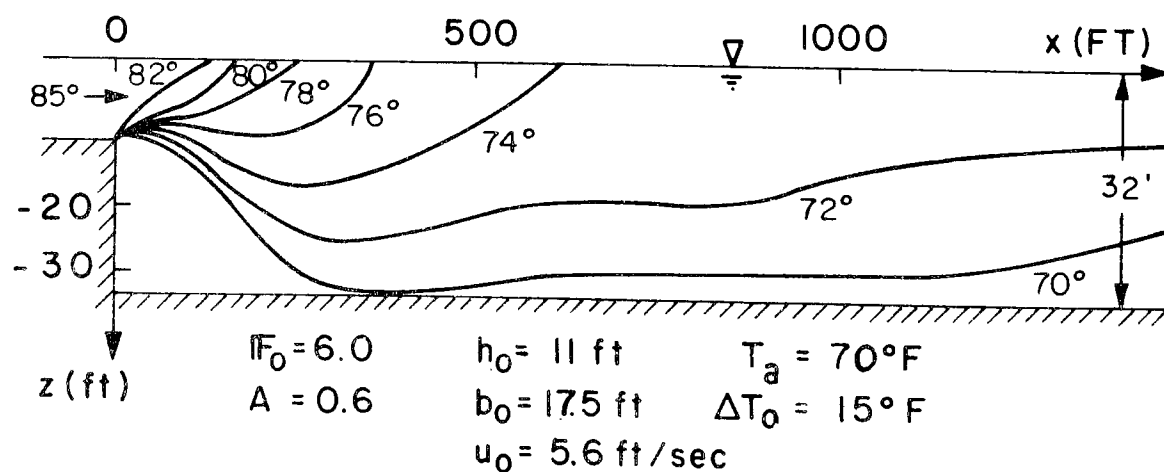
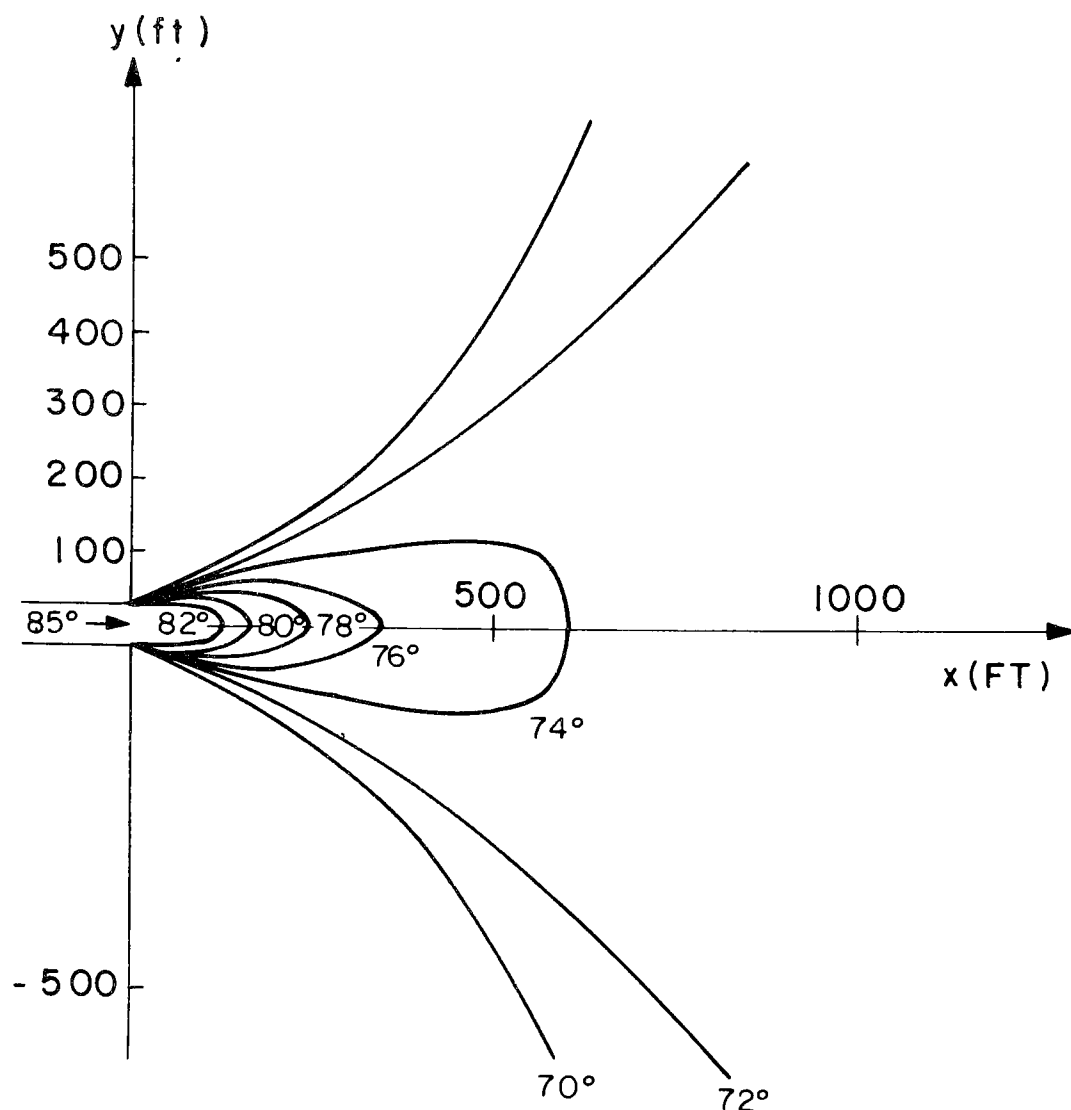


Fig. 4.7 Calculated Contours for the Case Study Example

ACKNOWLEDGEMENT

This study was partially supported by the Environmental Protection Agency under the National Thermal Pollution Research Program. The cooperation of Mr. Frank H. Rainwater, Chief of the National Thermal Pollution Research Program, is gratefully acknowledged.

Additional support for the study was received from the Public Service Electric and Gas Company of Newark, New Jersey, as part of a study of thermal discharges for the proposed Atlantic Generating Station, an offshore floating nuclear power facility.

Mr. Patrick Ryan, Research Assistant in the R.M. Parsons Laboratory for Water Resources and Hydrodynamics made substantial contributions in the development of the relationships used in Chapter IV. Numerical computations were carried out at the M.I.T. Information Processing Service Center. Our thanks to Miss Kathleen Emperor who typed the report.

References

1. Fan, L. N., "Turbulent Buoyant Jets into Stratified or Flowing Ambient Fluids", W. M. Keck Laboratory of Hydraulics and Water Resources, California Institute of Technology, Report No. KH-R-15, June 1967.
2. Fan, L. N. and N.H. Brooks, "Numerical Solutions of Turbulent Buoyant Jet Problems", W. M. Keck Laboratory of Hydraulics and Water Resources, California Institute of Technology, Report No. KH-R-18, 1969.
3. Tamai, N. and others, "Horizontal Surface Discharge of Warm Water Jets", ASCE Journal of the Power Division, No. 6847, PO 2, October 1969.
4. Wiegel, R. L. and others, "Discharge of Warm Water Jet Over Sloping Bottom", Technical Report HEL-3-4, University of California, November 1964.
5. Jen, Y. and others, "Surface Discharge of Horizontal Warm Water Jet", Technical Report HEL-3-3, University of California, December 1964.
6. Stefan, H. and F. R. Schiebe, "Experimental Study of Warm Water Flow Part I", Project Report No. 101, St. Anthony Falls Hydraulic Laboratory, University of Minnesota, December 1968.
7. Hayashi, T. and N. Shuto, "Diffusion of Warm Water Jets Discharged Horizontally at the Water Surface", IAHR Proceedings, Ft. Collins, Colorado, September 1967.
8. Ellison, T. H. and J. S. Turner, "Turbulent Entrainment in Stratified Flows", Journal of Fluid Mechanics, Vol. 6, Part 3, October 1959.
9. Hoopes, J. A. and others, "Heat Dissipation and Induced Circulations from Condenser Cooling Water Discharges into Lake Monona", Report No. 35, Engineering Experiment Station, University of Wisconsin, February 1968.
10. Motz, L. H. and B. A. Benedict, "Heated Surface Jet Discharged into a Flowing Ambient Stream", Department of Environmental and Water Resources Engineering, Vanderbilt University, Nashville, Tennessee, Report No. 4, August 1970.
11. Morton, B. R., Taylor, G. I. and J. S. Turner, "Turbulent Gravitational Convection from Maintained and Instantaneous Sources", Proc. Roy. Society, London, A 234:1-23, 1956.
12. Morton, B. R., J. Fluid Mech. 5:151-63, 1959.
13. Edinger, J. E., Duttweiler, D. W. and J. C. Geyer, "The Response of Water Temperature to Meteorological Conditions", Water Resources Research, 4:5, 1137-43, 1968.

14. Abramovich, G. N., The Theory of Turbulent Jets, The M.I.T. Press, M.I.T., Cambridge, Massachusetts, 1963.
- * 15. Stolzenbach, K. D. and D.R.F. Harleman, "An Analytical and Experimental Investigation of Surface Discharges of Heated Water", R. M. Parsons Laboratory for Water Resources and Hydrodynamics, Technical Report No. 135, Department of Civil Engineering, M.I.T., February 1971.
16. Ryan, P. J. and K. D. Stolzenbach, Chapter 1: "Environmental Heat Transfer", Engineering Aspects of Heat Disposal from Power Generation, (D.R.F. Harleman, Ed.), R. M. Parsons Laboratory for Water Resources and Hydrodynamics, Department of Civil Engineering, M.I.T., Cambridge, Massachusetts, June 1972.

* Also published as Water Pollution Control Research Series Report No. 16130 DJU 02/7. by the Water Quality Office, Environmental Protection Agency, Washington, D. C.

List of Symbols

A	- discharge channel aspect ratio, h_o/b_o
a_{ij}	- coefficient matrix in the governing differential equation set
b	- horizontal surface distance from core boundary to jet boundary
b_o	- one half the width of rectangular discharge channel
C	- coefficient in the exponent of Ellison and Turner's vertical entrainment velocity function
c_{ij}	- vector of the constants in the governing differential equation jet
D	- ratio of flow in the jet to the initial flow = dilution
D_s	- dilution in the stable region of the heated discharge
$\frac{db}{dx}$	- lateral spread of the turbulent region of a jet
ERR	- maximum allowable average roundoff error for each step in the numerical computation
IF_o	- densimetric Froude number of the discharge channel = $\frac{u_o}{\sqrt{\frac{\Delta\rho_o}{\rho}gh_o}}$
IF_L	- local densimetric Froude number in the jet = $\frac{u_c}{\sqrt{\frac{\Delta\rho}{\rho}gh}}$
IF'_o	- a characteristic Froude number = $IF_o A^{1/4}$
f	- similarity function for velocity = $(1 - \zeta^{3/2})^2$
g	- acceleration of gravity
HT	- ratio of heat flow in the jet to the initial discharge heat flow
H	- maximum allowable vertical penetration of the jet
h	- vertical centerline distance from core boundary to jet boundary
h_o	- depth of the discharge channel
h_o^*	- depth of the heated flow at the point of discharge if a cold water wedge is present
h_{max}	- maximum value of h obtained in a heated discharge
I_1	- $\int_0^1 f(\zeta)d\zeta = .4500$
I_2	- $\int_0^1 f^2(\zeta)d\zeta = .3600$
I_3	- $\int_0^1 t(\zeta)d\zeta = .6000$

$$I_4 - \int_0^1 \int_{\zeta}^1 t(\zeta) d\zeta d\zeta = .2143$$

$$I_5 - \int_0^1 f(\zeta) \zeta^{1/2} d\zeta = .2222$$

$$I_6 - \int_0^1 f^2(\zeta) \zeta^{1/2} d\zeta = .1333$$

$$I_7 - \int_0^1 f(\zeta) t(\zeta) d\zeta = .3680$$

K - surface heat loss coefficient

k - kinematic surface heat loss coefficient

P - pressure

Q_o - discharge channel flow

R - maximum allowable depth of discharge channel

r - vertical distance from the jet centerline to the boundary of the core region

S - maximum allowable half-width of discharge channel

s - horizontal distance from the jet centerline to the boundary of the core region

STEP - increment in $x/\sqrt{h_o b_o}$ at which numerical output is printed

T - temperature

T_a - ambient temperature

T_c - jet centerline surface temperature

T_o - temperature of the heated flow in the discharge channel

T_{*} - a particular temperature of interest

ΔT - temperature rise above ambient in the jet, T - T_a

ΔT_c - surface temperature rise above ambient at the jet centerline, T_c - T_a

ΔT_o - temperature difference between the discharge and the ambient water,
T_o - T_a

ΔT_{*} - T_{*} - T_a

TM - dimensionless time of travel along the jet centerline,

$$\frac{u_o}{\sqrt{h_o b_o}} \int_0^x \frac{dx}{u_c} .$$

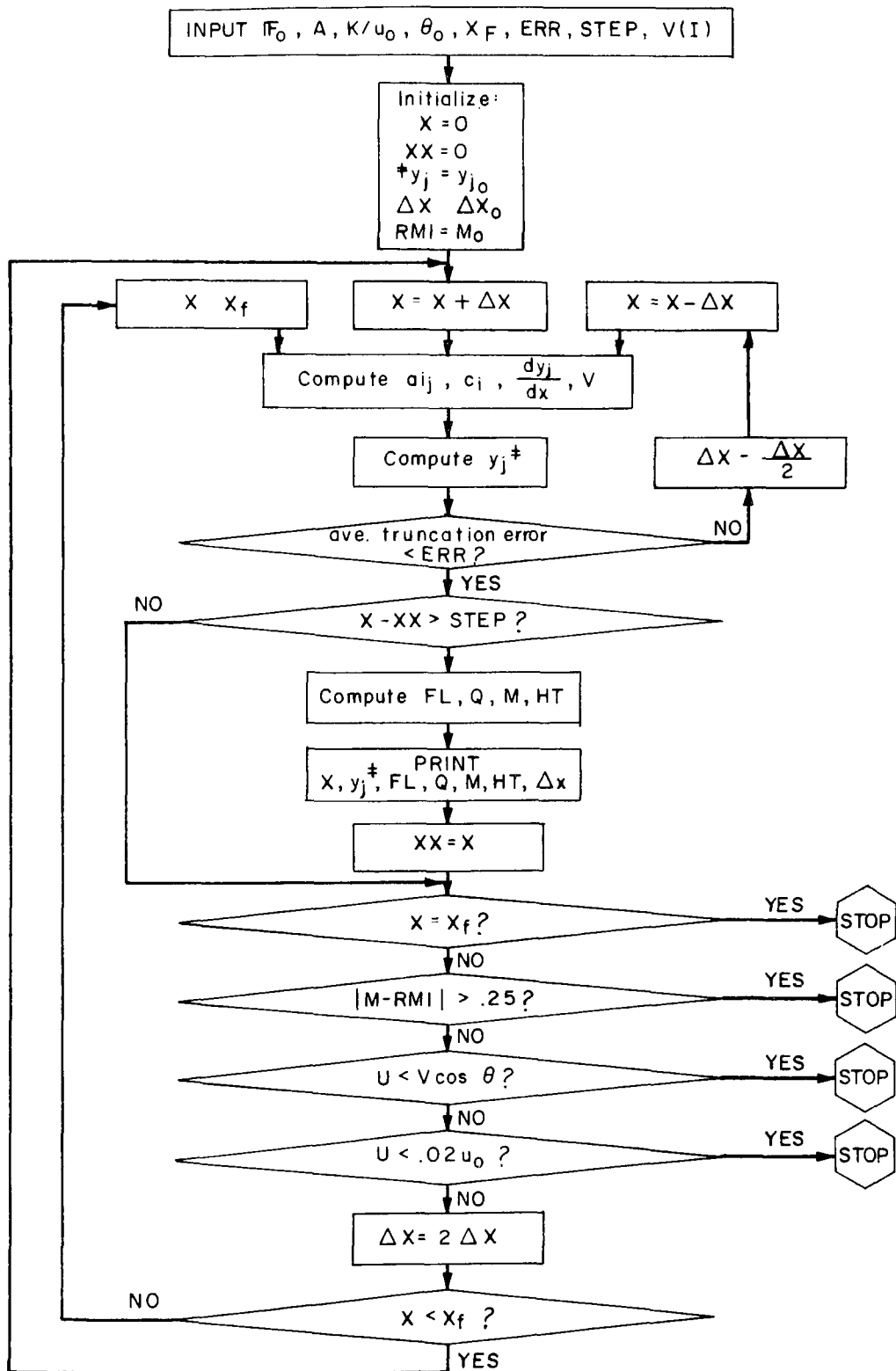
t - similarity function for temperature = (1-ζ^{3/2})

- u, v, w - velocity components in the coordinate system relative to the centerline of a deflected jet
 $\tilde{u}, \tilde{v}, \tilde{w}$ - velocity components in the fixed coordinate system
 U_o - maximum allowable velocity in the discharge channel
 u_o - velocity in the discharge channel
 u_o^* - velocity of the heated flow at the point of discharge if a cold water wedge is present
 u_c - surface centerline jet velocity
 V - ambient crossflow velocity
 $V_1 - V_8$ - ambient crossflow velocity components as input to the numerical program
 v_e - lateral velocity of the entrained flow at the jet boundary
 v_c - lateral velocity in the jet at $y = s+b$ and $-(h+r) < z < \eta$
 v_h - lateral velocity in the jet at $y = s$ and $-(h+r) < z < -r$
 v_s - lateral velocity in the jet at $y = s$ and $-r < z < \eta$
 w_c - vertical velocity in the jet at $z = -(r+h)$ and $0 < y < s+b$
 w_b - vertical velocity in the jet at $z = -r$ and $b < y < s+b$
 w_e - vertical velocity in the jet at $z = -r$ and $0 < y < s$
 x, y, z - coordinate direction relative to the centerline of a deflected jet
 $\tilde{x}, \tilde{y}, \tilde{z}$ - fixed coordinate direction
 x_* - value of x where $\Delta T = \Delta T_*$
 x_L - value of $x/\sqrt{h_o b_o}$ at which the numerical computation terminates
 y_j - vector of the variables ($\bar{u}, \bar{\Delta T}$, etc.) in the governing differential equation set
- α_y - lateral entrainment coefficient in non-buoyant and buoyant jets
 α_z - vertical entrainment coefficient in a non-buoyant jet
 α_{sz} - vertical entrainment coefficient in a buoyant jet
 β - coefficient of thermal expansion of water
 ϵ - spread, $\frac{db}{dx}$, of the turbulent region of a non-buoyant jet
 ϵ_o - spread, $\frac{db}{dx}$, of the turbulent region in an undeflected non-buoyant jet
 ζ_y - dimensionless width of the turbulent region of a jet, $\frac{|y|-s}{b}$
 ζ_z - dimensionless depth of the turbulent region of a jet, $\frac{z-r}{h}$

ζ - either of ζ_y or ζ_z
 θ - angle between the jet centerline (x axis) and the \tilde{y} axis
 θ_o - angle between the discharge channel centerline and the \tilde{y} axis
 ρ - density of water
 ρ_a - density of the ambient water
 ρ_o - density of the heated discharge
 $\Delta\rho$ - difference between the ambient water density and the water density, $\rho_a - \rho$
 $\Delta\rho_o$ - difference between the ambient water density and the density of
the heated flow in the discharge channel, $\rho_a - \rho_o$

superscript ' - indicates a turbulent fluctuating quantity
superscript - - indicates a dimensionless quantity. Note that variables
printed by the computer are dimensionless but are
capitalized.
subscript s - indicates a jet property in the stable region

Appendix I Flow Chart for Solution of $[a_{ij}] \frac{dy_j}{dx} c_i$



* y_j include $U, T, B, H, R, S, \frac{dB}{dx}, \theta, XP$, and YP ; $\frac{dB}{dx}$ is not printed

DOUBLE PRECISION DERY,Y,PRMT,X,TH,XP,YP,U,B,T,H,BX,S,R,XLIM,AUX,XX	PGM10001
DOUBLE PRECISION A,C,CCOS,DSIN,DELX	PGM10002
REAL I1,I2,I3,I4,I5,I6,I7,I8,M	PGM10003
INTEGER P,RR,REG,VFG,FLAG	PGM10004
DIMENSION PRMT(5),Y(10),AUX(8,10),DERY(10),A(10,10),C(10),VEL(8)	PGM10005
EQUIVALENCE (Y(8),TH),(Y(9),XP),(Y(10),YP),(Y(3),B),(Y(1),U)	PGM10006
EQUIVALENCE (Y(2),T),(Y(4),H),(Y(7),BX),(Y(6),S),(Y(5),R)	PGM10007
COMMON DERY,Y,PRMT,X,XLIM,AUX,XX,A,C,DELX	PGM10008
COMMON EPSB,G,DV,IER,IR,WI,VI,KMI,M,FR,AS,E	PGM10009
COMMON THID,THI,ERR,VEL,I1,I2,I3,I4,I5,I6,I7,I8,EPS,V,BXS,DT,FI	PGM10010
COMMON P,RR,NPAGE,NLINE,REG,NDIM,VFG,FLAG,IHLF,STEP,IM,XI	PGM10011
EPS=0.22	PGM10012
I1=.4500	PGM10013
I2=.3160	PGM10014
I3=.6000	PGM10015
I4=.2143	PGM10016
I5=.2220	PGM10017
I6=.13333	PGM10018
I7=.3680	PGM10019
RR=5	PGM10020
READ (RR,100) KK	PGM10021
100 FORMAT (I3)	PGM10022
K=1	PGM10023
10 READ(RR,101) FR,AS,E,THID,XLIM,ERR,STEP	PGM10024
101 FORMAT (2F10.5,F10.7,4F10.5)	PGM10025
READ (RR,102) (VEL(I),I=1,8)	PGM10026
102 FORMAT (8F10.5)	PGM10027
THI=3.14159*THID/180.0	PGM10028
R=AS** .5	PGM10029
S=1./R	PGM10030
H=.0001	PGM10031
XX =-2.0	PGM10032
B=H	PGM10033
T=1.0	PGM10034
BX=EPS	PGM10035
TH=THI	PGM10036

Appendix II Program Listing


```
XP=0.
YP=0.
CALL CROSS
U=1.0-V*COS(THI)
IER=0
TM=0
XI=0
NPAGE=0
NLINE=50
REG=1
FI=(1./(FR**2))*S
RMI=1.0+R*FI*.5
PRMT(1)=0.
PRMT(2)=XLIM
PRMT(3)=.00001
PRMT(4)=ERR
IF (VEL(1)) 2,1,2
1 NDIM=7
VFG=2
GO TO 3
2 NDIM=10
VFG=1
3 DO 4 N=1,NDIM
DERY(N)=1./NDIM
4 CONTINUE
CALL SRKGS
IF(K-KK) 7,8,8
7 K=K+1
GO TO 10
8 CALL EXIT
9 STOP
END
```

```
PGM10037
PGM10038
PGM10039
PGM10040
PGM10041
PGM10042
PGM10043
PGM10044
PGM10045
PGM10046
PGM10047
PGM10048
PGM10049
PGM10050
PGM10051
PGM10052
PGM10053
PGM10054
PGM10055
PGM10056
PGM10057
PGM10058
PGM10059
PGM10060
PGM10061
PGM10062
PGM10063
PGM10064
PGM10065
PGM10066
PGM10067
PGM10068
```


C	PREPARATIONS OF FIRST RUNGE-KUTTA STEP	SRKG0037
	DO 3 I=1,NDIM	SRKG0038
	AUX(1,I)=Y(I)	SRKG0039
	AUX(2,I)=DERY(I)	SRKG0040
	AUX(3,I)=0.DC	SRKG0041
3	AUX(6,I)=0.DC	SRKG0042
	IREC=0	SRKG0043
	H=H+H	SRKG0044
	IHLF=-1	SRKG0045
	ISTEP=0	SRKG0046
	IEND=0	SRKG0047
C		SRKG0048
C		SRKG0049
	4 IF((X+H-XEND)*H) 7,6,5	SRKG0050
C	START OF A RUNGE-KUTTA STEP	SRKG0051
	5 H=XEND-X	SRKG0052
	6 IEND=1	SRKG0053
C		SRKG0054
C	RECORDING OF INITIAL VALUES OF THIS STEP	SRKG0055
	7 CALL OUTP	SRKG0056
36	IF(PRMT(5))40,8,40	SRKG0057
	8 ITEST=0	SRKG0058
	9 ISTEP=ISTEP+1	SRKG0059
C		SRKG0060
C		SRKG0061
C	START OF INNERMOST RUNGE-KUTTA LOOP	SRKG0062
	J=1	SRKG0063
	DO 91 I=1,NDIM	SRKG0064
	AUX(3,I)=0.DC	SRKG0065
91	AUX(6,I)=0.DC	SRKG0066
10	AJ=A(J)	SRKG0067
	BJ=B(J)	SRKG0068
	CJ=C(J)	SRKG0069
	DO 11 I=1,NDIM	SRKG0070
	R1=H*DERY(I)	SRKG0071
	R2=AJ*(R1-BJ*AUX(6,I))	SRKG0072

	Y(I)=Y(I)+R2	SRKG0073
	R2=R2+R2+R2	SRKG0074
11	AUX(6,I)=AUX(6,I)+R2-CJ*R1	SRKG0075
	IF(J-4)12,15,15	SRKG0076
12	J=J+1	SRKG0077
	IF(J-3)13,14,13	SRKG0078
13	X=X+.5D0*H	SRKG0079
14	CALL FCT	SRKG0080
	GO TO 10	SRKG0081
C	END OF INNERMOST RUNGE-KUTTA LOOP	SRKG0082
C		SRKG0083
C	TEST OF ACCURACY	SRKG0084
15	IF(ITEST)16,16,20	SRKG0085
C		SRKG0086
C	IN CASE ITEST=0 TESTING OF ACCURACY IS IMPOSSIBLE	SRKG0087
16	DO 17 I=1,NDIM	SRKG0088
17	AUX(4,I)=Y(I)	SRKG0089
	ITEST=1	SRKG0090
	ISTEP=ISTEP+ISTEP-2	SRKG0091
18	IHLF=IHLF+1	SRKG0092
	X=X-H	SRKG0093
	H=.5D0*H	SRKG0094
	DO 19 I=1,NDIM	SRKG0095
	Y(I)=AUX(1,I)	SRKG0096
	DERY(I)=AUX(2,I)	SRKG0097
19	AUX(6,I)=AUX(3,I)	SRKG0098
	GO TO 9	SRKG0099
C		SRKG0100
C	IN CASE ITEST=1 TESTING OF ACCURACY IS POSSIBLE	SRKG0101
20	IMOD=ISTEP/2	SRKG0102
	IF(ISTEP-IMOD-IMOD)21,23,21	SRKG0103
21	CALL FCT	SRKG0104
	DO 22 I=1,NDIM	SRKG0105
	AUX(5,I)=Y(I)	SRKG0106
22	AUX(7,I)=DERY(I)	SRKG0107
	GO TO 9	SRKG0108

C		SRKG0109
C	COMPUTATION OF TEST VALUE DELT	SRKG0110
	23 DELT=0.D0	SRKG0111
	DO 24 I=1,NDIM	SRKG0112
	24 DELT=DELT+AUX(8,I)*DAES(AUX(4,I)-Y(I))	SRKG0113
	IF(DELT-PRMT(4))23,28,25	SRKG0114
C		SRKG0115
C	ERROR IS TOO GREAT	SRKG0116
	25 GO TO 26	SRKG0117
	26 DO 27 I=1,NDIM	SRKG0118
	27 AUX(4,I)=AUX(5,I)	SRKG0119
	ISTEP=ISTEP+ISTEP-4	SRKG0120
	X=X-H	SRKG0121
	IEND=0	SRKG0122
	GO TO 18	SRKG0123
C		SRKG0124
C	RESULT VALUES ARE GOOD	SRKG0125
	23 DO 50 K=1,6	SRKG0126
	IF (Y(K)) 25,50,50	SRKG0127
	50 CONTINUE	SRKG0128
	281 CALL FCT	SRKG0129
	DO 29 I=1,NDIM	SRKG0130
	AUX(1,I)=Y(I)	SRKG0131
	AUX(2,I)=DERY(I)	SRKG0132
	AUX(3,I)=AUX(6,I)	SRKG0133
	Y(I)=AUX(5,I)	SRKG0134
	29 DERY(I)=AUX(7,I)	SRKG0135
	IF(PRMT(5))40,30,40	SRKG0136
	30 DO 31 I=1,NDIM	SRKG0137
	Y(I)=AUX(1,I)	SRKG0138
	31 DERY(I)=AUX(2,I)	SRKG0139
	IREF=IHLF	SRKG0140
	IF(IEND)32,32,39	SRKG0141
C		SRKG0142
C	INCREMENT GETS DOUBLED	SRKG0143
	32 IHLF=IHLF-1	SRKG0144

```

        ISTEP=ISTEP/2
        H=H+H
33  IMOD=ISTEP/2
    IF (ISTEP-IMOD-IMOD) 4, 34, 4
34  GO TO 35
35  IHLF=IHLF-1
    ISTEP=ISTEP/2
    H=H+H
    GO TO 4

```

```

C
C      RETURNS TO CALLING PROGRAM
37  IHLF=12
    GO TO 39
38  IHLF=13
39  CALL OUTP
40  RETURN
    END

```

```

SRKG0145
SRKG0146
SRKG0147
SRKG0148
SRKG0149
SRKG0150
SRKG0151
SRKG0152
SRKG0153
SRKG0154
SRKG0155
SRKG0156
SRKG0157
SRKG0158
SRKG0159
SRKG0160
SRKG0161

```

SUBROUTINE OUTP	OUTP0001
DOUBLE PRECISION DERY,Y,PRMT,X,TH,XP,YP,U,B,T,H,BX,S,R,XLIM,AUX	OUTP0002
DOUBLE PRECISION A,C,XX,DCUS,DSIN,DELX	OUTP0003
REAL I1,I2,I3,I4,I5,I6,I7,I8,M	OUTP0004
INTEGER P,RR,REG,VFG,FLAG	OUTP0005
DIMENSION PRMT(5),Y(10),AUX(8,10),DERY(10),A(10,10),C(10),VEL(8)	OUTP0006
EQUIVALENCE (Y(8),TH),(Y(9),XP),(Y(10),YP),(Y(3),B),(Y(1),U)	OUTP0007
EQUIVALENCE (Y(2),T),(Y(4),H),(Y(7),BX),(Y(6),S),(Y(5),R)	OUTP0008
COMMON DERY,Y,PRMT,X,XLIM,AUX,XX,A,C,DELX	OUTP0009
COMMON EPSB,G,DV,IER,VIR,WI,VI,RMI,M,FR,AS,E	OUTP0010
COMMON THID,THI,ERR,VEL,I1,I2,I3,I4,I5,I6,I7,I8,EPS,V,BXS,DT,FI	OUTP0011
COMMON P,RR,NPAGE,NLINE,REG,NDIM,VFG,FLAG,IHLF,STEP,TM,XI	OUTP0012
P=6	OUTP0013
CALL CROSS	OUTP0014
GO TO (100,98,108,118), REG	OUTP0015
98 S=0.0	OUTP0016
100 IF(R-.01)101,101,109	OUTP0017
101 R=0	OUTP0018
REG=REG+2	OUTP0019
109 GO TO (110,105,110,105), REG	OUTP0020
108 R= 0.0	OUTP0021
110 IF(S-.01)111,111,105	OUTP0022
111 S=0.	OUTP0023
REG=REG+1	OUTP0024
GO TO 105	OUTP0025
113 R=0.0	OUTP0026
S=0.0	OUTP0027
105 CONTINUE	OUTP0028
120 IF(X-XX-STEP) 170,170,121	OUTP0029
121 XX=X	OUTP0030
122 IF (NLINE-50) 150,140,140	OUTP0031
140 NPAGE=NPAGE+1	OUTP0032
141 NLINE=0	OUTP0033
WRITE (P,202) NPAGE	OUTP0034
202 FORMAT(1H1,24HBUOYANT JET CALCULATIONS,10X,5HPAGE ,I2)	OUTP0035
WRITE (P,2021)	OUTP0036

```

2021 FORMAT(/2X,13HFRCODE NUMBER,8X,12HASPECT RATIO,7X,
118HANGLE OF DISCHARGE,6X,14HROUND OFF ERROR,7X,4HXLIM,14X,
214HHEAT LOSS COEF)
WRITE (P,203) FR,AS,THID,ERR,XLIM,E
203 FORMAT(1X,4(F9.5,12X),F10.5,11X,F8.7//)
WRITE (P,300) (I,VEL(I),I=1,3)
300 FORMAT(8(3X,3HVEL,I1,1H=,F8.3)//)
WRITE (P,199)
199 FORMAT(4X,1HX,8X,1HH,8X,1HB,8X,1HR,8X,1HS,8X,2HFL,7X,
11HQ,7X,1HM,5X,1HU,5X,1HT,4X,2HHT,5X,1HV,6X,2HXP,
27X,2HYP,5X,3HTHD,6X,2HTM/)
150 NLINE=NLINE+1
THD=180.0*TH/3.14159
FL=T*H/(U*U)
FL=FL/(AS**.5)
FL=ABS(FL)
FL=FL**.5
FL=FR/FL
Q=U*(S+B*I1)*(R+H*I1)+V*DCOS(TH)*(S+B)*(R+H)
M=U*U*(S+B*I2)*(R+H*I2)+Q*V*DCOS(TH)
M=M+U*V*DCOS(TH)*(S+B*I1)*(R+H*I1)
M=M+(R*R*.5+I3*H*R+I4*H*H)*(S+B*I3)*T*FI
HT=U*T*(S+B*I7)*(R+H*I7)+T*V*DCOS(TH)*(S+B*I3)*(R+H*I3)
DELX=X-XI
DTM=2*DELX/(L+UI)
TM=TM+DTM
95 IF(NDIM-7)96,96,97
96 XP=X
97 CONTINUE
WRITE (P,200) X,H,B,R,S,FL,Q,M,U,T,HT,V,XP,YP,THD,TM
200 FORMAT(7(1X,D8.3),5(1X,F5.3),2(1X,D3.3),1X,F5.1,2X,D3.3)
XI=X
UI=U
IF(ABS(M-RMI)-.25) 180,180,158
180 IF(U-V*DCOS(TH))160,160,159
159 IF(U-.02) 160,160,170

```

OUTP0037
 OUTP0038
 OUTP0039
 OUTP0040
 OUTP0041
 OUTP0042
 OUTP0043
 OUTP0044
 OUTP0045
 OUTP0046
 OUTP0047
 OUTP0048
 OUTP0049
 OUTP0050
 OUTP0051
 OUTP0052
 OUTP0053
 OUTP0054
 OUTP0055
 OUTP0056
 OUTP0057
 OUTP0058
 OUTP0059
 OUTP0060
 OUTP0061
 OUTP0062
 OUTP0063
 OUTP0064
 OUTP0065
 OUTP0066
 OUTP0067
 OUTP0068
 OUTP0069
 OUTP0070
 OUTP0071
 OUTP0072


```
158 WRITE (P,400)
400 FORMAT(/10X,43HMOMENTUM HAS EXCEEDED BOUNDS RUN TERMINATES)
    GO TO 190
160 WRITE (P,401)
401 FORMAT(/10X,48HJET VELOCITY HAS BECOME TOO SMALL RUN TERMINATES)
190 PRMT(5)=1.0
170 RETURN
    END
```

```
OUTP0073
OUTP0074
OUTP0075
OUTP0076
OUTP0077
OUTP0078
OUTP0079
OUTP0080
```

```

SUBROUTINE CROSS
DOUBLE PRECISION DERY,Y,PRMT,X,TH,XP,YP,L,B,T,F,BX,S,R,XLIM,AUX,XX
DOUBLE PRECISION AUN,CUN,DCOS,DSIN,DELX
REAL I1,I2,I3,I4,I5,I6,I7,I8,M
INTEGER P,RR,REG,VFG,FLAG
DIMENSION PRMT(5),Y(10),AUX(8,10),DERY(10),VEL(8)
DIMENSION AUN(10,10),CUN(10)
EQUIVALENCE (Y(8),TH),(Y(9),XP),(Y(10),YP),(Y(3),B),(Y(1),U)
EQUIVALENCE (Y(2),T),(Y(4),H),(Y(7),BX),(Y(6),S),(Y(5),R)
COMMON DERY,Y,PRMT,X,XLIM,AUX,XX,AUN,CUN,DELX
COMMON EPSB,G,DV,IER,WIR,WI,VI,RMI,M,FR,AS,E
COMMON THID,THI,ERR,VEL,I1,I2,I3,I4,I5,I6,I7,I8,EPS,V,BXS,DT,FI
COMMON P,RR,NPAGE,NLINE,REG,NDIM,VFG,FLAG,IHLF,STEP,TM,XI
A=XP*VEL(4)
A=A-VEL(5)
V=-A*2*VEL(3)*VEL(4)
A=A*A
A=VEL(3)*A
A=VEL(2)*EXP(-A)
DV=V*A
V=VEL(1)+A
RETURN
END

```

```

CROSS0001
CROSS0002
CROSS0003
CROSS0004
CROSS0005
CROSS0006
CROSS0007
CROSS0008
CROSS0009
CROSS0010
CROSS0011
CROSS0012
CROSS0013
CROSS0014
CROSS0015
CROSS0016
CROSS0017
CROSS0018
CROSS0019
CROSS0020
CROSS0021
CROSS0022
CROSS0023

```

```

SUBROUTINE FCT
DOUBLE PRECISION DERY,Y,PRMT,X,TH,XP,YP,U,B,T,H,BX,S,R,XLIM,AUX,XX
DOUBLE PRECISION A,C,CCOS,DSIN,DELX
REAL I1,I2,I3,I4,I5,I6,I7,I8,M
INTEGER P,RR,REG,VFG,FLAG
DIMENSION PRMT(5),Y(10),AUX(8,10),DERY(10),A(10,10),C(10),VEL(3)
EQUIVALENCE (Y(8),TH),(Y(9),XP),(Y(10),YP),(Y(3),B),(Y(1),U)
EQUIVALENCE (Y(2),T),(Y(4),H),(Y(7),BX),(Y(6),S),(Y(5),R)
COMMON DERY,Y,PRMT,X,XLIM,AUX,XX,A,C,DELX
COMMON EPSB,G,DV,IER,WIR,WI,VI,RMI,M,FR,AS,E
COMMON THID,THI,ERR,VEL,I1,I2,I3,I4,I5,I6,I7,I8,EPS,V,BXS,DT,FI
COMMON P,RR,NPAGE,NLINE,REG,NDIM,VFG,FLAG,IHLF,STEP,TM,XI
DO 50 I=1,10
C(I)=0.
DERY(I)=0.
DO 50 II=1,10
A(I,II)=0.
50 CONTINUE
101 FLAG=VFG
WI=EPS*U
VI=-WI
EPSB=EPS
ARG=5*T*H/(U*U*FR*FR)
ARG=ARG/(AS*.5)
IF(ARG)10100,10100,10101
10100 ARG=C.
10101 IF(ARG-100.)10103,10103,10102
10102 WIR=C.
GO TO 10104
10103 WIR=EXP(-ARG)
10104 GO TO (1011,1012), FLAG
1011 G=0.
BXS=BX
BX=0.
GO TO 1013
1012 G=FI*T

```

```

FCTN0001
FCTN0002
FCTN0003
FCTN0004
FCTN0005
FCTN0006
FCTN0007
FCTN0008
FCTN0009
FCTN0010
FCTN0011
FCTN0012
FCTN0013
FCTN0014
FCTN0015
FCTN0016
FCTN0017
FCTN0018
FCTN0019
FCTN0020
FCTN0021
FCTN0022
FCTN0023
FCTN0024
FCTN0025
FCTN0026
FCTN0027
FCTN0028
FCTN0029
FCTN0030
FCTN0031
FCTN0032
FCTN0033
FCTN0034
FCTN0035
FCTN0036

```

	WI=WI*WIR	FCTN0037
1013	GO TO (102,103,104,105), REG	FCTN0038
102	WI=WI*(I1-I2)	FCTN0039
	VI=VI*(I1-I2)	FCTN0040
	GO TO 110	FCTN0041
103	WI=WI*(I1-I2)	FCTN0042
	VI=VI*I1/2	FCTN0043
	GO TO 110	FCTN0044
104	WI=WI*I1/2	FCTN0045
	VI=VI*(I1-I2)	FCTN0046
	GO TO 110	FCTN0047
105	WI=WI*I1/2	FCTN0048
	VI=VI*I1/2	FCTN0049
110	H1=R+H*I1	FCTN0050
	B1=S+B*I1	FCTN0051
	A(1,1)=H1*B1	FCTN0052
	A(1,2)=U*I1*B1	FCTN0053
	A(1,3)=U*B1	FCTN0054
	A(1,4)=U*H1	FCTN0055
	C(1)=WI*B1-VI*H1-U*I1*H1*BX	FCTN0056
	H3=R+H*I3	FCTN0057
	B3=S+B*I3	FCTN0058
	H2=R+H*I2	FCTN0059
	B2=S+B*I2	FCTN0060
	HG=R*R/2+R*H*I3+H*H*I4	FCTN0061
	A(2,1)=2*U*H2*B2	FCTN0062
	A(2,2)=U*U*I2*B2+G*B3*(R*I3+2*H*I4)	FCTN0063
	A(2,3)=U*U*B2+G*B3*(R+H*I3)	FCTN0064
	A(2,4)=U*U*H2+G*HG	FCTN0065
	A(2,5)=FI*B3*HG	FCTN0066
	C(2)=- (U*U*I2*H2+G*I3*HG)*BX	FCTN0067
	B7=S+B*I7	FCTN0068
	H7=R+H*I7	FCTN0069
	A(3,1)=G*B7*H7	FCTN0070
	A(3,2)=U*G*I7*B7	FCTN0071
	A(3,3)=U*G*B7	FCTN0072

A(3,4)=U*G*H7	FCTN0073
A(3,5)=U*B7*H7*FI	FCTN0074
C(2)=-E*G*B3-U*G*I7*H7*B X	FCTN0075
GO TO (1,2,3,4), REG	FCTN0076
1 A(5,1)=U	FCTN0077
A(5,2)=G*I3	FCTN0078
A(5,3)=G	FCTN0079
A(5,5)=FI*(R/2+H*I3)	FCTN0080
GO TO 5	FCTN0081
2 A(5,4)=1.	FCTN0082
GO TO 5	FCTN0083
3 A(5,3)=1.0	FCTN0084
GO TO 5	FCTN0085
4 A(5,4)=1.	FCTN0086
A(4,3)=1.0	FCTN0087
GO TO 6	FCTN0088
5 I8=1.-I2/I1	FCTN0089
A(4,1)=U*((S*H+R*B)*I2+R*S*I8)	FCTN0090
A(4,2)=G*(2*S*H*I4+R*E*I3*I3)	FCTN0091
A(4,3)=U*U*S*I8+G*(S*I*I3+R*B*I3)	FCTN0092
A(4,4)=U*U*R*I8+G*(R*R/2+H*R*I3)	FCTN0093
A(4,5)=FI*(S*H*H*I4+I*R*R*I3/2+B*H*R*I3*I3)	FCTN0094
C(4)=U*(VI*R-WI*S)*I2/I1-G*(R*R/2+H*R*I3)*I3*B X	FCTN0095
6 GO TO (120,131), VFG	FCTN0096
120 CALL CROSS	FCTN0097
DERY(9)=DSIN(TH)	FCTN0098
DERY(10)=DCOS(TH)	FCTN0099
VST=V*DERY(9)	FCTN0100
VCT=V*DERY(10)	FCTN0101
DT=U*U*(S+B*I2)*(R+H*I2)+2*U*VCT*(S+B*I1)*(R+H*I1)	FCTN0102
1+VCT*VCT*(R+H)*(S+B)	FCTN0103
DT=-VST*(WI*(S+B*I1)-VI*(R+H*I1))/DT	FCTN0104
DERY(8)=DT	FCTN0105
H0=R+H	FCTN0106
DT=VST*DT-DERY(10)*OV*DERY(9)	FCTN0107
B0=S+B	FCTN0108

A(1,2)=A(1,2)+VCT*B0	FCTN0109
A(1,3)=A(1,3)+VCT*B0	FCTN0110
A(1,4)=A(1,4)+VCT*H0	FCTN0111
C(1)=C(1)-VCT*H0*BX+BC*H0*DT	FCTN0112
A(2,1)=A(2,1)+2*VCT*H1*B1	FCTN0113
A(2,2)=A(2,2)+VCT*(2*U*I1*B1+VCT*B0)	FCTN0114
A(2,3)=A(2,3)+VCT*(2*U*B1+VCT*B0)	FCTN0115
A(2,4)=A(2,4)+VCT*(2*U*H1+VCT*H0)	FCTN0116
C(2)=C(2)-VCT*(2*U*I1*H1+VCT*H0)*BX+2*(U*H1*H1+VCT*B0*H0)*DT	FCTN0117
1+VCT*(W1*B1-V1*H1)	FCTN0118
A(3,2)=A(3,2)+G*VCT*I3*B3	FCTN0119
A(3,3)=A(3,3)+G*VCT*B2	FCTN0120
A(3,4)=A(3,4)+G*VCT*H2	FCTN0121
A(3,5)=A(3,5)+F1*VCT*H3*B3	FCTN0122
C(3)=C(3)-G*VCT*I3*H2*BX+G*B3*H3*DT	FCTN0123
GO TO (7,8,9),REG	FCTN0124
7 A(5,1)=A(5,1)+VCT	FCTN0125
C(5)=(U+VCT)*DT	FCTN0126
GO TO 9	FCTN0127
8 A(4,1)=A(4,1)+VCT*I1*(R*B+S*H)	FCTN0128
A(4,2)=A(4,2)+S*U*VCT*(I1-I1/I2)	FCTN0129
A(4,3)=A(4,3)+S*U*VCT*I8	FCTN0130
A(4,4)=A(4,4)+R*U*VCT*I8	FCTN0131
C(4)=C(4)-R*U*VCT*(I1-I1/I2)*BX	FCTN0132
1+((U*(2*I1-I2/I1)+VCT)*(S*H+R*B)+R*S*U*I8)*DT	FCTN0133
9 GO TO (130,131),FLAG	FCTN0134
130 A(1,2)=A(1,2)+(U*I1*H1+VCT*H0)	FCTN0135
A(2,2)=A(2,2)+(U*U*I2*H2+2*U*VCT*I1*H1+VCT*VCT*H0)	FCTN0136
GO TO (10,10,10,11),REG	FCTN0137
10 A(4,2)=A(4,2)+R*U*VCT*(I1-I2/I1)	FCTN0138
11 CALL SGELG(5)	FCTN0139
EPSB=C(2)	FCTN0140
BX=BXS	FCTN0141
FLAG=2	FCTN0142
G=FI*T	FCTN0143
WI=WI*WIR	FCTN0144

GO TO 110	FCTN0145
131 DB=BX-EP SB	FCTN0146
A(6,1)=DB*2*U*B*H2*I6	FCTN0147
A(6,2)=DB*U*U*B*I2*I6	FCTN0148
A(6,3)=DB*U*U*B*I6	FCTN0149
A(6,6)=U*U*B*H2*I6	FCTN0150
C(6)=G*HG-U*L*I6*DB*H2*BX	FCTN0151
GO TO (132,133),VFG	FCTN0152
132 A(6,1)=A(6,1)+2*B*VCT*I5*H2*DB	FCTN0153
A(6,2)=A(6,2)+VCT*B*(2*U*I5*I1+VCT)*DB	FCTN0154
A(6,3)=A(6,3)+VCT*B*(2*U*I5+VCT)*DB	FCTN0155
A(6,6)=A(6,6)+VCT*B*(2*U*I5*H1+VCT*H0)	FCTN0156
C(6)=C(6)-DB*VCT*(2*U*I5*H1+VCT*H0)*BX+2*DB*B*(U*I5*H1+VCT	FCTN0157
1*H0)*DT	FCTN0158
133 CALL SGELG(5)	FCTN0159
DERY(1)=C(1)	FCTN0160
DERY(2)=C(5)	FCTN0161
DERY(3)=BX	FCTN0162
DERY(4)=C(2)	FCTN0163
DERY(5)=C(3)	FCTN0164
DERY(6)=C(4)	FCTN0165
DERY(7)=C(6)	FCTN0166
RETURN	FCTN0167
END	FCTN0168

	SUBROUTINE SGELG(M)	SGEL0001
	DOUBLE PRECISION AD, AI, XX, DABS, DCOS, DSIN, SAVE, S, R, XLIM, AUX	SGEL0002
	DOUBLE PRECISION DERY, Y, PRMT, X, TH, XP, YP, U, B, T, H, BX	SGEL0003
	DOUBLE PRECISION A, PIV, TB, TOL, PIVI, DELX	SGEL0004
	REAL MUN	SGEL0005
	INTEGER P, RR, REG, VFG, FLAG	SGEL0006
	DIMENSION PRMT(5), Y(10), AUX(8, 10), DERY(10), AI(100), R(10), VEL(8)	SGEL0007
	DIMENSION A(100), AD(10, 10)	SGEL0008
	DIMENSION SAVE(10)	SGEL0009
	EQUIVALENCE (AI(1), AD(1, 1))	SGEL0010
	COMMON DERY, Y, PRMT, X, XLIM, AUX, XX, AI, R, DELX	SGEL0011
	COMMON EPSB, G, DV, IER, VIR, WI, VI, RMI, MUN, FR, AS, E	SGEL0012
	COMMON THID, THI, ERR, VEL, I1, I2, I3, I4, I5, I6, I7, I8, EPS, V, BXS, DT, FI	SGEL0013
	COMMON P, RR, NPAGE, NLINE, REG, NDIM, VFG, FLAG, IHLF, STEP, TM, XI	SGEL0014
	N=1	SGEL0015
	EPSS=.1E-16	SGEL0016
C	SCALE THE MATRIX	SGEL0017
	DO 54 I=1, M	SGEL0018
	AMAX=R(I)	SGEL0019
	DO 52 J=1, M	SGEL0020
	DA=DABS(AD(I, J))	SGEL0021
	IF(DA-AMAX) 52, 52, 51	SGEL0022
51	AMAX=DA	SGEL0023
52	CONTINUE	SGEL0024
	DO 53 J=1, M	SGEL0025
	AD(I, J)=AD(I, J)/AMAX	SGEL0026
53	CONTINUE	SGEL0027
	R(I)=R(I)/AMAX	SGEL0028
54	CONTINUE	SGEL0029
C	SAVE THE Y EQUATION ROW	SGEL0030
	MM=M+1	SGEL0031
	DO 999 I=1, MM	SGEL0032
	SAVE(I)=AD(MM, I)	SGEL0033
999	CONTINUE	SGEL0034
C	CONVERT MATRIX TO COLUMN FORM	SGEL0035
	IJ=0	SGEL0036


```

        NM=0
        DO 1100 K=1,M
        DO 1000 L=1,M
        IJ=IJ+1
        NM=NM+1
1000    A(IJ)=A1(NM)
1100    NM=NM+10-M
        IF(M)23,23,1
C
C      SEARCH FOR GREATEST ELEMENT IN MATRIX A
1    IER=0
      PIV=C.DO
      MM=M*M
      NM=N*M
      DO 3 L=1,MM
      TB=DABS(A(L))
      IF(TB-PIV)3,3,2
2    PIV=TB
      I=L
3    CONTINUE
      TOL=EPSS*PIV
C      A(I) IS PIVOT ELEMENT. PIV CONTAINS THE ABSOLUTE VALUE OF A(I)
C
C
C      START ELIMINATION LOOP
      LST=1
      DO 17 K=1,M
C
C      TEST ON SINGULARITY
      IF(PIV)23,23,4
4    IF(IER)7,5,7
5    IF(PIV-TOL)6,6,7
6    IER=K-1
7    PIVI=1.DO/A(I)
      J=(I-1)/M
      I=I-J*M-K

```

```

SGEL0037
SGEL0038
SGEL0039
SGEL0040
SGEL0041
SGEL0042
SGEL0043
SGEL0044
SGEL0045
SGEL0046
SGEL0047
SGEL0048
SGEL0049
SGEL0050
SGEL0051
SGEL0052
SGEL0053
SGEL0054
SGEL0055
SGEL0056
SGEL0057
SGEL0058
SGEL0059
SGEL0060
SGEL0061
SGEL0062
SGEL0063
SGEL0064
SGEL0065
SGEL0066
SGEL0067
SGEL0068
SGEL0069
SGEL0070
SGEL0071
SGEL0072

```

	J=J+1-K	SGEL0073
C	I+K IS ROW-INDEX, J+K COLUMN-INDEX OF PIVOT ELEMENT	SGEL0074
C		SGEL0075
C	PIVOT ROW REDUCTION AND ROW INTERCHANGE IN RIGHT HAND SIDE R	SGEL0076
	DO 8 L=K,NM,M	SGEL0077
	LL=L+I	SGEL0078
	TB=PIVI*R(LL)	SGEL0079
	R(LL)=R(L)	SGEL0080
	8 R(L)=TB	SGEL0081
C		SGEL0082
C	IS ELIMINATION TERMINATED	SGEL0083
	IF(K-M)9,18,18	SGEL0084
C		SGEL0085
C	COLUMN INTERCHANGE IN MATRIX A	SGEL0086
	9 LEND=LST+M-K	SGEL0087
	IF(J)12,12,10	SGEL0088
	10 II=J*M	SGEL0089
	DO 11 L=LST,LEND	SGEL0090
	TB=A(L)	SGEL0091
	LL=L+II	SGEL0092
	A(L)=A(LL)	SGEL0093
	11 A(LL)=TB	SGEL0094
C		SGEL0095
C	ROW INTERCHANGE AND PIVOT ROW REDUCTION IN MATRIX A	SGEL0096
	12 DO 13 L=LST,NM,M	SGEL0097
	LL=L+I	SGEL0098
	TB=PIVI*A(LL)	SGEL0099
	A(LL)=A(L)	SGEL0100
	13 A(L)=TB	SGEL0101
C		SGEL0102
C	SAVE COLUMN INTERCHANGE INFORMATION	SGEL0103
	A(LST)=J	SGEL0104
C		SGEL0105
C	ELEMENT REDUCTION AND NEXT PIVOT SEARCH	SGEL0106
	PIV=0.DO	SGEL0107
	LST=LST+1	SGEL0108

J=0	SGEL0109
DO 16 II=LST,LEND	SGEL0110
PIVI=-A(II)	SGEL0111
IST=II+M	SGEL0112
J=J+1	SGEL0113
DO 15 L=IST,MM,M	SGEL0114
LL=L-J	SGEL0115
A(L)=A(L)+PIVI*A(LL)	SGEL0116
TB=DABS(A(L))	SGEL0117
IF(TB-PIV)15,15,14	SGEL0118
14 PIV=TB	SGEL0119
I=L	SGEL0120
15 CONTINUE	SGEL0121
DO 16 L=K,NM,M	SGEL0122
LL=L+J	SGEL0123
16 R(LL)=R(LL)+PIVI*R(L)	SGEL0124
17 LST=LST+M	SGEL0125
END OF ELIMINATION LCCP	SGEL0126
C	SGEL0127
C	SGEL0128
C	SGEL0129
C BACK SUBSTITUTION AND BACK INTERCHANGE	SGEL0130
18 IF(M-1)23,22,19	SGEL0131
19 IST=MM+M	SGEL0132
LST=M+1	SGEL0133
DO 21 I=2,M	SGEL0134
II=LST-I	SGEL0135
IST=IST-LST	SGEL0136
L=IST-M	SGEL0137
L=A(L)+.5D0	SGEL0138
DO 21 J=II,NM,M	SGEL0139
TB=R(J)	SGEL0140
LL=J	SGEL0141
DO 20 K=IST,MM,M	SGEL0142
LL=LL+1	SGEL0143
20 TB=TB-A(K)*R(LL)	SGEL0144
K=J+L	

```

      R(J)=K(K)
21  R(K)=TB
22  GO TO (223,221), FLAG
221 MM=M+1
    DO 222 I=1,M
      R(MM)=R(MM)-SAVE(I)*R(I)
222 CONTINUE
    R(MM)=R(MM)/SAVE(MM)
223 DO 24 I=1,100
    A(I)=0.
24  CONTINUE
    RETURN
C
C
C  ERROR RETURN
23  IER=-1
    RETURN
    END

```

```

SGEL0145
SGEL0146
SGEL0147
SGEL0148
SGEL0149
SGEL0150
SGEL0151
SGEL0152
SGEL0153
SGEL0154
SGEL0155
SGEL0156
SGEL0157
SGEL0158
SGEL0159
SGEL0160
SGEL0161
SGEL0162

```

Input:

1							
6.0	0.6	0.0	90.0	500.0	0.01	1.0	
0.0	0.0	0.0	0.0	0.0	0.0	0.0	0.0

Output:

BUOYANT JET CALCULATIONS

PAGE 1

FROUDE NUMBER 6.00000		ASPECT RATIO 0.60000		ANGLE OF DISCHARGE 90.00000		ROUND OFF ERROR 0.01000		XLIM 500.00000		HEAT LOSS COEF .0					
VEL1=	0.0	VEL2=	0.0	VEL3=	0.0	VEL4=	0.0	VEL5=	0.0	VEL6=	0.0	VEL7=	0.0	VEL8=	0.0

X	H	B	R	S	FL	Q	M	U	T	HT	V	XP	YP	THD	TM
.0	.100D-03	.100D-03	.775D 00	.129D 01	.528E 03	.100E 01	1.014	1.000	1.000	1.000	0.0	.0	.0	90.0	.0
.131D 01	.190D 00	.585D 00	.521D 00	.152D 01	.124E 02	.109E 01	1.014	1.005	0.971	1.000	0.0	.131D 01	.0	90.0	.131E 01
.262D 01	.378D 00	.116D 01	.450D 00	.137D 01	.890E 01	.118E 01	1.014	1.004	0.940	1.000	0.0	.262D 01	.0	90.0	.261E 01
.524D 01	.724D 00	.239D 01	.218D 00	.144D 01	.664E 01	.138E 01	1.014	1.006	0.884	1.000	0.0	.524D 01	.0	90.0	.522E 01
.786D 01	.104D 01	.377D 01	.293D-01	.153D 01	.574E 01	.161E 01	1.014	1.007	0.828	1.000	0.0	.786D 01	.0	90.0	.782E 01
.918D 01	.119D 01	.450D 01	.0	.152D 01	.517E 01	.177E 01	0.995	0.931	0.759	0.984	0.0	.918D 01	.0	90.0	.918E 01
.105D 02	.134D 01	.527D 01	.0	.148D 01	.465E 01	.196E 01	0.997	0.847	0.692	0.986	0.0	.105D 02	.0	90.0	.107E 02
.131D 02	.161D 01	.652D 01	.0	.130D 01	.391E 01	.232E 01	1.000	0.726	0.597	0.988	0.0	.131D 02	.0	90.0	.140E 02
.157D 02	.185D 01	.873D 01	.0	.100D 01	.342E 01	.265E 01	1.002	0.645	0.535	0.990	0.0	.157D 02	.0	90.0	.178E 02
.210D 02	.221D 01	.125D 02	.0	.195D 00	.283E 01	.321E 01	1.002	0.539	0.457	0.990	0.0	.210D 02	.0	90.0	.267E 02
.236D 02	.224D 01	.153D 02	.0	.103D 00	.267E 01	.347E 01	0.999	0.492	0.424	0.987	0.0	.236D 02	.0	90.0	.317E 02
.249D 02	.227D 01	.166D 02	.0	.0	.258E 01	.360E 01	0.996	0.471	0.409	0.985	0.0	.249D 02	.0	90.0	.345E 02
.262D 02	.228D 01	.180D 02	.0	.0	.250E 01	.373E 01	0.996	0.449	0.394	0.985	0.0	.262D 02	.0	90.0	.373E 02
.275D 02	.228D 01	.196D 02	.0	.0	.244E 01	.387E 01	0.997	0.429	0.381	0.985	0.0	.275D 02	.0	90.0	.403E 02
.288D 02	.227D 01	.211D 02	.0	.0	.238E 01	.400E 01	0.997	0.411	0.368	0.985	0.0	.288D 02	.0	90.0	.434E 02
.315D 02	.225D 01	.246D 02	.0	.0	.227E 01	.426E 01	0.997	0.380	0.346	0.985	0.0	.315D 02	.0	90.0	.501E 02
.367D 02	.220D 01	.324D 02	.0	.0	.211E 01	.476E 01	0.997	0.329	0.310	0.985	0.0	.367D 02	.0	90.0	.648E 02
.419D 02	.215D 01	.415D 02	.0	.0	.197E 01	.523E 01	0.997	0.290	0.282	0.985	0.0	.419D 02	.0	90.0	.818E 02
.472D 02	.209D 01	.516D 02	.0	.0	.186E 01	.568E 01	0.997	0.260	0.260	0.985	0.0	.472D 02	.0	90.0	.101E 03
.524D 02	.204D 01	.629D 02	.0	.0	.177E 01	.609E 01	0.997	0.235	0.242	0.985	0.0	.524D 02	.0	90.0	.122E 03
.629D 02	.202D 01	.884D 02	.0	.0	.151E 01	.683E 01	0.994	0.189	0.215	0.984	0.0	.629D 02	.0	90.0	.171E 03
.734D 02	.211D 01	.124D 03	.0	.0	.107E 01	.707E 01	0.995	0.134	0.208	0.984	0.0	.734D 02	.0	90.0	.236E 03
.839D 02	.195D 01	.174D 03	.0	.0	.868E 00	.715E 01	0.994	0.104	0.206	0.983	0.0	.839D 02	.0	90.0	.325E 03
.105D 03	.156D 01	.324D 03	.0	.0	.658E 00	.720E 01	0.991	0.070	0.204	0.981	0.0	.105D 03	.0	90.0	.565E 03
.126D 03	.125D 01	.552D 03	.0	.0	.543E 00	.723E 01	0.988	0.052	0.202	0.978	0.0	.126D 03	.0	90.0	.909E 03
.147D 03	.102D 01	.864D 03	.0	.0	.470E 00	.723E 01	0.985	0.040	0.202	0.974	0.0	.147D 03	.0	90.0	.136E 04
.168D 03	.359D 00	.126D 04	.0	.0	.418E 00	.722E 01	0.981	0.033	0.201	0.971	0.0	.168D 03	.0	90.0	.194E 04
.210D 03	.641D 00	.235D 04	.0	.0	.349E 00	.720E 01	0.973	0.024	0.200	0.963	0.0	.210D 03	.0	90.0	.342E 04
.252D 03	.506D 00	.382D 04	.0	.0	.304E 00	.716E 01	0.965	0.018	0.200	0.956	0.0	.252D 03	.0	90.0	.542E 04

JET VELOCITY HAS BECOME TOO SMALL RUN TERMINATES

SELECTED WATER RESOURCES ABSTRACTS INPUT TRANSACTION FORM		1. Report No. 2. 3. Accession No. <div style="font-size: 2em; font-weight: bold; text-align: center;">W</div>	
4. Title A User's Manual for Three-Dimensional Heated Surface Discharge Computations		5. Report Date 6. 8. Performing Organization Report No. 10. Project No.	
7. Author(s) K.D. Stolzenbach, E. Eric Adams, and Donald R.F. Harleman		11. Contract/Grant No. 16130 DJU 13. Type of Report and Period Covered	
9. Organization Department of Civil Engineering, Massachusetts Institute of Technology, Cambridge, Massachusetts 02139 12. Sponsoring Organization Environmental Protection Agency 15. Supplementary Notes Environmental Protection Agency Report Number EPA-R2-73-133; January 1973.		16. Abstract <p>The temperature distribution induced in an ambient body of water by a surface discharge of heated condenser cooling water must be determined for evaluation of thermal effects upon the natural environment, for prevention of recirculation of the heated discharge into the cooling water intake, for improved design of laboratory scale models and for insuring that discharge configurations meet legal temperature regulations. This report presents a review of the theoretical background for a three-dimensional temperature prediction model, a detailed discussion of the computer program and a case study illustrating the procedure for optimizing the design of a surface discharge channel. Flow chart, program listing and a sample of the input and output data are given in the appendices. The model presented here includes modifications of the report by Keith D. Stolzenbach and Donald R. F. Harleman, published in February 1971 entitled, "An Analytical and Experimental Investigation of Surface Discharges of Heated Water."</p>	
17a. Descriptors Waste heat disposal, heated surface discharge, turbulent buoyant jets, temperature prediction, thermal pollution.			
17b. Identifiers			
17c. COWRR Field & Group 05G			
18. Availability	19. Security Class. (Report) 20. Security Class. (Page)	21. No. of Pages 22. Price	Send To: WATER RESOURCES SCIENTIFIC INFORMATION CENTER U.S. DEPARTMENT OF THE INTERIOR WASHINGTON, D.C. 20240
Abstractor		Institution Massachusetts Institute of Technology	